

# UC Berkeley

## UC Berkeley Electronic Theses and Dissertations

### Title

Global Analysis of Murine Cytomegalovirus Open Reading Frames Using Yeast Two-Hybrid and Growth Phenotype Analysis

### Permalink

<https://escholarship.org/uc/item/0177z7vw>

### Author

Umamoto, Sean

### Publication Date

2011

Peer reviewed|Thesis/dissertation

Global Analysis of Murine Cytomegalovirus Open Reading Frames Using Yeast Two-Hybrid and  
Growth Phenotype Analysis

By

Sean Noritoshi Umamoto

A dissertation submitted in partial satisfaction of the

requirements for the degree of

Doctor of Philosophy

In

Comparative Biochemistry

in the

Graduate Division

of the

University of California, Berkeley

Committee in charge:

Professor Fenyong Liu, Chair

Professor Bing K. Jap

Professor Lee Riley

Spring 2011





## Abstract

# Global Analysis of Murine Cytomegalovirus Open Reading Frames Using Yeast Two-Hybrid and Growth Phenotype Analysis

By

Sean Noritoshi Umamoto

Doctor of Philosophy in Comparative Biochemistry

University of California, Berkeley

Professor Fenyong Liu, Chair

Human cytomegalovirus (HCMV), a beta-herpesvirus, is an important opportunistic pathogen that primarily affects individuals with compromised or immature immune systems. It is of great significance in AIDS patients where it can cause serious morbidity through retinitis-associated blindness, and other complications, such as pneumonia and enteritis. In developed nations, it is a leading viral cause of congenital disease, where in-utero infection manifests in mental and behavioral disorders. In order to control infection and HCMV associated disease, new compounds and novel strategies must be developed. Understanding the role viral proteins play during the course of infection will help elucidate the mechanisms of HCMV pathogenesis and provide important information on potential targets for new treatments.

However, the strict species specificity of HCMV prevents any studies into the pathogenesis of the virus in an animal host. This limitation can be overcome through the use of murine cytomegalovirus (MCMV). MCMV, like HCMV, is a beta-herpesvirus that exhibits similar pathogenesis in mice to HCMV infection in the human host. The genetic structure of MCMV contains significant sequence homology to HCMV AD169 in at least 78 ORFs and can thereby be used as an important tool in elucidating the functions of these ORFs in a complete *in vivo* system.

In our study, we have conducted a comprehensive YTH screen to identify potential interactions between approximately 170 MCMV ORFs. Growth phenotype analysis were also conducted using five different cell lines potentially involved in various aspects of CMV infection. Between these 170 predicted proteins we have identified 94 potential interactions that exhibit varying levels of essentiality depending on the type of cell infected.

We aim to understand the nature of the interactions between the viral particle and proteins encoded by the virus in order to elucidate potential mechanisms by which these proteins help to assemble and create new progeny viruses. The interactions that we have identified in this study provide a framework to predict the functions of uncharacterized viral proteins. And understanding the importance of each protein in the context of infection can further help to determine the nature of these unknown viral proteins. Together using information about known viral proteins that interact with these unknown elements, we can develop a better understanding of how all of these components contribute to viral infection

which can be used to determine more effective methods to treat or prevent CMV associated diseases.

To my parents  
and my family, of blood and of heart

## Table of Contents

Abstract	pg. 1
Dedication	pg. i
Table of Contents	pg. ii
Acknowledgments	pg. iii
Chapter 1 - Introduction	pg. 1
Chapter 2 – MCMV Virion	pg. 11
Introduction	pg. 12
Materials and Methods	pg. 13
Results	pg. 14
Discussion	pg. 17
Figures	pg. 21
References	pg. 26
Chapter 3 – MCMV Interactome	pg. 29
Introduction	pg. 30
Materials and Methods	pg. 32
Results	pg. 33
Discussion	pg. 36
Figures	pg. 42
References	pg. 78
Chapter 4 – Deletion Mutant Virus Screens	pg. 80
Introduction	pg. 81
Materials and Methods	pg. 82
Results	pg. 84
Discussion	pg. 87
Figures	pg. 90
References	pg. 100
Chapter 5 – M43	pg. 102
Introduction	pg. 103
Materials and Methods	pg. 104
Results	pg. 108
Discussion	pg. 110
Figures	pg. 115
References	pg. 120
Chapter 6 – Conclusion	pg. 122

## Acknowledgements

Some of the greatest moments in time are preceded by seemingly impossible or insurmountable challenges, challenges that when overcome form the cornerstones of a great life. Every great journey requires an opportunity and for that, my gratitude goes to Dr. Fenyong Liu for providing me with the chance to accomplish an amazing goal.

Among the many mentors that I've had the honor to meet and have been inspired by, I would like to thank the members of my qualifying and dissertation committees. To Dr. Barry Shane for chairing my qualifying exam and providing me with many key points that would help me pass this challenging exam. Dr. Stewart Linn, who at the doorstep of retirement, chose to help guide a naïve student. And I would especially like to thank Dr. Lee Riley and Dr. Bing K. Jap, who served on both my qualifying exam and dissertation committees. Without their guidance, the road to the finish would have been longer and more treacherous. I would also like to thank Dr. Robert Beatty, who has always provided me with sound advice in both my undergraduate and graduate education at Berkeley.

Along this journey I have been fortunate to encounter many sterling individuals with strong drives to reach their own lofty heights. My thanks goes out to Drs. Manfred Lee, Phong Trang, Walter Dunn, Alice Chu, Aaron To, Kihoon Kim and Rong Hai who helped provide a friendly environment for a new undergrad to assimilate into. My gratitude goes out to Dr. Karen Chan, for the many exciting adventures spent in and out of the laboratory and Dr. Qiu Zhong, whose expertise in both food and facts led to many fulfilling and intellectual moments. Edward Yang provided the means to many great birthday dinners and bowling outings. And Dr. Paul Rider, who has shared the road I've taken from the very beginning, helped me realize that some things need not be taken so seriously. To Dr. Yong Bai and Dr. Hao Gong, two amazing scholars from China. And to the soul of Liu Lab, Dr. Gerry Abenes, whose kindness and generosity has never known any boundaries.

The credit for the completion of this journey will always be shared with the many amazing young minds that I've been fortunate to mentor directly. My thanks for the attainment of my degree goes to Cheryl Ma, Jody Shen, Tina Thai, Mari Fitzgibbons, Bin Lin, Daniel Lee, Katherine Sue, Katherine Ha, Kristina Dang, Theo Sottero, Samantha Ngaw, Victoria Chu, Tiffany Shih, Jing Gao, Shauna Trinh, Elaine Lee and Ben Lee. An amazing group of individuals that not only provided the man and womanpower to complete an extraordinary amount of work but also created an amazingly fun environment to work in. And no group of individuals would be complete without mentioning Dr. Patty Ku and Kevin Lin, who were both there at the beginning and whose hard work and delightful personalities set the bar by which all those who would follow would be held to. My thanks again for the fun times spent in both Barker and Warren. Always know that you will forever have a friend in me.

I would be remiss to forget my many friends outside of the Liu laboratory who helped steady me on the climb to the finish. Amazingly, bowling would be the answer to not only my boredom but also my quest for friendship. Thank you to Hiromi Chiyoda, John Kim, and more recently, Reiko Golobic, Terry "Bee" Woo, Wayne and Anna Yamaguchi, Tony Tam and all of the ridiculously amazing bowlers at Serra Bowl.

Each step towards a remarkable summit requires the vision to choose the right stone or rock to climb on and to that, I thank my friends from optometry, who proved that in order to

see straight, moments of double vision are often required. Thanks to Drs. Joycelyn Niimi, John Shan, Darren Ng, and Kuni Kanai and my fellow pseudo-optometrists, Yuri Kanai and Alice Vu who were always around to provide many good times and that occasional ride from the emergency room. But more importantly, reminded me that kindness and generosity needn't require any strings attached. I would however, have never met any of these fantastic friends without knowing Dr. Phong Vu, who has used his skill in perfecting vision long before obtaining his degree. Without his guidance and expertise in the field of life, I would surely have fallen from the path long before I reached the top.

In thanking my bowling friends, I left out one very important individual. He would also show me that kindness has no bounds, friendship has no strings, thoughtfulness should never be forgotten and the only limits that you truly have are the ones that you set on yourself. No summit metaphor would be complete or completed without mentioning Dr. Eric Yabu. After reaching many lofty heights with him in the past year, I'm happy to have shared this latest accomplishment with him. The last stretch to the top always seems to be the hardest and I would not have finished this and any of the other climbs without his encouragement and unwavering faith in my abilities, when even I had my doubts.

While many may say in a negative connotation that upon reaching a summit the only direction left to go is down, the truth for me is, there would be no climbs and no reason to climb without the possibility of returning to celebrate with the people who encouraged me to start it. My base camp will always be my family, who has never stopped encouraging me, never stopped believing in me and have never stopped helping me to achieve my goals. My thanks goes to Jimmy and Merle Yoshida, who may not be family by blood but will always be so in my heart. To my many wonderful uncles and aunties, but especially to Irene Umamoto, who gave me the strength of family in the mainland and to Brian, Karen, Chaz and Neal Umamoto who alone, make Hawaii a wonderful place to return to. I can't mention family without thanking Adrian Oliberos, who allowed an only child the remarkable experience of having a brother. And to my grandparents, who created the memories that I will always carry with me. Memories that allow me to bring Hawaii with me wherever I go. And finally, this journey would not be complete without the love and guidance that started it. I will forever be thankful to my parents, Gary and Amy Umamoto, who are my strong heart that refuses to let me quit no matter what obstacles I face.

I have been fortunate to be influenced on this journey by many amazing individuals and many more than I have the space to mention. And with the completion of all great summits, the next adventure is just around the corner. And I am forever grateful that I can bring with me each and every individual who have made me who I am.

## **Chapter 1**

### **Introduction**



## **Herpesviridae**

The family Herpesviridae contains over 130 different viruses across a wide range of species [1, 2]. The basic structure of all herpesviruses consists of an icosahedral capsid that contains linear double stranded DNA. The capsid is surrounded by an amorphous electron dense region called the tegument. And is enclosed by a lipid envelope of host origin that contains many glycolipids of viral origin.

The herpes family share several biological characteristics including a large amount of enzymes that are involved in nucleic acid metabolism, DNA synthesis and protein kinase activity. The synthesis of genetic material and the assembly of capsids occurs inside the nucleus where creation of viral progeny leads to the destruction of the host cell. And a key feature of herpesviruses are their ability to go latent in their hosts after primary infection with the potential to reactivate and resume lytic infection [2].

The herpesvirus family can be further classified into three groups that are based on DNA sequence homology, similarities in genome arrangement, and relatedness of several viral proteins important in infection. These subfamilies, deemed alpha-, beta- and gamma-herpesviruses, can also be characterized by their ability to infect and cause disease. The alpha-herpesviruses can be of variable host range, tend to have short infection cycles (~24 hours) and establish latent infection primarily in sensory ganglia neuronal cells. Beta-herpesviruses have a restricted host range, and can infect and establish latency in a variety of host cells. They generally have longer infection cycles (~72 hours) and infection will result in enlarged cells (cytomegaly). The final subfamily—gamma-herpesviruses, have a restricted host range and infect lymphocyte, epithelial and fibroblast cells. They generally go latent in T- and B-lymphocytes [2].

Of the over 100 herpesviruses, eight are members of the human herpesvirus family and consist of alpha-, beta- and gamma- sub family viruses. Of the alpha-herpesviruses, herpes simplex virus 1 and 2 (HSV-1, HHV-1 and HSV-2, HHV-2) are the causative agents of cold-sores and genital herpes and Varicella-zoster virus (VZV, HHV-3) causes chicken pox and the reactivation disease, shingles. The beta-herpesviruses include human cytomegalovirus (HCMV, HHV-5)—an opportunistic pathogen primarily involved in infection of immunocompromised patients, human herpesvirus 6 (HHV-6)—a T-cell trophic virus and human herpesvirus 7 (HHV-7)—which is also T-cell trophic and functions as a helper virus for HHV-6 [3]. The last two viruses, Epstein-Barr virus (EBV, HHV-4) and Kaposi's sarcoma virus (KSHV, HHV-8) are gamma-herpesviruses. EBV infection can result in mononucleosis or Burkitt's lymphoma and KSHV can cause cancer in immunocompromised states such as AIDS.

### **Human Cytomegalovirus Characteristics**

As mentioned previously, human cytomegalovirus (HCMV) is a member of the beta-herpesvirus subgroup. It is a species specific, ubiquitous pathogen that can infect a variety of cell types. In cell culture, HCMV is able to infect neuronal cells, muscle cells, connective tissue, endothelial cells, epithelial cells and leukocytes [4].

The structure of the virion shares the same basic characteristics of all herpesviruses. It is the largest of all human herpesviruses, consisting of an icosahedral capsid surrounding a 235

kb double stranded DNA genome that contains more than 140 genes [5]. The tegument which surrounds the nucleocapsid makes up approximately 40% of the mass of the virus and can contain viral and cellular RNA along with proteins that can be involved in viral structure, entry, egress and modulation of host defenses [5]. The surrounding envelope contains glycoproteins that may facilitate virus entry into a wide range of host cells that facilitate both permissive and non-permissive infection.

The overall structure of the HCMV virion has been found to contain 71 viral encoded proteins and over 70 host cellular proteins [6]. Of these 71 proteins, 5 make up the capsid, 14 are found in the tegument, 19 are glycoproteins, 12 are transcription-replication related and 9 remain uncharacterized.

Attachment of the viral particle can potentially occur via a number of viral glycoproteins. These glycoproteins may function in a cell type specific manner allowing CMV entry into the large range of host cells that can be infected. Of the glycoproteins found in the virion, strong evidence suggests a universal requirement involving glycoprotein B, a highly conserved core glycoprotein. gB binding of heparin sulfate is an important process that facilitates the initial entry event [5, 7]. The mode of viral entry can vary based on cell type, with direct fusion of the virus occurring in fibroblast cells and endocytic pathways occurring in cells such as epithelial and endothelial cells [8, 9].

Viral infection and replication occurs in three stages, taking around 48 to 72 hours to complete the release of viral particles. The genes involved in these three stages of viral replication are classified as alpha or immediate-early genes (IE), beta or early genes (E), and gamma or late genes (L). The immediate early genes expressed immediately upon entry into the host cell, serve to modulate host cell functions that can involve cellular or immune responses to viral infection. These virally encoded genes can suppress apoptotic responses, disrupt CTL surveillance, and serve to prime the cell for early gene expression and viral replication [5]. Early genes are expressed starting at 6 hours post infection (hpi), and continues to the point at which viral DNA replication begins, at around 24 hpi. The proteins expressed during this period are mainly involved in initiation of viral DNA replication or alteration of the host cell to help facilitate viral replication. However, they can include proteins that continue to control the host cell response to infection. The final class of genes, gamma or late genes, are expressed after viral DNA replication occurs. These genes are responsible for viral structure, DNA packaging, viral maturation and egress.

Viral DNA synthesis occurs within the nucleus of the infected cell and is initiated via the activation of a region found in the CMV genome called oriLyt [10]. This region activates transcription along with viral-encoded replication machinery, UL54 (DNA polymerase), UL44 (processivity factor), UL57 (single stranded binding protein) and a heterotrimeric helicase protein [5]. The linear viral DNA circularizes in the ND-10 region where it follows a rolling circle model of replication.

Viral packaging and maturation occurs in the nucleus where replicated DNA is packaged into capsids that have been assembled in the nuclear compartment. These capsids take on multiple forms both mature and immature—nucleocapsids and procapsids, respectively, as well as unpackaged, potentially defective forms. Packaged mature capsids egress through the nuclear membrane where it obtains its envelope and exits the cell via an exocytic pathway.

## **Human Cytomegalovirus Associated Disease**

HCMV is able to establish both persistent and latent infection and is highly species specific. Generally, HCMV infection rarely leads to CMV-mediated disease because the virus is primarily an opportunistic pathogen. In developing countries, anywhere from 90% to 100% of the population will have been infected with HCMV during childhood [11], while in developed countries only 40% to 80% of the population will be infected due to better hygiene [12]. Due to this decrease in exposure to HCMV during childhood, the incidence of first time mothers who have not been exposed to HCMV has increased, resulting in HCMV's rise as one of the leading causes of congenital disease in the developed countries such as the United States [12]. In utero infections can manifest in mental and behavioral disorders [13].

HCMV infection has also been attributed to various other diseases. It has been associated as a risk factor or potential agent for atherosclerosis [14, 15]. The ability for HCMV to infect a variety of cell types which line or are involved in blood vessel structure or maintenance such as endothelial cells, smooth muscle cells, leukocytes, macrophages and epithelial cells, provide support that HCMV infection could be related to an increased risk of heart disease [4, 5]. Other factors that could potentially be involved is the ability of the virus to upregulate cell adhesion molecules such as VCAM-1, ICAM-1 and E-selectin in infected smooth vascular endothelial cells in in vitro cell cultures and in biopsies taken from transplant patients [16-20]. There is also evidence in both murine cytomegalovirus (MCMV) animal models and HCMV cell cultures of an increased immune response, caused by upregulated chemokines, in infected areas, which could lead to damage to the lining of the blood vessels [21-23]. In addition to being able to upregulate cellular chemokines, HCMV encodes its own chemokine receptor homolog, US28, which is involved in cell migration and has the potential to promote angiogenesis and tumor formation [24, 25].

Another area of morbidity due to HCMV infection being realized is HCMV related diseases of the intestine. HCMV infection of the intestines during solid organ transplants has led to a variety of intestinal problems from hemorrhaging, colitis, and perforation to relapses of inflammatory bowel disease [26-29]. Cases of HCMV infection of the bowel have also been of major concern in both immunocompetent infants and neonates, with symptoms leading to intestinal blockage and bleeding [30, 31].

HCMV has been found to infect several tissue types from the gastrointestinal tract including smooth muscle cells, endothelial cells and epithelial cells [32]. Cytomegalovirus has also been shown to infect intestinal epithelial cells in vitro [33]. Infection in vitro has been observed from the basolateral surface of polarized Caco-2 cells to levels of  $10^3$  PFU, 28 days post infection [33-35]. In simian immunodeficiency virus (SIV) infected animals, CMV associated masses in the small intestines were found, highlighting the opportunistic nature of CMV to infect and cause disease in immunocompromised patients [36]. The importance of infection of intestinal epithelia of the small intestines may be in its ability to serve as a reservoir for persistent infection as seen in HIV-1 infection of gastrointestinal epithelial cells and mucosal cells [37-39].

## **Human Cytomegalovirus and AIDS**

HCMV is of great importance in acquired immunodeficiency syndrome (AIDS) where it can cause significant morbidity by leading to CMV retinitis, a leading cause of AIDS-related blindness, as well as other complications such as pneumonia and enteritis [40-42].

HCMV represents one of the most common opportunistic infections associated with AIDS patients. In HIV infected individuals, HCMV infection can lead to severe diseases such as CMV-associated pneumonia, gastrointestinal diseases, and CNS complications. Furthermore, HCMV is also among the most common causes of oral diseases associated with AIDS patients [43-45]. During primary infection, HCMV usually travels to the salivary glands after initial primary infection [43, 46]. Subsequently, the virus engages in a high level of replication in the serous acinar cells of the salivary glands. Salivary glands are a major source of persistent virus production and have also been shown to be a site for CMV latent infections [43, 46]. Extremely high levels of viral production in the salivary glands are a hallmark of CMV primary infections and reactivation from latent infections [43, 46].

## **Treatment**

As CMV is a prominent cause of infection in transplant and immunocompromised patients, there are treatments that are available that reduce the severity of disease. Common agents used in intestinal transplantation, solid organ transplants and other immunocompromised individuals are ganciclovir and valganciclovir—as first line treatments, and foscarnet or cidovir—as second line treatments, when life threatening CMV infections are resistant to ganciclovir (Eksborg 2003, Abete 2004). However, with an increasing incidence of resistance to these drugs, new targets for future therapeutics need to be identified.

## **Murine Cytomegalovirus**

Strict species specificity has prevented the study of HCMV in any animal model. Thus there is currently no animal model suitable for HCMV infections. And it is impossible to study the function of viral genes in HCMV pathogenesis in the human host. Consequently, little is known about the mechanism of HCMV pathogenesis, and related viruses, such as murine CMV (MCMV) must be used to provide insight into the tissue tropism, virulence, and latency of HCMV. Murine cytomegalovirus (MCMV) provides an excellent model to study the biology of CMV infection. MCMV offers several advantages including rapid viral growth, the availability of a reliable animal model, and sequence homology to HCMV [43, 46-48]. Moreover, infection of mice by MCMV resembles in many ways its human counterpart with respect to pathogenesis during acute infection, establishment of latency, and reactivation after immunosuppression, transfusion, or transplantation [43, 46-48]. The MCMV genome of 230 kb is predicted to encode more than 170 open reading frames (ORF), 78 of which have extensive homology to those of HCMV [49-52]. However, many of these MCMV genes have not been characterized and their functions in viral pathogenesis have not been investigated.

MCMV infection in salivary gland and the oral cavity shares many characteristics with HCMV. Like HCMV, MCMV travels to the salivary glands after initial primary infection. Subsequently, the viruses engage in a high level of replication in the acinar cells of the salivary glands and the resulting viruses are then shed via saliva [47, 48]. Persistent and latent MCMV

infections have been found in the salivary glands and are believed to be one of the major sources for oral infections as well as horizontal transmission. However, little is known about the mechanism of how MCMV establishes infection in the salivary glands and equally elusive is the nature of the viral genes responsible for infection in the organ.

### **Yeast Two-Hybrid**

Yeast two-hybrid has been applied to large-scale analyses of interactomes of multiple organisms. Because of the relatively large size of complex organisms, the importance of individual proteins in relation to these systems may be difficult to ascertain if investigated individually. Therefore, these large-scale analyses that are used to form global interactomes can be of great importance in determining the significance of individual proteins by analyzing their relation to other proteins in the organism. Organisms that have been studied using YTH include humans, *Drosophila melanogaster*, *Caenorhabditis elegans*, *Saccharomyces cerevisiae*, *Plasmodium falciparum* and *Helicobacter pylori* [53-57]. Viral interactions have also been studied in this fashion. Viral global genetic YTH studies have been conducted in vaccinia virus, three herpesviruses and Hepatitis C virus [58-62]. In respect to herpesviruses, YTH analysis have been conducted in Kaposi's sarcoma (KSHV) and Varicella Zoster (VZV). This method was used to discover 123 interactions in KSHV and 173 in VZV, in genomes predicting 89 ORFs and 69 ORFs, respectively [61].

## References

1. Roizman, B., *Herpesviridae*, in *Fields Virology*, B.N. Fields, D.M. Knipe, and P.M. Howley, Editors. 1996, Lippincott - Raven Press: New York. p. pp. 2221-2230.
2. Roizman, B.N. and P.E. Pellet, *The Family Herpesviridae: A Brief Introduction*, in *Fields Virology*, B.N. Fields, et al., Editors. 2001, Lippincott Williams and Wilkins: Philadelphia. p. 2 v. (xix, 3087 p.).
3. Frenkel, N. and E. Roffman, *Human Herpesvirus 7*, in *Fields Virology*, B.N. Fields, D.M. Knipe, and P.M. Howley, Editors. 1996, New York.
4. Gerna, G., F. Baldanti, and M.G. Revello, *Pathogenesis of human cytomegalovirus infection and cellular targets*. *Hum Immunol*, 2004. **65**(5): p. 381-6.
5. Mocarski, E., T. Shenk, and R. Pass, *Cytomegalovirus*, in *Fields Virology*, B.N. Fields, D.M. Knipe, and P.M. Howley, Editors. 2007, Wolters Kluwer Health/Lippincott Williams & Wilkins.
6. Varnum, S.M., et al., *Identification of proteins in human cytomegalovirus (HCMV) particles: the HCMV proteome*. *J Virol*, 2004. **78**(20): p. 10960-6.
7. Compton, T., D.M. Nowlin, and N.R. Cooper, *Initiation of human cytomegalovirus infection requires initial interaction with cell surface heparan sulfate*. *Virology*, 1993. **193**(2): p. 834-41.
8. Jarvis, M.A. and J.A. Nelson, *Human cytomegalovirus tropism for endothelial cells: not all endothelial cells are created equal*. *J Virol*, 2007. **81**(5): p. 2095-101.
9. Ryckman, B.J., et al., *Human cytomegalovirus entry into epithelial and endothelial cells depends on genes UL128 to UL150 and occurs by endocytosis and low-pH fusion*. *J Virol*, 2006. **80**(2): p. 710-22.
10. Anders, D.G., et al., *Boundaries and structure of human cytomegalovirus oriLyt, a complex origin for lytic-phase DNA replication*. *J Virol*, 1992. **66**(6): p. 3373-84.
11. Fields, B.N., D.M. Knipe, and P.M. Howley, *Fields virology*. 3rd ed. 1996, New York: Lippincott - Raven Press. 2 v. (xxi, 2950) p.
12. Fields, B.N., et al., *Field's Virology*. 4th ed. Field's Virology. 2001, Philadelphia: Lippincott Williams & Wilkins. 2 v. (xix, 3087 p.).
13. Fields, B.N., D.M. Knipe, and P.M. Howley, *Fields' virology*. 5th ed ed. 2007, Philadelphia: Wolters Kluwer Health/Lippincott Williams & Wilkins. 2 v. (xix, 3091, 86 p.).
14. Sorlie, P.D., et al., *A prospective study of cytomegalovirus, herpes simplex virus 1, and coronary heart disease: the atherosclerosis risk in communities (ARIC) study*. *Arch Intern Med*, 2000. **160**(13): p. 2027-32.
15. Nieto, F.J., et al., *Cohort study of cytomegalovirus infection as a risk factor for carotid intimal-medial thickening, a measure of subclinical atherosclerosis*. *Circulation*, 1996. **94**(5): p. 922-7.
16. Allen, M.D., et al., *VCAM-1 and E-selectin expression during cytomegalovirus infection in post-transplant myocardial biopsies*. *Clin Transplant*, 1996. **10**(6 Pt 1): p. 528-37.
17. Shahgaspour, S., S.B. Woodroffe, and H.M. Garnett, *Alterations in the expression of ELAM-1, ICAM-1 and VCAM-1 after in vitro infection of endothelial cells with a clinical isolate of human cytomegalovirus*. *Microbiol Immunol*, 1997. **41**(2): p. 121-9.

18. Shahgasempour, S., et al., *Alteration in the expression of endothelial cell integrin receptors alpha 5 beta 1 and alpha 2 beta 1 and alpha 6 beta 1 after in vitro infection with a clinical isolate of human cytomegalovirus*. Arch Virol, 1997. **142**(1): p. 125-38.
19. Sedmak, D.D., et al., *Divergent patterns of ELAM-1, ICAM-1, and VCAM-1 expression on cytomegalovirus-infected endothelial cells*. Transplantation, 1994. **58**(12): p. 1379-85.
20. Koskinen, P.K., et al., *Vascular cell adhesion molecule-1 (VCAM-1) is induced during cytomegalovirus infection in vascular structures of heart allografts*. Transpl Int, 1994. **7 Suppl 1**: p. S363-4.
21. MacDonald, M.R., X.Y. Li, and H.W.t. Virgin, *Late expression of a beta chemokine homolog by murine cytomegalovirus*. J Virol, 1997. **71**(2): p. 1671-8.
22. Penfold, M.E., et al., *Cytomegalovirus encodes a potent alpha chemokine*. Proc Natl Acad Sci U S A, 1999. **96**(17): p. 9839-44.
23. Saederup, N., et al., *Cytomegalovirus-encoded beta chemokine promotes monocyte-associated viremia in the host*. Proc Natl Acad Sci U S A, 1999. **96**(19): p. 10881-6.
24. Stropes, M.P. and W.E. Miller, *Functional analysis of human cytomegalovirus pUS28 mutants in infected cells*. J Gen Virol, 2008. **89**(Pt 1): p. 97-105.
25. Maussang, D., et al., *Human cytomegalovirus-encoded chemokine receptor US28 promotes tumorigenesis*. Proc Natl Acad Sci U S A, 2006. **103**(35): p. 13068-73.
26. Choi, S.W., et al., *Lower gastrointestinal bleeding due to cytomegalovirus ileal ulcers in an immunocompetent man*. Yonsei Med J, 2001. **42**(1): p. 147-51.
27. Jang, H.J., et al., *Cytomegalovirus infection of the graft duodenum and urinary bladder after simultaneous pancreas-kidney transplantation*. Transplant Proc, 2004. **36**(7): p. 2200-2.
28. Takahashi, Y. and T. Tange, *Prevalence of cytomegalovirus infection in inflammatory bowel disease patients*. Dis Colon Rectum, 2004. **47**(5): p. 722-6.
29. Siegal, D.S., N. Hamid, and B.A. Cunha, *Cytomegalovirus colitis mimicking ischemic colitis in an immunocompetent host*. Heart Lung, 2005. **34**(4): p. 291-4.
30. Bonnard, A., et al., *Cytomegalovirus infection as a possible underlying factor in neonatal surgical conditions*. J Pediatr Surg, 2006. **41**(11): p. 1826-9.
31. Hinds, R., et al., *Another cause of bloody diarrhoea in infancy: cytomegalovirus colitis in an immunocompetent child*. J Paediatr Child Health, 2004. **40**(9-10): p. 581-2.
32. Sinzger, C., et al., *Fibroblasts, epithelial cells, endothelial cells and smooth muscle cells are major targets of human cytomegalovirus infection in lung and gastrointestinal tissues*. J Gen Virol, 1995. **76 ( Pt 4)**: p. 741-50.
33. Esclatine, A., et al., *Human cytomegalovirus infects Caco-2 intestinal epithelial cells basolaterally regardless of the differentiation state*. J Virol, 2000. **74**(1): p. 513-7.
34. Jarvis, M.A., et al., *Human cytomegalovirus infection of caco-2 cells occurs at the basolateral membrane and is differentiation state dependent*. J Virol, 1999. **73**(6): p. 4552-60.
35. Esclatine, A., et al., *Differentiation-dependent redistribution of heparan sulfate in epithelial intestinal Caco-2 cells leads to basolateral entry of cytomegalovirus*. Virology, 2001. **289**(1): p. 23-33.

36. Hutto, E.H., D.C. Anderson, and K.G. Mansfield, *Cytomegalovirus-associated discrete gastrointestinal masses in macaques infected with the simian immunodeficiency virus*. *Vet Pathol*, 2004. **41**(6): p. 691-5.
37. Smith, P.D., et al., *Macrophage HIV-1 infection and the gastrointestinal tract reservoir*. *J Leukoc Biol*, 2003. **74**(5): p. 642-9.
38. Moyer, M.P. and H.E. Gendelman, *HIV replication and persistence in human gastrointestinal cells cultured in vitro*. *J Leukoc Biol*, 1991. **49**(5): p. 499-504.
39. Moyer, M.P., et al., *Infection of human gastrointestinal cells by HIV-1*. *AIDS Res Hum Retroviruses*, 1990. **6**(12): p. 1409-15.
40. Moorman, A.C., et al., *Changing conditions and treatments in a dynamic cohort of ambulatory HIV patients: the HIV outpatient study (HOPS)*. *Ann Epidemiol*, 1999. **9**(6): p. 349-57.
41. Sissons, J.G. and A.J. Carmichael, *Clinical aspects and management of cytomegalovirus infection*. *J Infect*, 2002. **44**(2): p. 78-83.
42. Jabs, D.A., C. Enger, and J.G. Bartlett, *Cytomegalovirus retinitis and acquired immunodeficiency syndrome*. *Arch Ophthalmol*, 1989. **107**(1): p. 75-80.
43. Pass, R.F., *Cytomegalovirus*, in *Fields Virology*, D.M. Knipe and P.M. Howley, Editors. 2001, Lippincott-William & Wilkins: Philadelphia, Pa. p. 2675-2706.
44. Itin, P.H. and S. Lautenschlager, *Viral lesions of the mouth in HIV-infected patients*. *Dermatology*, 1997. **194**(1): p. 1-7.
45. Greenberg, M.S., *HIV-associated lesions*. *Dermatol Clin*, 1996. **14**(2): p. 319-26.
46. Mocarski, E.S. and C.T. Courcelle, *Cytomegalovirus and their replication*, in *Fields Virology*, D.M. Knipe and P.M. Howley, Editors. 2001, Lippincott-William & Wilkins: Philadelphia, Pa. p. 2629-2673.
47. Hudson, J.B., *The murine cytomegalovirus as a model for the study of viral pathogenesis and persistent infections*. *Arch Virol*, 1979. **62**(1): p. 1-29.
48. Jordan, M.C., *Latent infection and the elusive cytomegalovirus*. *Rev Infect Dis*, 1983. **5**(2): p. 205-15.
49. Rawlinson, W.D., H.E. Farrell, and B.G. Barrell, *Analysis of the complete DNA sequence of murine cytomegalovirus*. *J Virol*, 1996. **70**(12): p. 8833-49.
50. Murphy, E., et al., *Coding potential of laboratory and clinical strains of human cytomegalovirus*. *Proc Natl Acad Sci U S A*, 2003. **100**(25): p. 14976-81.
51. Davison, A.J., et al., *The human cytomegalovirus genome revisited: comparison with the chimpanzee cytomegalovirus genome*. *J Gen Virol*, 2003. **84**(Pt 1): p. 17-28.
52. Chee, M.S., et al., *Analysis of the protein-coding content of the sequence of human cytomegalovirus strain AD169*. *Curr Top Microbiol Immunol*, 1990. **154**: p. 125-69.
53. Giot, L., et al., *A protein interaction map of Drosophila melanogaster*. *Science*, 2003. **302**(5651): p. 1727-36.
54. Ito, T., et al., *A comprehensive two-hybrid analysis to explore the yeast protein interactome*. *Proc Natl Acad Sci U S A*, 2001. **98**(8): p. 4569-74.
55. LaCount, D.J., et al., *A protein interaction network of the malaria parasite Plasmodium falciparum*. *Nature*, 2005. **438**(7064): p. 103-7.
56. Li, S., et al., *A map of the interactome network of the metazoan C. elegans*. *Science*, 2004. **303**(5657): p. 540-3.



57. Rain, J.C., et al., *The protein-protein interaction map of Helicobacter pylori*. Nature, 2001. **409**(6817): p. 211-5.
58. McCraith, S., et al., *Genome-wide analysis of vaccinia virus protein-protein interactions*. Proc Natl Acad Sci U S A, 2000. **97**(9): p. 4879-84.
59. Calderwood, M.A., et al., *Epstein-Barr virus and virus human protein interaction maps*. Proc Natl Acad Sci U S A, 2007. **104**(18): p. 7606-11.
60. Rozen, R., et al., *Virion-wide protein interactions of Kaposi's sarcoma-associated herpesvirus*. J Virol, 2008. **82**(10): p. 4742-50.
61. Uetz, P., et al., *Herpesviral protein networks and their interaction with the human proteome*. Science, 2006. **311**(5758): p. 239-42.
62. de Chassey, B., et al., *Hepatitis C virus infection protein network*. Mol Syst Biol, 2008. **4**: p. 230.

## **Chapter 2**

### **MCMV Virion**

## Introduction

Human cytomegalovirus (HCMV), a beta-herpesvirus, is an important opportunistic pathogen that primarily affects individuals with compromised or immature immune systems [1]. It is of great importance in AIDS patients where it can cause significant morbidity through retinitis-associated blindness, and other complications, such as pneumonia and enteritis [2-4]. In developed nations, it is a leading viral cause of congenital disease, where in-utero infection manifests in mental and behavioral disorders [1]. In order to control infection and HCMV associated disease, new compounds and novel strategies must be developed. Understanding the role viral proteins play in the formation and maturation of the virion will help elucidate the mechanisms of HCMV pathogenesis, providing important information on potential targets for new treatments.

However, the strict species specificity of HCMV prevents any studies into the pathogenesis of the virus in an animal host. This limitation can be overcome through the use of murine cytomegalovirus (MCMV). MCMV, like HCMV, is a betaherpesvirus that exhibits similar pathogenesis in mice to HCMV infection in the human host [5]. The genetic structure of MCMV contains significant sequence homology to HCMV AD169 in at least 78 ORFs and can thereby be used as an important tool in elucidating the functions of these ORFs in a complete *in vivo* system [6]. Due to these similarities, MCMV provides a good model to study infection with regards to host genetics, latency and the immune system [7, 8].

Because of the important role of MCMV as a tool for helping to determine the effects of HCMV infection in a human host, understanding the structure of the virion and its interactions can provide important information in understanding how CMV infects and causes disease. MCMV, like HCMV, is one of the largest herpesviruses, containing a ~230 kb genome which encodes for roughly 170 ORFs [6, 9]. There are potentially, 57 proteins that have been found to be associated with the MCMV virion [10]. These proteins compose the icosahedral capsid, which surround the genome and associated proteins and an outer layer of proteins comprising what is called the tegument, all of which, is enclosed by a viral envelope derived from a cellular lipid bilayer containing viral glycoproteins.

Determining how MCMV virion proteins interact can be useful in helping not only elucidate viral pathogenesis in mouse infection, but due to the high degree of homology to the HCMV virion, can also provide important clues to the function of these proteins in human infection. To determine MCMV virion protein interactions we take advantage of the yeast two-hybrid assay (YTH). This method uses transcription activation (AD) and DNA-binding domains (BD) of the GAL4 transcription factor, which can be separated into two components [11]. To study potential one to one interactions between proteins, genes can be cloned into AD or BD expression vectors resulting in either AD or BD-fusion proteins when expressed in haploid yeast cells. When the yeasts are mated these fusion proteins are allowed to interact and can bind to form a functional GAL4 transcription factor that activates transcription that is detectable by nutrient selection.

YTH has been applied to large-scale analyses of interactomes of multiple organisms. Because of the relatively large size of complex organisms, the importance of individual proteins in relation to these systems may be difficult to ascertain. Therefore, these large-scale analyses that are used to form global interactomes can be of great importance in determining the

significance of individual proteins. Organisms studied using YTH include humans, *Drosophila melanogaster*, *Caenorhabditis elegans*, *Saccharomyces cerevisiae*, *Plasmodium falciparum* and *Helicobacter pylori* [12-16]. Viral interactions have also been studied in this fashion. To date, viral global genetic YTH studies have been conducted in vaccinia virus, three herpesviruses and more recently, Hepatitis C virus [17-21]. The usefulness of this method can be seen through studies with Kaposi's sarcoma (KSHV) and Varicella Zoster (VZV), where yeast two-hybrid analyses were used to discover 123 interactions in KSHV and 173 in VZV, in genomes predicting 89 ORFs and 69 ORFs, respectively [20].

In our study, we have conducted a comprehensive YTH screen to identify potential interactions between 57 MCMV ORFs that are found to be associated with the virion. We have identified 15 potential interactions involving the capsid, tegument and associated proteins of known and unknown functions. To our knowledge, 12 of these interactions have not been previously identified. Our studies have observed the presence of "hub" proteins, which interact with multiple partners. These hub proteins may be involved as organizing centers for connecting or recruiting viral proteins to the mature virion. It is also possible that these hubs may be involved in viral entry or egress, helping to traffic the virion through the cell. The interactions that we have identified in this study also provide a framework to predict functions of uncharacterized virion proteins. Together with known viral proteins, the elucidation of the MCMV viral interactome allows for the better understanding of how these components contribute to virion formation and maturation and provide information that can be used to discover their importance by providing a direction for the study of pathogenesis through animal studies.

## **Materials and Methods**

### **Construction of plasmids**

MCMV Smith and pSM3fr, a MCMV Smith<sub>BAC</sub> construct, were used for all PCR amplification of full-length virion ORFs. Primers to virion ORFs (Table 1) were designed for cloning into the pGBK-T7 bait and pGAD-T7 prey plasmids for yeast expression and further subcloning in pCMV-myc and pCMV-HA mammalian expression plasmids (Clontech). Each primer sequence contains an outer and inner restriction enzyme site for cloning in the multiple cloning site (MCS) of the yeast and mammalian expression plasmids, respectively (Table 1). PCR amplification was through the use of iProof High-fidelity DNA polymerase (Bio-Rad). The resulting constructs were confirmed by restriction digest profile and sequencing. A total of fifty-seven MCMV-encoded virion ORFs were cloned into each of the pGBK-T7 and pGAD-T7 vectors.

### **Yeast two-hybrid screen**

The one hundred fourteen viral ORFs that were cloned into both pGBK-T7 and pGAD-T7 vectors were transformed into AH109 (MAT<sub>a</sub>) and Y187 (MAT<sub>α</sub>) yeast strains, respectively (Matchmaker 3 System, Clontech). AH109 strains harboring pGBK-T7 plasmids were maintained in minimal SD media with tryptophan dropout supplement (SD/-Trp) while Y187 strains harboring pGAD-T7 plasmids were maintained in minimal SD media with leucine dropout supplement (SD/ -Leu).

Prior to performing the matings, all pGBK-T7-fusion proteins in AH109 strains were tested for autoactivation. Individual AH109 strains were plated on SD/ -Ade/ -His/ -Trp agar with 40 µg/mL X-α-Gal. Four AH109 strains containing pGBK-T7 ORFs (M82, m18, M87, and M95) were determined to be autoactivators in the absence of any pGAD-T7 cloned ORFs, and subsequently eliminated from further matings.

Yeast mating was carried out by inoculating fresh colonies (<2 weeks old) of both AH109 and Y187 strains into 1.5 mL microcentrifuge tubes containing 0.5 mL of YPDA media and incubated at 30°C with shaking at 200 rpm for 24 hours. There were a total of 3021 possible combinations (53 AH109 x 57 Y187) and each mating combination was performed in duplicate. To select for diploids that have successfully mated, mated yeast were pelleted at 14,000 rpm for 15 seconds. Each pellet was resuspended in 0.5 mL Tris-EDTA buffer and 10 µL of each was plated in one well of 48-well plates containing 1 mL of SD/-Leu/ -Trp agar and incubated at 30°C for 3-5 days. Diploid colonies from each successful mating was then picked from each well and resuspended with 100 µL of TE buffer in a 1.5 mL microcentrifuge tube and 10 µL was plated in one well of 48-well plates containing 1 mL of SD/ -Ade/ -His/ -Leu/ -Trp (quadruple drop-out (QDO)) agar with 40 µg/ mL of X-α-Gal.

Mating controls used was via the comparison of combinations of transformed AH109 and Y187 strains together and individually in 0.5 mL of YPDA, that were shaken overnight at 200 rpm. These mating cultures were plated onto SD/ -Leu/ -Trp plates. Only diploid yeasts from the mating of AH109 and Y187 yeast were able to grow on the SD/ -Leu/ -Trp plates while individual AH109 and Y187 yeast were unable to grow.

Three weeks after plating the mated diploid yeasts, QDO plates were scored for positive protein-protein interactions. QDO/ X-α-Gal plates were used as a high stringency screen for eliminating possible false positives. AH109 strains contained three reporters—ADE2, HIS3, and MEL1 (encodes α-galactosidase)—under the control of unique GAL4 upstream activating sequences (UAS) and TATA boxes. The positive control used was AH109 yeast transformed with BD-p53 fusion protein mated with Y187 yeast transformed with AD-T (SV40 T-antigen), while the negative control was transformation of AH109 with BD-Lamin C with and Y187 with AD-T.

When scoring the duplicate matings, wells containing the MCMV ORF fusion proteins that showed no yeast growth after three weeks were considered to be non-interacting partners. Duplicate wells containing blue yeast colonies in both wells or in one well were chosen for repeated screening to confirm that positive interaction exists. Confirmation of a positive interaction was through consistent results from at least two of three independent experiments.

## Results

### **Cloning of MCMV open reading frames coding for virion proteins and construction of plasmids for yeast two-hybrid screen**

Cloned MCMV open reading frames were determined by using MCMV sequence analysis as determined by Rawlinson et al. 1996 and annotated sequences determined by Brocchieri et al. 2005 [6, 9].

The protein composition of MCMV virions was determined by using proteomic analysis of MCMV infectious particles by Kattenhorn et al. 2004 including, M78, which is reported as

having an association with the tegument but not found in their study [10, 22]. In this study, we have cloned and expressed, in the yeast two-hybrid system, fifty-seven proteins associated with the MCMV virion. The proteins cloned and expressed include the four capsid proteins (M46, m48.2, M85 and M86), fifteen tegument proteins (M25, M32, M35, M47, M48, M51, M69, M72, M78, M82, M83, M94, M97, M99, and M104), five glycoproteins (m02, M55, M74, M75 and M100), six proteins involved in replication (M44, M54, M57, M70, M102, and M105), two immunomodulatory proteins (M43, and M45), and twenty-five additional proteins (M56, M77, M80, M98, m18, m20, m25.2, M28, M31, m39, M71, M87, M88, m90, m107, M116, m117.1, m121, m147, m150, m151, m163, m165, and m166.5).

For each ORF, we designed an optimal PCR primer pair. The primer pairs were designed as follows: The forward primer (from 5' to 3') contains the sequence immediately after the predicted translation initiation codon AUG and 20-25 additional nucleotides of the coding sequence. The reverse primer contains the reverse complement of both the predicted translation termination codon and the preceding 20-25 nucleotides at the end of the ORF (Table 1). In addition, the primers also contain 15-20 nucleotide common sequences that contain sites for restriction enzymes for cloning of the PCR products into the yeast two-hybrid screening vectors (pGADT7 and pGBKT7) and the mammalian expression vectors (pCMV-HA and pCMV-myc)(Table 1).

Each ORF encoding MCMV virion proteins were amplified individually by PCR with a specific set of primers. The amplified PCR products cover the entire ORF sequence minus the initiation codon and were cloned into yeast two-hybrid "prey" pGADT7 and "bait" pGBKT7 vectors, respectively, resulting in the generation of one hundred fourteen constructs. The viral ORF sequences in each of these constructs were confirmed using DNA sequencing analysis.

### **Identification of potential interactions among MCMV-encoded virion proteins using yeast two-hybrid screen**

The strategy employed used pair-wise combinations of MCMV-encoded virion proteins to test interactions in the yeast two-hybrid assay using a 48-well protein array format. The array consisted of a set of yeast transformants, each expressing one MCMV virion ORF, as a hybrid protein containing a GAL4 DNA binding domain. The yeast construct contained in each well of this array was mated to a set of yeast transformants, of the opposite mating type, which carried one of the MCMV ORFs, as a hybrid protein with containing a GAL4 activation domain. The resulting diploids were cultured on medium selective for the two-hybrid reporter genes. Using this approach a single protein could be tested for interaction against every one of the cloned MCMV virion protein constructs. By generating different sets of activation and DNA binding domain constructs we were able to assay more than 3000 combinations representing potential interacting pairs between MCMV virion proteins.

In order to generate yeast transformants for the two-hybrid screen, plasmid DNA from each of the fifty-seven generated "bait" pGBKT7-derived constructs were isolated from *E. coli* and transformed into the AH109 yeast strain resulting in a collection of transformants expressing a set of DNA-binding domain MCMV hybrid proteins. Similarly, plasmid DNA from each of the generated "prey" pGADT7-derived constructs were isolated and transformed into the yeast strain, Y187, in order to create transformants expressing a set of fifty-seven DNA activation domain MCMV hybrid proteins. Analysis of the recovered plasmid DNAs from these

yeast transformants indicated that the constructs were present and exhibited similar restriction profiles as those in *E. coli*.

Prior to performing the matings, all fifty-seven pGBKT7-fusion proteins in AH109 strains were tested for autoactivation. Four AH109 strains, which contained ORFs M82, m18, M87 and M95, were determined to be autoactivators in the absence of any pGADT7-cloned ORF (Table 2), and subsequently eliminated from any further matings. Each of the rest of the fifty-three AH109 constructed strains were mated, in duplicate, with each of the fifty-seven Y187 constructed stains, and the resulting diploid cells were plated in duplicate on selective medium. In addition to selecting for the presence of the two plasmids based on leucine and tryptophan selection, we used a high stringency screening method, selecting for positive protein interactions using three more reporter genes to eliminate potential false positives: histidine, adenine, and Mel1, which encodes alpha-galactosidase for blue/white screening of yeast colonies. The growth of colonies of diploid yeast cells with blue staining within three weeks after plating were scored as a positive pair-wise interaction between the two proteins tested. While all other results (e.g. no growth of yeast colonies) were scored as a negative interaction (Table 2, Figure 1).

Two-hybrid screens may generate a significant number of false positives that represent the random generation histidine-positive colonies. This is possibly due to rearrangement and deletion of the DNA-binding domain plasmid, recombinational events between the DNA-binding and activation domain plasmids, or genomic rearrangement of the host strain. To exclude these possibilities, three sets of experiments were carried out. First, plasmid DNA constructs from the yeast transformants were recovered and analyzed. Our results indicated that these constructs were present in all transformants analyzed and exhibited similar restriction enzyme profiles as those in *E. coli*. Second, all screens were carried out in duplicate to determine whether the results were reproducible. Lastly, any protein that resulted in histidine positive growth with any of the four controls (the yeast protein Mec3, human lamin, and the empty vectors, pGADT7 and pGBKT7) was classified as a false positive and removed from the set of positive interactions.

After screening more than 3000 mating combinations between the fifty-three MCMV GAL4 DNA-binding domain fusion proteins with the fifty-seven MCMV GAL4-activating domain fusion proteins we revealed fifteen positive interactions between thirteen virion proteins (Table 3, Figure 2). Of the thirteen, interacting virion proteins consisted of two capsid proteins (M46 and M85), eight tegument proteins (M32, M35, M72, M82, M88, M94, M97, M99), and three proteins of unknown localization: one protein of known function (M98) and two of unknown function (M28, m107). One of these proteins, M28, was found to be self-interacting, suggesting that this protein may form dimers or possibly, self-assemble into polymers.

All interactions were detected in one direction, either AD to BD interaction or BD to AD interaction but not both. This can be a common phenomenon in two-hybrid assays and can be attributed to steric hindrance of either the bait or prey fusion proteins [18, 20]. Among the fourteen interactions, five were found to be involved with M35, four with M72 and M94, three with M88, and two with M99 and m107 (Table 3, Figure 2). These results suggest that these proteins may function as a hub or organizing center for viral proteins in the mature virion or for recruiting other viral proteins during virion maturation and assembly. M35 and M72, tegument proteins, were found to interact with a capsid protein, M46. As M35, was found to be involved

with many of the tegument associated proteins, this may suggest an important role for M35 in formation of the tegument around the capsid.

## Discussion

Yeast two-hybrid analyses have been used to determine the interactomes of a variety of different organisms such as humans, *Drosophila melanogaster*, *Caenorhabditis elegans*, *Saccharomyces cerevisiae*, *Plasmodium falciparum* and *Helicobacter pylori* [12-16]. Studies using the yeast two-hybrid assay have also encompassed potential interactions between virally expressed proteins both through global analysis of protein expression and through studies of the proteins comprising the virion. These studies have been conducted on vaccinia virus, three herpesviruses and more recently, Hepatitis C virus [17-21]. The data generated through the formation of the interactomes mentioned represent a powerful amount of information that forms important building blocks for the beginnings of additional studies needed to determine the biological significance of these interactions and the role each protein plays in the survival of the organism. This makes yeast two-hybrid an important tool in system-level studies [23]. In this study, we have used the yeast two-hybrid system to study potential interactions among MCMV-encoded virion proteins. Our results have identified 15 potential interactions between various ORFs located in different components of the virion.

Before mentioning our results, it is important to understand that yeast two-hybrid screens have been found to generate a number of false positives [11]. One potential source is through the random generation of histidine-positive colonies. This can be due to rearrangement and deletion of the DNA-binding domain plasmid, recombinational events between the DNA-binding and activation domain plasmids, or genomic rearrangement of the host strain. Another type of false positive is due to the non-specific activation of different reporter systems. And the third type is due to autoactivation, which is caused by activators of transcription caused by binding only domain fusion proteins. False negatives may also arise from the YTH screens. This is due to the potential for systems that test for protein interactions in the nucleus to lead to erroneous results because of the expression of proteins that are normally not found in the nucleus. This system may also miss interactions involving proteins with significant hydrophobic domains such as membrane proteins that prevent proper folding or transport to the nucleus.

To exclude these possibilities, five different sets of experiments have been carried out. First, plasmid DNA from the yeast transformants was recovered and analyzed. Our results indicated that these constructs were present in all transformants examined and each exhibited similar restriction enzyme profiles as those in *E. coli*, suggesting that there is no significant change or rearrangement of the sequence of the transformants during the screening process. Second, all screens were carried out in duplicate to determine whether the results were reproducible. Third, we used the highest stringency protocol in our system by utilizing 4 different reporters to ensure the validity of the data. Any protein that resulted in histidine-positive growth with any of the four controls (the yeast protein Mec3, human lamin, and the empty vectors pGADT7 and pGBKT7) was classified as a false positive and removed from the set of positive interactions. Fourth, prior to any matings in our experiments, all of the binding



domain-fusion proteins have been tested for autoactivation and positive fusion proteins from this screen were removed from further study.

To the best of our knowledge, 12 of the 15 interactions that we have identified in our yeast two-hybrid screens have not been previously reported. While, three of these interactions have been found in HCMV or other herpesvirus homologs (Table 3)[24-28]. The interactions that we have found can be classified into four categories based on the locations and known functions of the viral proteins in association with the construction of the virion.

(A) Interactions of viral capsid proteins. Extensive studies between capsid proteins have been carried out in HCMV [24, 29]. In MCMV, the capsid is comprised of four different proteins, M46, m48.2, M85 and M86. Of these four capsid proteins, we have found interactions between the minor capsid proteins, M46 and M85 [10]. This is similar to interactions previously reported in both HSV1 and HCMV homologs [24, 25].

(B) Interactions between viral capsid and tegument proteins. The cytomegalovirus tegument is a generally unstructured region of proteins surrounding the capsid that has potential roles in the formation of the virion, egress of the viral particle, immune evasion and entry during initial infection [30]. During maturation of the virion, some of the components of the tegument have been shown to assume an icosahedrally ordered structure around precursor capsids [31]. And further analysis through cryoelectron microscopy of the capsid shows potential anchoring sites for tegument proteins [32]. This evidence suggests that these proteins may have a role in serving as a hub or center for further assembly of additional tegument components, as these same studies show that there are distinct densities of tegument proteins extending from the initial icosahedrally ordered layer [31]. While the exact identities of these interacting proteins have yet to be determined, in HCMV, the amino terminus of UL32 was found to interact with intranuclear B and C capsids [33]. However, the investigators state that this interaction seems to depend on preformed capsids and cannot be detected through yeast two-hybrid screens. This observation seems to hold true for the MCMV homolog M32, as we have been unable to detect interaction with any individual capsid components.

Our results have discovered two potential interactions between tegument proteins and the nucleocapsid. M46, the minor capsid protein, interacts with M35 and M72. M35 and UL35 have been shown to be essential through gene deletion studies [34, 35]. The HCMV homolog UL35 is expressed late and localizes to the nucleus [36]. Suggesting that M35 may have a role in the maturation of the virus. M72 encodes a viral dUTPase—also found in other herpesvirus, poxvirus and HIV1—that is thought to facilitate replication in differentiated cells [37]. The M72 homolog, UL72, exhibits late gene expression and accumulates in the cytoplasm, however is non-essential in fibroblast cells [38]. While it is possible that M72's incorporation into the virion may occur due to its proximity at the site of virion maturation, its interaction with the minor capsid protein as well as other tegument proteins, to be discussed, may suggest that its recruitment may be important in the assembly process or that it may be needed to facilitate the initial stages of viral infection.

(C) Interactions between tegument proteins. Interactions between tegument proteins may be important in recruitment of other tegument proteins to the precursor virion for roles in the assembly and maturation process but they also may represent important steps in entry and

replication of the infecting viral particle [39]. We have observed eight interactions between tegument proteins in our study.

In addition to its interaction with M46, we have found that M35 potentially interacts with M32, M72, M82 and M99. Of these four interactions, three are novel interactions. Whereas, previous studies have shown the interaction between homologs, UL35 and UL82, in HCMV, although the exact role of this interaction is still unknown [27]. M99 exhibits structural and functional similarity to UL99, which is involved in the cytoplasmic assembly of the maturing viral particle [40, 41]. UL32, the HCMV M32 homolog, previously mentioned through its interaction with the maturing capsid, has also been shown to play a large role in cytoplasmic virion maturation and egress [42]. These findings seem to provide further evidence that M35 has a role in the maturation process of the virion and may serve as a recruitment hub to the maturing viral particle through its interaction with the nucleus.

M99, in addition to interacting with M35, has been found to interact with M94, a putative DNA binding protein thought to also have a potential role in DNA maturation and cleavage[43]. This interaction has been previously observed in HCMV and HSV1 [28, 43]. M94 also serves as hub interacting with M88, M97, and M98. While the function of M88 is unknown, M97, a phosphotransferase, has a potential role in protein modification and has been shown to affect capsid distribution [44, 45].

(D) Interaction between tegument and additional proteins of unknown localization. Interactions between tegument proteins and previously uncharacterized proteins m107 and M98 may show a potential role for the functions of these proteins. m107 interacts with the tegument proteins M72, the dUTPase and M88. And M98, an exonuclease, binds to M94, the aforementioned DNA binding protein [46]. While the role m107 plays in the virion presents a potential mystery as its function and the functions of its binding partners M72 and M88 remains largely unknown. The association between M94 and M98 seems to show a functional similarity in potentially interacting with the viral genome to facilitate maturation. In addition to these interactions, we have also found self-interaction with M28, whose function and localization is unknown.

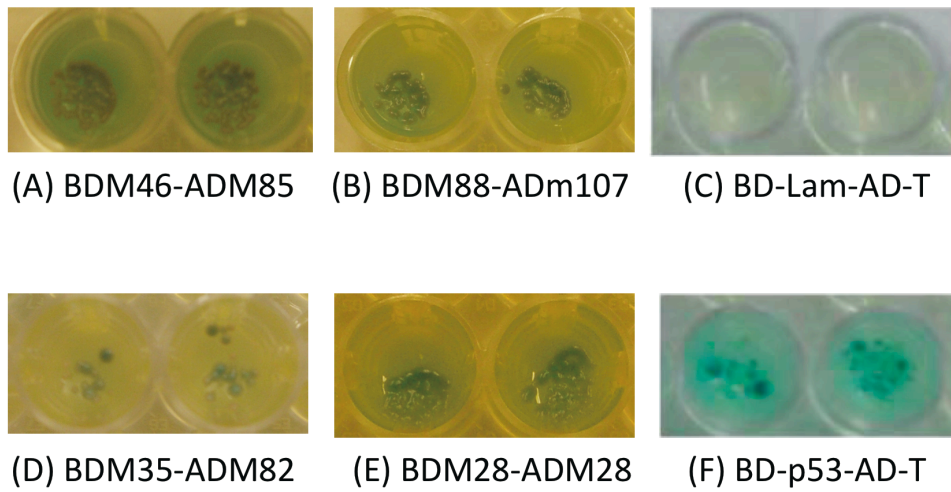
In our study we fail to identify any interactions between viral glycoproteins and any virion components. This may be due to the improper folding of viral glycoproteins in our yeast two-hybrid system, which may result in improper conformation for binding and interaction. It may also be due to the limitation of the YTH system to test and express proteins that are normally not found in the nuclear environment.

The murine cytomegalovirus virion represents a complex network of viral particles that interact to efficiently infect and replicate in a host cell. Its structure has been found to contain 57 proteins that make up the capsid, tegument and outer envelope of the virus in addition to several proteins of cellular origin [10]. Of the 57 ORFs studied, we have discovered 15 interactions between virion proteins that suggest intricate roles for the formation and maturation of the viral particle. However, we cannot exclude the possibility that we were unable to identify interactions between these ORFs and the other proteins found associated with the virion. It is possible that there are interactions that occur in human cells that cannot be detected with our YTH assays. And also feasible, like in the case of the interaction between UL32 and precursor capsids, that interactions may require changes in conformation only present in the formation of complexes that are unable to be observed in the one to one

interactions limited by our assay. There may also be small peptides, human proteins other constituents found in viral particles, such as lipids, that may be involved in potential unseen interactions.

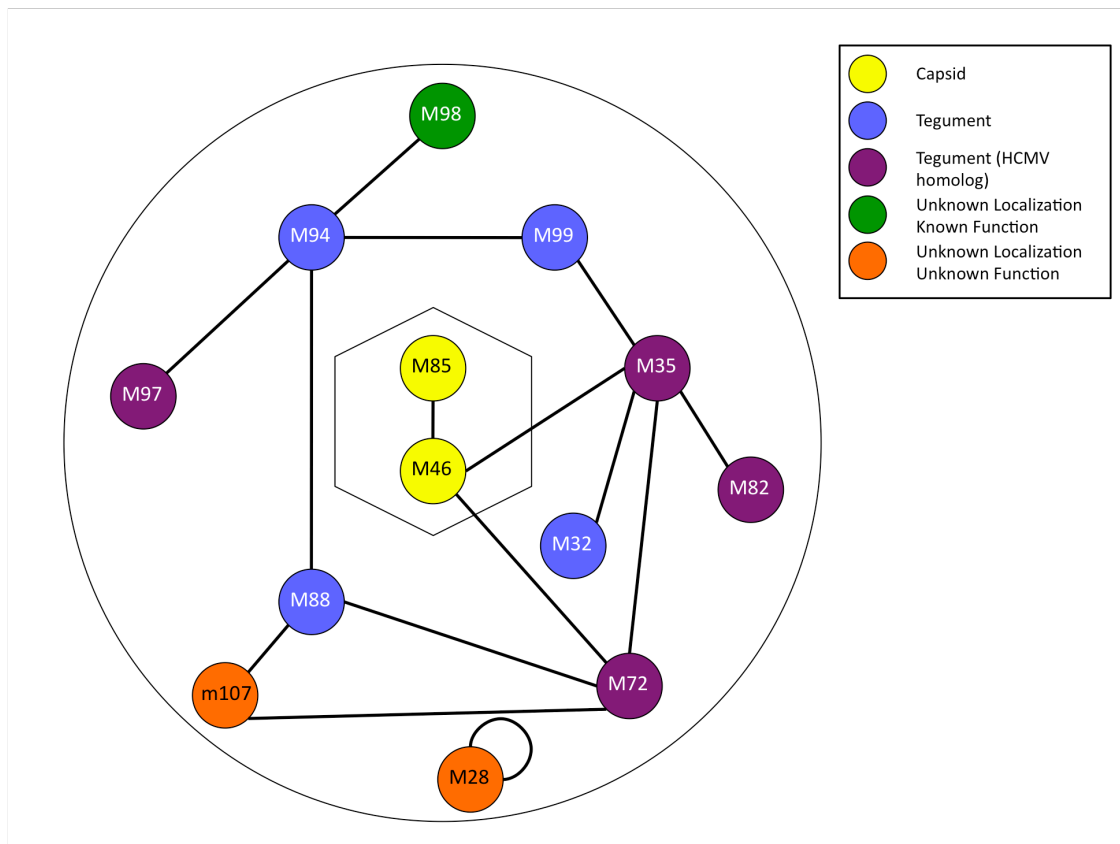
However, the interactions that we have uncovered through our screen will potentially provide insight into potential mechanisms of CMV virion assembly and formation that can be experimented through the use of the MCMV animal model. Future studies into these interactions are required in order to facilitate the development of new strategies and treatments for HCMV associated disease and infection.

FIGURE 1



**Figure 1. Yeast Two Hybrid Interactions**

Examples of positive yeast two-hybrid interactions are shown (A, B, D and E). Positive (F) and negative (C) controls were used to test the validity of the assay.



**Figure 2. MCMV Virion interaction Map.**

The interaction map displays the interactions between MCMV virion proteins as found by yeast two-hybrid analysis. Each node or protein is shown as a circle and each interaction is shown as a single solid line. Circle borders are colored to depict the localization of each MCMV ORF in the virion. Yellow: Capsid, Blue: Tegument, Purple: Tegument as determine by HCMV homolog, Green: known function and unknown localization, and Orange: unknown function and unknown localization.

Table 1

m02U	CCGGAATTC AAGCCATG GAGGCCG GAGCCGCTGTCGGGAGA	m02D	CGCGGATCCGGTACCTCAACCGTCTCGAGCGTAGT
m18U	GGGAATTCATATGCTCGAGGTGCTGACACTGGGCACGGTA	m18D	CCGGAATTCGCGCCGCTCAATCATCCACCAGAGAGG
m20U	AAAAGTGCAGCGCTGACAACGCTCAACCGGAAT	m20D	AAAAGTGCAGCTAGCGTACAGCTCCGAAAG
M25U	CCGGAATTCGGTACCGCAGTTCGTACAGCACGT	M25D	CGCGGATCCGGTACCTTACAGAAAGGTACGCTTGGAA
m25.2U	GGGAATTCATATGCTCGAGGTAGGTGCGCTCCCTTTCC	m25.2D	CCGGAATTCGCGGCCGCTCAGACCGCTTTCAAAAAGAAC
M28U	GGGAATTCATATGGCGGCCGCAAGCCTGGAAGCTGTGGTAT	M28D	CCGGAATTCGCGCCGCTCACCAGCGCTGGGCAC
M31U	CCGGAATTCAGATCTCTCAGCGCAAGCAGGAAAC	M31D	CGCGGATCCGGTACCTCAGCCGGTGTGAAACG
M32U	GGGAATTCATATGGCGGCCGCTCCGCTCGAGGGCGCGG	M32D	CGCGGATCCGCGCCGCTCAGTGAGACGACGAGATTTT
M35U	CCGGAATTCAGATCTCTGCGCTCCGACGGAAGAA	M35D	CGCGGATCCAGATCTTACACTTCGCTCTCGTGC
m39U	GGGAATTCATATGCTCGAGGTCTGTACTCAGTTTTGGGGA	m39D	CCGGAATTCGCGCCGCTCAGAAGTTGTGCAGCGTAC
M43U	GGGAATTCATATGGGTACCACAACGACGTTGACGGGG	M43D	CCGGAATTCGGTACCTTATTGATGTCGCAACACAC
M44U	CCGGAATTCCTGACCGAGGGTGTAGAAAGTTCG	M44D	CGCGGATCCGGTACCTCAGCCCGCACCTTTTGT
M45U	GGGAATTCATATGGGTACCATCCGAATCCTCACCTGCC	M45D	CGCGGATCCGGTACCTCAGCGATAATTCAGGAAAG
M46U	CCGGAATTCCTCGAGGTGCGAACGTCAGCAGCTTCG	M46D	CGCGGATCCGCGCCGCTCAGCGAACTCAGCAGAG
M47U	GGGAATTCATATGTTGTCGACCGCCGCTTCGCGAAGGACC	M47D	GGGAATTCATATGGGTACCTCATGCTGCGCTTCTGTAC
M48U	GGGAATTCATATGGGTACCAAGATCGTCCGCGCAAGCC	M48D	GGGAATTCATATGGGTACCTCAGTGAGGTAGAGGATCTT
m48.2U	CCGGAATTCCTCGAGGTCTAGCTCTCTACTTTACT	m48.2D	CGCGGATCCGCGCCGCTTATTGATGACGCGTGCGCTT
M51U	GGGAATTCATATGAAGATCTCTGACGATCGCGCACAGGT	M51D	CCGGAATTCGGTACCTCAGTCCGCTGTTTCCCTGC
M54U	CCGGAATTCGACACTTGCSTGGAGACTTTC	M54D	CCGGAATTCCTCAGCTCTCCATCGCTCGT
M55U	GGGAATTCATATGGCGCCGCTTCAAGAAGAAACGAAAGAGGATG	M55D	CGCGGATCCGCGCCGCTCAGTACTCGAAATCGGAGTCC
M56U	CCGGAATTC AAGCCATG GAGGCCG CAATGAATACGTTACA AAAA AACTG	M56D	CGCGGATCCGGTACCTCACTTGTACAGGCAAGGAGG
M57U	GGGAATTCATATGGGTACCGCGGACGATCTCTCCAG	M57D	GGGAATTCATATGGGTACCTCACAACCGAGACCGTTTGTCT
M69U	GGGAATTCATATGTTGTCGACCTCGCGCCGCTCAAGA	M69D	CCGGAATTCGGTACCTCAGTACAGAGTCCATCTCGCT
M70U	CGCGGATCCGTCGCGCCGCTACCGTCTGTTCCGCAC	M70D	CGCGGATCCGCGCCGCTAATACTGCGAGGGCAGGGA
M71U	GGGAATTCATATGGGTACCAGTACGAATCTATACGGTTCG	M71D	GGGAATTCATATGGGTACCTCAGAGCGGCCATCTGCT
M72U	GGGAATTCATATGTTGTCGACCGCGAAGCACAAGAAAGAA	M72D	CCGGAATTCGGTACCTCAGCCCTGTTCCAGCAG
m74U	GGGAATTCATATGTTGTCGACCAACCCCTTATTACTCATGTCCG	m74D	CCGGAATTCGGTACCTCAGACACGGCTAAAGGATAT
M75U	GGGAATTCATATGCTCGAGGTGCGGAGAAATTAACCTCCATC	M75D	CGCGGATCCGCGCCGCTTATCTTTTTGCGCGCACAGC
M77U	CCGGAATTCAGATCTCTAGTCCGTTAAAACTTTCAGC	M77D	CGCGGATCCGGTACCTCAGTACACTCACACTCACACAG
M78U	GGGAATTCATATGAAGATCTCTCCGACTTCATCGTCCGCGCT	M78D	CCGGAATTCGGTACCTCAGACACAGAGGAGGAGGTA
M80U	GGGAATTCATATGAAGATCTCTACGGCGCAGCCGCTCCG	M80D	CCGGAATTCAGATCTTCAITTCATTTTATTGAGGAGGGA
M82U	GGGAATTCATATGCTCGAGGTGCGGAGAAATTAACCTCCG	M82D	CCGGAATTCCTCGAGTACGAGGTTGATGATGTGGG
M83U	GGGAATTCATATGCTCGAGGTAAACCCATGAACAACAGGACC	M83D	CCGGAATTCGCGCCGCTCATGAACGACGAGTCTCC
M85U	CCGGAATTCCTGTCGACCGAAACGACGGTTTTGTGTCAGC	M85D	CGCGGATCCGGTACCTCAACCTTGTAGATGCACAGG
M86U	GGGAATTCATATGGGTACCGGGGAGAAGTGGACGGCGAC	M86D	CCGGAATTCGGTACCTCAGGATTAATAAGATGCTTTG
M87U	CCGGAATTCGCGCCGCAAGCCTGACGCGAGCGATGGGT	M87D	CGCGGATCCGCGCCGCTCAGCGAGCGTGAAGTGCACAGT
M88U	CCGGAATTCCTCGAGGTGACGAAGAAGACGCGCGCA	M88D	CGCGGATCCGCGCCGCTTAAAGCTGTAACACCTGATCA
m90U	CCGGAATTCCTGTCGACCGACTCGCGAGACGAAACA	m90D	CGCGGATCCGGTACCTCAGTCTTTGTACATGAACCC
M94U	CCGGAATTCCTGTCGACCGGACGCTCCAGACTATCCGT	M94D	CGCGGATCCGGTACCTCAGATGTGCTCGAGAACGAT
M95U	GGGAATTCATATGGGTACCGCTACAGCGCCGCGGCT	M95D	CCGGAATTCGGTACCTCAGACCGCGCTCGCGGTG
M97U	CCGGAATTCGCGCCGCAAGCCTGAGCTGACGCGG	M97D	CGCGGATCCGCGCCGCTCAGGAAAGATCTTGTACGGA
M98U	GGGAATTCATATGGGTACCTCGTACAAGATCTTCCCTG	M98D	CCGGAATTCGGTACCTCAGGGAGTCCGCGCGGTA
M99U	GGGAATTCATATGTTGTCGACCGGTGCAAGTGTGTAACA	M99D	CGCGGATCCGGTACCTCACAAGCCCTGACTTTTTTC
M100U	CCGGAATTCGGTACCTCTCACTATTTGACCCGC	M100D	CGCGGATCCGGTACCTCACTCTGCGTCTGCTCCGA
M102U	GGGAATTCATATGGGTACCGGAATTCGCGATGGAGAGGC	M102D	CCGGAATTCGGTACCTCAGTTCATAGAAAAGAAAGGC
M104U	GGGAATTCATATGGGTACCTGGCGGAACAGTCTTGTGA	M104D	CCGGAATTCGGTACCTCAACATTAAGGTGCTGGAC
M105U	GGGAATTCATATGGCGCCGCGAGAGAGGTCAGCGACGA	M105D	CCGGAATTCGCGCCGCTCAGAAAACAGAGTGGTATCT
m107U	CCGGAATTCAGATCTCTGACGACGCGGCGGGGG	m107D	CGCGGATCCGGTACCTCAACTAGTGGCGCTCCTCG
M116U	CCGGAATTCGGTACCGGGCACGACATCATGTTTCGT	M116D	CCGGAATTCGGTACCTCATATGAAGTCTGCGGGTGT
m117.1U	CCGGAATTCGCGCCGCTCCGAGACGTCGGTATGCC	m117.1D	CGCGGATCCGCGCCGCTTACTTAGCCGCTGCTGCT
M121U	GGGAATTCATATGGGTACCGCGTCCAGTAGACACCGT	M121D	GGGAATTCATATGGGTACCTCAGTAGACAGAACGCGTCCG
m147U	CCGGAATTCCTCGAGGTTTTGTAATCTATATGTAATTTTC	m147D	CGCGGATCCGCGCCGCTTATTATCTGTCGGGACCGCA
m150U	CCGGAATTCCTGTCGACCTGTATTGTCGCGGTTCTCTCT	m150D	CGCGGATCCGGTACCTCAGACGCTCGCTGCTCAC
m151U	CGCGGATCCGTCGCGCCGCTATTGGCGTGATACGTGCGCT	m151D	CGCGGATCCGCGCCGCTTATCGAAAGCTGAGCTCGCT
m163U	CCGGAATTCGGTACCGAGGGCCGCAACGACGCT	m163D	CGCGGATCCGGTACCTTATACCGGTTATAGGGAAC
m165U	CCGGAATTCGGTACCGCCCTCGGCGCTACGATG	m165D	CGCGGATCCGGTACCTCATGAGTATCTGAGAGGA
m166.5U		m166.5D	



Table 3

BD ORFs	Function	AD ORFs	Function	Co-IP	Reported in MCMV	Reported in HCMV
<b>Capsid-Capsid Protein Interactions</b>						
M46	Minor Capsid Protein	M85	Capsid Protein			UL46-UL85
<b>Capsid-Tegument Protein Interactions</b>						
M46	Minor Capsid Protein	M35	M25/UL25 gene family			
M46	Minor Capsid Protein	M72	dUTPase			
<b>Tegument-Tegument Protein Interactions</b>						
M32	Tegument	M35	M25/UL25 gene family			
M35	M25/UL25 gene family	M72	dUTPase			
M35	M25/UL25 gene family	M82	pp71 Upper matrix phosphoprotein			UL35-UL82
M88	Tegument (HCMV)	M72	dUTPase			
M88	Tegument (HCMV)	M94	Putative DNA binding protein (HCMV)			
M94	Putative DNA binding protein (HCMV)	M99	Tegument (pp28 phosphoprotein)			
M97	Phosphotransferase	M94	Putative DNA binding protein (HCMV)			
M99	Tegument (pp28 phosphoprotein)	M35	M25/UL25 gene family			
<b>Tegument-Additional Protein Interactions</b>						
M72	dUTPase	m107	unknown			
M88	Tegument (HCMV)	m107	unknown			
M98	Exonuclease	M94	Putative DNA binding protein (HCMV)			
<b>Additional Protein-Protein Interactions</b>						
M28	unknown	M28	unknown			



## References

1. Fields, B.N., D.M. Knipe, and P.M. Howley, *Fields' virology*. 5th ed ed. 2007, Philadelphia: Wolters Kluwer Health/Lippincott Williams & Wilkins. 2 v. (xix, 3091, 86 p.).
2. Sissons, J.G. and A.J. Carmichael, *Clinical aspects and management of cytomegalovirus infection*. *J Infect*, 2002. **44**(2): p. 78-83.
3. Jabs, D.A., C. Enger, and J.G. Bartlett, *Cytomegalovirus retinitis and acquired immunodeficiency syndrome*. *Arch Ophthalmol*, 1989. **107**(1): p. 75-80.
4. Moorman, A.C., et al., *Changing conditions and treatments in a dynamic cohort of ambulatory HIV patients: the HIV outpatient study (HOPS)*. *Ann Epidemiol*, 1999. **9**(6): p. 349-57.
5. Krmpotic, A., et al., *Pathogenesis of murine cytomegalovirus infection*. *Microbes Infect*, 2003. **5**(13): p. 1263-77.
6. Rawlinson, W.D., H.E. Farrell, and B.G. Barrell, *Analysis of the complete DNA sequence of murine cytomegalovirus*. *J Virol*, 1996. **70**(12): p. 8833-49.
7. Scalzo, A.A., et al., *The interplay between host and viral factors in shaping the outcome of cytomegalovirus infection*. *Immunol Cell Biol*, 2007. **85**(1): p. 46-54.
8. Reddehase, M.J., J. Podlech, and N.K. Grzimek, *Mouse models of cytomegalovirus latency: overview*. *J Clin Virol*, 2002. **25 Suppl 2**: p. S23-36.
9. Brocchieri, L., et al., *Predicting coding potential from genome sequence: application to betaherpesviruses infecting rats and mice*. *J Virol*, 2005. **79**(12): p. 7570-96.
10. Kattenhorn, L.M., et al., *Identification of proteins associated with murine cytomegalovirus virions*. *J Virol*, 2004. **78**(20): p. 11187-97.
11. Fields, S. and O. Song, *A novel genetic system to detect protein-protein interactions*. *Nature*, 1989. **340**(6230): p. 245-6.
12. Giot, L., et al., *A protein interaction map of Drosophila melanogaster*. *Science*, 2003. **302**(5651): p. 1727-36.
13. Ito, T., et al., *A comprehensive two-hybrid analysis to explore the yeast protein interactome*. *Proc Natl Acad Sci U S A*, 2001. **98**(8): p. 4569-74.
14. LaCount, D.J., et al., *A protein interaction network of the malaria parasite Plasmodium falciparum*. *Nature*, 2005. **438**(7064): p. 103-7.
15. Li, S., et al., *A map of the interactome network of the metazoan C. elegans*. *Science*, 2004. **303**(5657): p. 540-3.
16. Rain, J.C., et al., *The protein-protein interaction map of Helicobacter pylori*. *Nature*, 2001. **409**(6817): p. 211-5.
17. McCraith, S., et al., *Genome-wide analysis of vaccinia virus protein-protein interactions*. *Proc Natl Acad Sci U S A*, 2000. **97**(9): p. 4879-84.
18. Calderwood, M.A., et al., *Epstein-Barr virus and virus human protein interaction maps*. *Proc Natl Acad Sci U S A*, 2007. **104**(18): p. 7606-11.
19. Rozen, R., et al., *Virion-wide protein interactions of Kaposi's sarcoma-associated herpesvirus*. *J Virol*, 2008. **82**(10): p. 4742-50.
20. Uetz, P., et al., *Herpesviral protein networks and their interaction with the human proteome*. *Science*, 2006. **311**(5758): p. 239-42.

21. de Chassey, B., et al., *Hepatitis C virus infection protein network*. Mol Syst Biol, 2008. **4**: p. 230.
22. Oliveira, S.A. and T.E. Shenk, *Murine cytomegalovirus M78 protein, a G protein-coupled receptor homologue, is a constituent of the virion and facilitates accumulation of immediate-early viral mRNA*. Proc Natl Acad Sci U S A, 2001. **98**(6): p. 3237-42.
23. Cusick, M.E., et al., *Interactome: gateway into systems biology*. Hum Mol Genet, 2005. **14 Spec No. 2**: p. R171-81.
24. Gibson, W., *Structure and assembly of the virion*. Intervirology, 1996. **39**(5-6): p. 389-400.
25. Desai, P. and S. Person, *Molecular interactions between the HSV-1 capsid proteins as measured by the yeast two-hybrid system*. Virology, 1996. **220**(2): p. 516-21.
26. Douglas, M.W., et al., *Herpes simplex virus type 1 capsid protein VP26 interacts with dynein light chains RP3 and Tctex1 and plays a role in retrograde cellular transport*. J Biol Chem, 2004. **279**(27): p. 28522-30.
27. Schierling, K., et al., *Human cytomegalovirus tegument proteins ppUL82 (pp71) and ppUL35 interact and cooperatively activate the major immediate-early enhancer*. J Virol, 2004. **78**(17): p. 9512-23.
28. Vittone, V., et al., *Determination of interactions between tegument proteins of herpes simplex virus type 1*. J Virol, 2005. **79**(15): p. 9566-71.
29. Liu, F., and Z.H. Zhou *Comparative virion structures of human herpesviruses*, in *Human herpesviruses : biology, therapy, and immunoprophylaxis*, A.M. Arvin, Editor. 2007, Cambridge University Press: Cambridge ; New York. p. xx, 1388 p.
30. Kalejta, R.F., *Tegument proteins of human cytomegalovirus*. Microbiol Mol Biol Rev, 2008. **72**(2): p. 249-65, table of contents.
31. Chen, D.H., et al., *Three-dimensional visualization of tegument/capsid interactions in the intact human cytomegalovirus*. Virology, 1999. **260**(1): p. 10-6.
32. Trus, B.L., et al., *Capsid structure of simian cytomegalovirus from cryoelectron microscopy: evidence for tegument attachment sites*. J Virol, 1999. **73**(3): p. 2181-92.
33. Baxter, M.K. and W. Gibson, *Cytomegalovirus basic phosphoprotein (pUL32) binds to capsids in vitro through its amino one-third*. J Virol, 2001. **75**(15): p. 6865-73.
34. Tam, A., et al., *Murine cytomegalovirus with a transposon insertional mutation at open reading frame M35 is defective in growth in vivo*. J Virol, 2003. **77**(14): p. 7746-55.
35. Schierling, K., et al., *Human cytomegalovirus tegument protein ppUL35 is important for viral replication and particle formation*. J Virol, 2005. **79**(5): p. 3084-96.
36. Liu, Y. and B.J. Biegalko, *The human cytomegalovirus UL35 gene encodes two proteins with different functions*. J Virol, 2002. **76**(5): p. 2460-8.
37. Chen, R., H. Wang, and L.M. Mansky, *Roles of uracil-DNA glycosylase and dUTPase in virus replication*. J Gen Virol, 2002. **83**(Pt 10): p. 2339-45.
38. Caposio, P., et al., *Evidence that the human cytomegalovirus 46-kDa UL72 protein is not an active dUTPase but a late protein dispensable for replication in fibroblasts*. Virology, 2004. **325**(2): p. 264-76.
39. Kalejta, R.F., *Functions of human cytomegalovirus tegument proteins prior to immediate early gene expression*. Curr Top Microbiol Immunol, 2008. **325**: p. 101-15.

40. Seo, J.Y. and W.J. Britt, *Cytoplasmic envelopment of human cytomegalovirus requires the postlocalization function of tegument protein pp28 within the assembly compartment*. J Virol, 2007. **81**(12): p. 6536-47.
41. Cranmer, L.D., C. Clark, and D.H. Spector, *Cloning, characterization, and expression of the murine cytomegalovirus homologue of the human cytomegalovirus 28-kDa matrix phosphoprotein (UL99)*. Virology, 1994. **205**(2): p. 417-29.
42. AuCoin, D.P., et al., *Betaherpesvirus-conserved cytomegalovirus tegument protein ppUL32 (pp150) controls cytoplasmic events during virion maturation*. J Virol, 2006. **80**(16): p. 8199-210.
43. Liu, Y., et al., *The tegument protein UL94 of human cytomegalovirus as a binding partner for tegument protein pp28 identified by intracellular imaging*. Virology, 2009. **388**(1): p. 68-77.
44. Rawlinson, W.D., et al., *The murine cytomegalovirus (MCMV) homolog of the HCMV phosphotransferase (UL97(pk)) gene*. Virology, 1997. **233**(2): p. 358-63.
45. Buser, C., et al., *Quantitative investigation of murine cytomegalovirus nucleocapsid interaction*. J Microsc, 2007. **228**(Pt 1): p. 78-87.
46. Sheaffer, A.K., S.P. Weinheimer, and D.J. Tenney, *The human cytomegalovirus UL98 gene encodes the conserved herpesvirus alkaline nuclease*. J Gen Virol, 1997. **78 ( Pt 11)**: p. 2953-61.

## **Chapter 3**

### **MCMV Interactome**

## Introduction

Herpesviruses represent a family of complex viruses that infect a wide range of species. Eight of these viruses are known to infect humans and fall into one of three subfamilies: alpha-, beta- and gamma-herpesviruses. Alphaherpesviruses are characterized by a fast replication cycle of around 24 hours, variable host range, and latency in neuronal cells. Betaherpesviruses are characterized by their long replication cycle of around 72 hours, strict species specificity and infection of many cell types. And gammaherpesviruses, have a restricted host range and establish latency in B and T cells.

Of these human herpesviruses, human cytomegalovirus (HCMV), a beta-herpesvirus, contains one of the largest genomes, encoding for approximately 170 open reading frames (ORFs). Approximately, 40 of these proteins are considered core proteins and are conserved among all herpesviruses [1]. These proteins consist of components of the viral capsid, DNA replication and packaging machinery, and glycoproteins. While the rest of the viral proteins, consist of structural and non-structural proteins conserved within betaherpesviruses and cytomegaloviruses.

While one approach to determine the functions of these genes may be through traditional hypothesis driven methods, characterized as “vertical” approaches by Vidal, 2001 [2]. This approach, while highly detailed, is limited by its focus on a small number of genes and lacks efficiency when applied to a large number of unknown genes. On the other hand, a “horizontal approach” can focus on characterizing many genes through high-throughput assays though at the expense of detail.

However, using these high-throughput methods to create large scale maps, as in the case of the protein interactome, we can utilize both the data obtained through this large scale project and existing data, developed using vertical approaches to help deduce the functions of a large number of unknowns as is found in HCMV.

Our laboratory has undertaken the task of creating this HCMV interactome. And we have also decided to take the creation of this map one step further by investigating the protein interactome of murine cytomegalovirus (MCMV) in order to take advantage of in vivo studies that can be done using murine version of the virus.

The strict species specificity of HCMV prevents any studies into the pathogenesis of the virus in an animal host. This limitation can be overcome through MCMV. MCMV, like HCMV, is a betaherpesvirus that exhibits similar pathogenesis in mice to HCMV infection in the human host [3]. The genetic structure of MCMV contains significant sequence homology to HCMV AD169 in at least 78 ORFs and can thereby be used as an important tool in elucidating the functions of these ORFs in a complete in vivo system [4]. Due to these similarities, MCMV provides a good model to study infection with regards to host genetics, latency and the immune system [5, 6].

Because of the important role of MCMV as a tool for helping to determine the effects of HCMV infection in a human host, understanding the structure of the virion and the complete interactions between structural and nonstructural proteins can provide important information in understanding how CMV infects and causes disease. MCMV, like HCMV, is one of the largest herpesviruses, containing a ~230 kb genome which encodes for roughly 170 ORFs [4, 7].

As in Chapter 2, determining how MCMV proteins interact can be useful in helping not only elucidate viral pathogenesis in mouse infection, but due to the high degree of homology to the HCMV virion, can also provide important clues to the function of these proteins in human infection. This homology can also work in reverse by using information about homologous HCMV proteins to provide clues to understand unknown MCMV proteins. In this chapter we hope to expand on the prior research, which focused primarily on the components that comprised the viral particle in order to develop a better understanding of how all the viral proteins encoded by the virus work to facilitate productive infection in the host.

In order to determine these MCMV protein interactions we once again take advantage of the yeast two-hybrid assay (YTH). This method uses transcription activation (AD) and DNA-binding domains (BD) of the GAL4 transcription factor, which can be separated into two components [8]. To study the potential one to one interactions between proteins, genes can be cloned into AD or BD expression vectors resulting in either AD or BD-fusion proteins when expressed in haploid yeast cells. When the yeasts are mated these fusion proteins are allowed to interact and can bind to form a functional GAL4 transcription factor that activates transcription that is detectable by nutrient selection.

YTH has been applied to large-scale analyses of interactomes of multiple organisms. Because of the relatively large size of complex organisms, the importance of individual proteins in relation to these systems may be difficult to ascertain. Therefore, these large-scale analyses that are used to form global interactomes can be of great importance in determining the significance of individual proteins. Organisms studied using YTH include humans, *Drosophila melanogaster*, *Caenorhabditis elegans*, *Saccharomyces cerevisiae*, *Plasmodium falciparum* and *Helicobacter pylori* [9-13]. Viral interactions have also been studied in vaccinia virus, three herpesviruses and Hepatitis C virus [14-18]. These interactome studies have helped show novel interactions elucidating how components of the organism interact to form cellular or viral structures and have also provided insight into the interaction between networks of proteins involved in different aspects of cellular regulation from transcription, to signaling to immune responses. The yeast two-hybrid study can also be used to support predicted function from previous studies by showing that the proteins involved can interact with each other in the context of the YTH assay as in the case of components of transcription thought to interact in vaccinia virus replication [14].

In our study, we have conducted a comprehensive YTH screen to identify potential interactions between approximately 170 MCMV ORFs. Between these 170 predicted proteins we have identified 94 potential interactions. Our studies have also observed the presence of “hub” proteins, which interact with multiple partners. These hub proteins may be involved as organizing centers for connecting or recruiting viral proteins to the mature virion. It is also possible that these hubs may be involved in viral entry or egress, helping to traffic the virion through the cell. We aim to understand the nature of these hub proteins as well as elucidate the interactions between the viral particle and proteins encoded by the virus that are not included in its structure to elucidate potential mechanisms by which these proteins help to assemble and create new progeny viruses. The interactions that we have identified in this study also provide a framework to predict the functions of uncharacterized viral proteins. Together with known viral proteins, the elucidation of the MCMV viral interactome allows for the better understanding of how these components contribute to viral infection and

pathogenesis, and can be used to discover their importance by providing a direction for the study of pathogenesis through animal studies.

## Materials and Methods

### Construction of plasmids

MCMV Smith and pSM3fr, a MCMV Smith<sub>BAC</sub> construct, were used for all PCR amplification of full-length virion ORFs. Primers to virion ORFs (Table 1) were designed for cloning into the pGBK-T7 bait and pGAD-T7 prey plasmids for yeast expression and further subcloning in pCMV-myc and pCMV-HA mammalian expression plasmids (Clontech). Each primer sequence contains an outer and inner restriction enzyme site for cloning in the multiple cloning site (MCS) of the yeast and mammalian expression plasmids, respectively (Table 1). PCR amplification was through the use of iProof High-fidelity DNA polymerase (Bio-Rad). The resulting constructs were confirmed by restriction digest profile and sequencing. A total of fifty-seven MCMV-encoded virion ORFs were cloned into each of the pGBK-T7 and pGAD-T7 vectors.

### Yeast two-hybrid screen

The three hundred and fifty three viral ORFs that were cloned into both pGBK-T7 and pGAD-T7 vectors were transformed into AH109 (*MATa*) and Y187 (*MATα*) yeast strains, respectively (Matchmaker 3 System, Clontech). AH109 strains harboring pGBK-T7 plasmids were maintained in minimal SD media with tryptophan dropout supplement (SD/-Trp) while Y187 strains harboring pGAD-T7 plasmids were maintained in minimal SD media with leucine dropout supplement (SD/ -Leu).

Prior to performing the matings, all pGBK-T7-fusion proteins in AH109 strains were tested for autoactivation. Individual AH109 strains were plated on SD/ -Ade/ -His/ -Trp agar with 40 µg/mL X-α-Gal. AH109 strains containing pGBK-T7 ORFs were determined to be autoactivators if growth was detected in the absence of any pGAD-T7 cloned ORFs, and subsequently eliminated from further matings.

Yeast mating was carried out by inoculating fresh colonies (<2 weeks old) of both AH109 and Y187 strains into 1.5 mL microcentrifuge tubes containing 0.5 mL of YPDA media and incubated at 30°C with shaking at 200 rpm for 24 hours. There were a total of 31,152 possible combinations (176 AH109 x 177 Y187) and each mating combination was performed in duplicate. To select for diploids that have successfully mated, mated yeast were pelleted at 14,000 rpm for 15 seconds. Each pellet was resuspended in 0.5 mL Tris-EDTA buffer and 10 µL of each was plated in one well of 48-well plates containing 1 mL of SD/-Leu/ -Trp agar and incubated at 30°C for 3-5 days. Diploid colonies from each successful mating was then picked from each well and resuspended with 100 µL of TE buffer in a 1.5 mL microcentrifuge tube and 10 µL was plated in one well of 48-well plates containing 1 mL of SD/ -Ade/ -His/ -Leu/ -Trp (quadruple drop-out (QDO)) agar with 40 µg/ mL of X-α-Gal.

Mating controls used was via the comparison of combinations of transformed AH109 and Y187 strains together and individually in 0.5 mL of YPDA, that were shaken overnight at 200 rpm. These mating cultures were plated onto SD/ -Leu/ -Trp plates. Only diploid yeasts from

the mating of AH109 and Y187 yeast were able to grow on the SD/ -Leu/ -Trp plates while individual AH109 and Y187 yeast were unable to grow.

Three weeks after plating the mated diploid yeasts, QDO plates were scored for positive protein-protein interactions. QDO/ X- $\alpha$ -Gal plates were used as a high stringency screen for eliminating possible false positives. AH109 strains contained three reporters—ADE2, HIS3, and MEL1 (encodes  $\alpha$ -galactosidase)—under the control of unique GAL4 upstream activating sequences (UAS) and TATA boxes. The positive control used was AH109 yeast transformed with BD-p53 fusion protein mated with Y187 yeast transformed with AD-T (SV40 T-antigen), while the negative control was transformation of AH109 with BD-Lamin C with and Y187 with AD-T (Figure 7).

When scoring the duplicate matings, wells containing the MCMV ORF fusion proteins that showed no yeast growth after three weeks were considered to be non-interacting partners. Duplicate wells containing blue yeast colonies in both wells or in one well were chosen for repeated screening to confirm that positive interaction exists. Confirmation of a positive interaction was through consistent results from at least two of three independent experiments.

## **Results**

### **Cloning of MCMV open reading frames coding for virion proteins and construction of plasmids for yeast two-hybrid screen**

Cloned MCMV open reading frames were determined by using MCMV sequence analysis as determined by Rawlinson et al. 1996 and annotated sequences determined by Brocchieri et al. 2005 [4, 7].

In this study, we have cloned and expressed, in the yeast two-hybrid system, one hundred and seventy-seven predicted proteins associated with the MCMV genome.

For each ORF, we designed an optimal PCR primer pair. The primer pairs were designed as follows: The forward primer (from 5' to 3') contains the sequence immediately after the predicted translation initiation codon AUG and 20-25 additional nucleotides of the coding sequence. The reverse primer contains the reverse complement of both the predicted translation termination codon and the preceding 20-25 nucleotides at the end of the ORF. In addition, the primers also contain 15-20 nucleotide common sequences that contain sites for restriction enzymes for cloning of the PCR products into the yeast two-hybrid screening vectors (pGADT7 and pGBKT7) and the mammalian expression vectors (pCMV-HA and pCMV-myc).

Each ORF encoding MCMV proteins was amplified individually by PCR with a specific set of primers. The amplified PCR products cover the entire ORF sequence minus the initiation codon and were cloned into yeast two-hybrid “prey” pGADT7 and “bait” pGBKT7 vectors, respectively, resulting in the generation of one hundred fourteen constructs. The viral ORF sequences in each of these constructs were confirmed using DNA sequencing analysis.

### **Identification of potential interactions among MCMV-encoded proteins using yeast two-hybrid screen**

The strategy employed used pair-wise combinations of MCMV-encoded proteins to test interactions in the yeast two-hybrid assay using a 48-well protein array format. The array



consisted of a set of yeast transformants, each expressing one MCMV virion ORF, as a hybrid protein containing a GAL4 DNA binding domain. The yeast construct contained in each well of this array was mated to a set of yeast transformants, of the opposite mating type, which carried one of the MCMV ORFs, as a hybrid protein with containing a GAL4 activation domain. The resulting diploids were cultured on medium selective for the two-hybrid reporter genes. Using this approach a single protein could be tested for interaction against every one of the cloned MCMV protein constructs. By generating different sets of activation and DNA binding domain constructs we were able to assay more than 31,000 combinations representing potential interacting pairs between MCMV proteins.

In order to generate yeast transformants for the two-hybrid screen, plasmid DNA from each of the 177 generated “bait” pGBKT7-derived constructs were isolated from *E. coli* and transformed into the AH109 yeast strain resulting in a collection of transformants expressing a set of DNA-binding domain MCMV hybrid proteins. Similarly, plasmid DNA from each of the generated “prey” pGADT7-derived constructs were isolated and transformed into the yeast strain, Y187, in order to create transformants expressing a set of 177 DNA activation domain MCMV hybrid proteins. Analysis of the recovered plasmid DNAs from these yeast transformants indicated that the constructs were present and exhibited similar restriction profiles as those in *E. coli*.

Prior to performing the matings, all 176 pGBKT7-fusion proteins in AH109 strains were tested for autoactivation. Ten AH109 strains, which contained ORFs: m18, m23.1, M34, M82, M87, M95, M113, m123.2, m123.3, m140 were determined to be autoactivators in the absence of any pGADT7-cloned ORF (Table 2), and subsequently eliminated from any further matings. Each of the rest of the one hundred and sixty-six AH109 constructed strains were mated, in duplicate, with each of the one hundred and seventy-seven Y187 constructed stains, and the resulting diploid cells were plated in duplicate on selective medium. In addition to selecting for the presence of the two plasmids based on leucine and tryptophan selection, we used a high stringency screening method, selecting for positive protein interactions using three more reporter genes to eliminate potential false positives: histidine, adenine, and Mel1, which encodes alpha-galactosidase for blue/white screening of yeast colonies. The growth of colonies of diploid yeast cells with blue staining within three weeks after plating were scored as a positive pair-wise interaction between the two proteins tested (Figure 7). While all other results (e.g. no growth of yeast colonies) were scored as a negative interaction.

Two-hybrid screens have the potential to generate a significant number of false positives that represent the random generation histidine-positive colonies. This is possibly due to rearrangement and deletion of the DNA-binding domain plasmid, recombinational events between the DNA-binding and activation domain plasmids, or genomic rearrangement of the host strain. To exclude these possibilities, three sets of experiments were carried out. First, plasmid DNA constructs from the yeast transformants were recovered and analyzed. Our results indicated that these constructs were present in all transformants analyzed and exhibited similar restriction enzyme profiles as those in *E. coli*. Second, all screens were carried out in duplicate to determine whether the results were reproducible. Lastly, any protein that resulted in histidine positive growth with any of the four controls (the yeast protein Mec3, human lamin, and the empty vectors, pGADT7 and pGBKT7) was classified as a false positive and removed from the set of positive interactions.

### **MCMV Interactome**

Of the 31,000 pair-wise interactions, there were ninety-four PPIs between sixty-four individual proteins (Figure 1 and 2, Table 1 and 3). Fifteen interactions were between virion proteins only, three were self-interactions and the rest were between virion and non-virion proteins.

### **Conservation class interactions**

While there are many aspects of MCMV pathogenesis and infection that can be viewed as novel and interesting, one of MCMV's most important roles as a research tool can be viewed as a conduit for studying HCMV using similarities between the two viruses. With respect to herpesviruses in general there are approximately forty-one conserved core genes [1]. These core genes are usually involved in virion assembly, replication, attachment and entry. In our study we found interactions involving thirteen herpesvirus core proteins (M99, M52, M53, M50, M70, M93, M72, M76, M85, M46, M77, M94, and M97) (Table 1). These proteins represent DNA machinery, capsid proteins, nuclear egress components, and tegument proteins. There are twenty-one PPIs between these thirteen core proteins as well as interactions between core and non-core proteins. Of these twenty-one PPIs, seven of these interactions were between only core proteins. Eight interactions were between core proteins and MCMV proteins with homology to HCMV proteins. And six of these interactions resulted between core proteins and genes related to MCMV only. Three of these six interactions were involved with *sgg1* (m132.2), a major hub protein found in this study (Table 1, Table 2, Figure 2).

The remaining interactions were between MCMV specific proteins, and MCMV proteins with homology to HCMV. Of the 170 MCMV predicted ORFs, approximately 42% of these genes have either sequence or functional homology to HCMV proteins [4]. There are thirty-two (34%) PPIs between proteins specific to MCMV, twenty-four (25%) between proteins that are homologous to HCMV and thirty-eight (40%) PPIs between HCMV homologous proteins and MCMV specific proteins. Of the twenty-four PPIs between HCMV homologous proteins four, M32-M35, M82-M35, M85-M46 and M99-M94 were found in a HCMV yeast two-hybrid assay also conducted in our laboratory (To, unpublished results) (Table 1).

### **Gene deletion phenotype interactions**

Considering the limitations of the virus in terms of encoding DNA, viral proteins are important in determining the formation of the viral particle as well as facilitating infection and pathogenesis in the host. This information can provide important insight into the role interacting partners have in the basic survival of the virus in an infected cell. This determination of essentiality can be conducted through systematic deletions in each ORF in the MCMV genome resulting in the creation of a library of mutant viruses containing single deletions in a specific encoded gene. Our laboratory has created this library and tested the essentiality of each predicted ORF through multiple time-point infections in murine NIH-3T3 fibroblast cells (Chan and Umamoto, unpublished results). These studies have resulted in the observation of three distinct phenotypes that can be used to categorize each predicted protein in regards to NIH-3T3 infection. These categories with respect to viral replication are: essential (no growth or titer obtainable), defective (there is either moderate or severe attenuation as

compared to the wild-type infection), and wild-type like or non-essential (growth of the deletion mutant resembles wild-type infection, indicating that in that particular cell line this gene is dispensable for viral growth).

Twenty-six (26%) of the ninety-four PPIs observed are between non-essential proteins. Ten (10%) interactions were found between essential proteins. Twenty-five (25%) were between non-essential and essential proteins. Sixteen were between non-essential and attenuated proteins and eight were between essential and attenuated proteins.

### Hub Proteins

Interactomes from a variety of different organisms including *Drosophila melanogaster*, *Caenorhabditis elegans*, *Saccharomyces cerevisiae*, *Plasmodium falciparum* and *Helicobacter pylori* and viruses such as vaccinia virus, herpesviruses and Hepatitis C virus has shown that certain proteins interact with more partners than others [9-13]. These proteins that tend to interact with many other proteins are termed “hub proteins.” And are thought to be of significance and importance to an organism due to large number of interactions that it may participate in. Comparisons between hub proteins and essentiality have been undertaken to a great degree in yeast and have resulted in mixed results in determining the link between the two [19-21]. This may be due to the methods used to determine hub proteins and the databases used to determine essentiality. It may also determine on the conditions and circumstances by which these proteins are expressed and determined to be essential in. This may be different physiological conditions involved in in vivo infection or different environments such as those found in different cellular conditions (Figures 2-6).

In our screen we have determined that five proteins interact with at least ten other partners while two proteins interact with at least seven different proteins. The largest number of interactions between a single hub and numerous partners were twenty-three total PPIs. The seven proteins identified as hub proteins in MCMV are M27 (11 PPIs), M35 (7 PPIs), M72 (7 PPIs), M88 (12 PPIs), m128.3 (12 PPIs), m132.2 (23 PPIs) and m169 (11 PPIs) (Table 2, Figure 3).

The essentiality of the identified hub proteins reveals that MCMV hub proteins can be both essential and non-essential. Two hub proteins are essential, four are non-essential and one is attenuated. Essentiality does not depend on homology to HCMV and the phenotype of the hub protein does not determine the essentiality of the network proteins. Hub proteins in MCMV can be structural and non-structural components.

Only one of these hub proteins is one of the core proteins, M72. However, the other interacting hub proteins do contain interactions with core proteins.

### Discussion

Yeast two-hybrid analyses have been used to determine the interactomes of a variety of different organisms such as humans, *Drosophila melanogaster*, *Caenorhabditis elegans*, *Saccharomyces cerevisiae*, *Plasmodium falciparum* and *Helicobacter pylori* [9-13]. Studies using the yeast two-hybrid assay have also encompassed potential interactions between virally expressed proteins both through global analysis of protein expression and through studies of the proteins comprising the virion. These studies have been conducted on vaccinia virus, three herpesviruses and Hepatitis C virus [14-18]. The data generated through the formation of the

interactomes mentioned represent a powerful set of information that forms important building blocks for the beginnings of additional studies needed to determine the biological significance of these interactions and the role each protein plays in the survival of the organism making yeast two-hybrid an important tool in system-level studies [22]. In this study, we have used the yeast two-hybrid system to study potential interactions among MCMV-encoded proteins. Our results have identified ninety-four PPIs between sixty-four individual proteins in a screen of 31,000 pairwise interactions (Figure 1 and 2, Table 1 and 3). Fifteen of these interactions were between virion proteins only, three were self-interactions and the remaining interactions were between virion and non-virion proteins.

Before mentioning our results, it is important to understand that yeast two-hybrid screens have been found to generate a number of false positives [8]. One potential source is through the random generation of histidine-positive colonies. This can be due to rearrangement and deletion of the DNA-binding domain plasmid, recombinational events between the DNA-binding and activation domain plasmids, or genomic rearrangement of the host strain. Another type of false positive is due to the non-specific activation of different reporter systems. And the third type is due to autoactivation, which is caused by activators of transcription caused by binding only domain fusion proteins. False negatives may also arise from the YTH screens. This is due to the potential for systems that test for protein interactions in the nucleus to lead to erroneous results because of the expression of proteins that are normally not found in the nucleus. This system may also miss interactions involving proteins with significant hydrophobic domains such as membrane proteins that prevent proper folding or transport to the nucleus.

To exclude these possibilities, five different sets of experiments have been carried out. First, plasmid DNA from the yeast transformants was recovered and analyzed. Our results indicated that these constructs were present in all transformants examined and each exhibited similar restriction enzyme profiles as those in *E. coli*, suggesting that there is no significant change or rearrangement of the sequence of the transformants during the screening process. Second, all screens were carried out in duplicate to determine whether the results were reproducible. Third, we used the highest stringency protocol in our system by utilizing four different reporters to ensure the validity of the data. Any protein that resulted in histidine-positive growth with any of the four controls (the yeast protein Mec3, human lamin, and the empty vectors pGADT7 and pGBKT7) was classified as a false positive and removed from the set of positive interactions. Fourth, prior to any matings in our experiments, all of the binding domain-fusion proteins have been tested for autoactivation and positive fusion proteins from this screen were removed from further study.

### **Conservation Class**

One of MCMV's most important features is the ability to compare MCMV infection with HCMV. Due to the strict species interactions, there is no animal model for HCMV infection and thus studies involving pathogenesis must be done using a related virus, for example, MCMV. MCMV infection of mice provides a useful platform to study CMV infection as both the virus and the research animal has been studied and characterized to great detail. Allowing for the comparative analysis between the two different viruses.

Of even more significance, with respect to herpesviruses in general, there are approximately forty-one conserved core genes [1]. These core genes are usually involved in virion assembly, replication, attachment and entry. In our study we found interactions involving thirteen herpesvirus core proteins (M46, M50, M52, M53, M70, M72, M76, M77, M85, M93, M94, M97, and M99) (Table 1). There are twenty-one PPIs involving these thirteen core proteins as well as interactions between non-core proteins. Of these twenty-one PPIs, seven of these interactions were between core proteins. These interactions involve nuclear egress machinery M50 and M53 which form the nuclear egress complex (NEC), confirmed by published data [23]. Also found were interactions between capsid proteins, M85 and M46, the DNA binding protein, M94 and the protein kinase, M97, and the tegument phosphoprotein, M99.

Eight interactions were between core proteins and MCMV proteins with homology to HCMV proteins. These interactions range from structural components, M25 and M99 (tegument) to possible immune regulatory proteins (M27). Six of these interactions resulted between core proteins and genes related to MCMV only. Three of these six interactions were involved with *sgg1*, *m132.2*, a major hub protein found in this study important in salivary gland replication and discussed in more detail in the protein hubs section (Table 1, Table 2, Figure 2).

The remaining interactions were between MCMV specific proteins, and MCMV proteins with homology to HCMV. Of the 170 MCMV predicted ORFs, approximately 42% of these genes have either sequence or functional homology to HCMV proteins [4]. There are thirty-two (34%) PPIs between proteins specific to MCMV, twenty-four (25%) between proteins that are homologous to HCMV and thirty-eight (40%) PPIs between HCMV homologous proteins and MCMV specific proteins. Of the twenty-four PPIs between HCMV homologous proteins four, M32-M35, M82-M35, M85-M46 and M99-M94 were found in an HCMV yeast two-hybrid also conducted in our laboratory (To, unpublished results) (Table 1).

The interactions involving core-conserved proteins confirms the importance of these proteins with respect to the virion, as discussed in chapter 2, as many of these core interactions are between the viral components which form the infectious particle [24]. The interactions discovered can also be used to identify the potential function of unknown components such as M93, which interacts with M88, a tegument protein and M46, a capsid protein. While more data and investigation into the function of M93 must be taken, it may be of interest to investigate M93 as a transporter or bridge between the capsid and the tegument—a unique feature of herpesvirus structure. The fact that M93 has not been identified as part of the virion may further suggest a role as a transport protein in early stages of viral assembly.

In terms of determining the level of interactions or types of interactions based on the conservation class of the protein, the data from both core-conserved proteins, proteins homologous to HCMV and those specific to MCMV, suggest there is no correlation between conservation class and number or types of interactions.

### **Gene deletion phenotype**

An interesting area of analysis is through the identification of essentiality in the interacting proteins identified in our screen. Using a library of deletion mutants, the

essentiality of each predicted ORF was determined through multiple time-point infections in murine NIH-3T3 fibroblast cells (Chan and Umamoto, unpublished results).

When applied to our yeast two hybrid screen. Twenty-six (26%) of the ninety-four PPIs observed are between non-essential proteins. Ten (10%) interactions were found between essential proteins. Twenty-five (25%) were between non-essential and essential proteins. Sixteen (16%) were between non-essential and attenuated proteins and eight (8%) were between essential and attenuated proteins. This data suggests that there is no correlation between gene deletion phenotype and interacting partners.

It is important to note, when considering the phenotype of gene deletions, that the data used was determined by infection of fibroblast cells. However, both MCMV and HCMV are known to infect a wide variety of cell types, and the determination of essentiality of each gene can possibly change depending on the cell type that has been infecting. This phenomenon is more evident as data from the cell line screening project discussed in chapter 4 is merged with the MCMV yeast two-hybrid data to add further layers of analysis to the horizontal research methodology which can take advantage of multiple global screens (Figures 2-6).

As observed with the MCMV interaction map created using NIH-3T3 viral growth data, many of the interacting ORF show a wild-type like growth phenotype (black) (Figure 2). However, in the other cell lines in which viral deletion mutants were assayed for growth phenotype the level of essentiality of these protein components changes. Interestingly, two hub proteins M27 and m132.2 that maintain non-essential growth phenotypes in fibroblast cells show signs of attenuation in the other cell types (Figures 3-6). This supports the previous discussion suggesting that the environment in which the virus finds itself may be important in determining the level of functional importance in each of the viral components.

Two of the more drastic changes between the cell lines occur with the ORFs, m117 and M38. Both of these proteins share only one identified interaction with another viral protein. M38, a protein potentially involved in apoptosis, shows an enhanced growth phenotype in J774A.1, macrophage cells. This phenomenon will be discussed in more detail in the next chapter (Figure 5). The m117 protein product is non-essential in fibroblast and bone marrow stromal cells (Figure 2 and 3) but shows severe attenuation in SCA-9, salivary gland cells (Figure 6). It shares an interaction with a virion component, M88, a tegument protein. While the function of m117 is unknown, this is an example of a situation where multiple global data sets can be merged to help identify the importance of an unknown viral protein. Through these studies we have potentially narrowed our investigation to salivary gland cells and may have a potential avenue of investigation with respect to M88. As it is not part of the initial infectious viral particle, m117 may interact at late stages of infection such as assembly or viral egress. Though it is important to note that the identification of components that comprise the viral particle was conducted using infected fibroblast cells [24]. And as potentially shown using rat CMV, there is differential gene expression depending on the organ or cell type infected [25]. Therefore, the actual components of the viral particle may change depending on the infected cell type. While all statements made here are purely speculative, they provide an avenue of investigation not initially available with before conducting the yeast two-hybrid study and the essentiality screens.

One final note on the determination of essentiality and its correlation with interacting partners, it is important to realize that all of these essentiality studies discussed in this chapter

and the following chapters have been conducted in vitro. The true phenotype of a gene deletion may only be discovered via in vivo infection. And this may provide a better correlation between interacting partners, as this is one of the significant reasons behind conducting a YTH assay with MCMV and using the virus as a research tool in other studies.

### Hub proteins

Interactomes of a variety of different organisms including *Drosophila melanogaster*, *Caenorhabditis elegans*, *Saccharomyces cerevisiae*, *Plasmodium falciparum* and *Helicobacter pylori* and viruses such as vaccinia virus, herpesviruses and Hepatitis C virus has shown that certain proteins interact with more partners than others [9-13]. Comparisons between hub proteins and essentiality have been undertaken to a great degree in yeast and have resulted in mixed results in determining the link between the two [19-21]. This may be due to the methods used to determine hub proteins and the databases used to determine essentiality. It may also determine on the conditions and circumstances by which these proteins are expressed and determined to be essential in, as discussed in the previous paragraph with respect to figures 2-6.

In our screen, we have determined that five proteins interact with at least ten other partners while two proteins interact with at least seven different proteins. The largest number of interactions between a single hub and numerous partners were twenty-three total PPIs. The seven proteins identified as hub proteins in MCMV are M27 (11 PPIs), M35 (7 PPIs), M72 (7 PPIs), M88 (12 PPIs), m128.3 (12 PPIs), m132.2 (23 PPIs) and m169 (11 PPIs) (Table 2, Figure 3).

In comparison, the HCMV interactome contained thirteen hub proteins identified with ten or more interactions with the largest number of interactions at thirty-four. From the MCMV screen, four of these hub proteins had homology to HCMV proteins however only one, M27, had a homologous hub protein, UL27, in the HCMV screen. However, UL27 was found to have eighteen interacting partners, seven more than what was found in MCMV. None of the homologous interactions in the M27 hub network correspond to those that were found in the UL27 hub network. This may be due to the limitation of the assay in detecting all possible interaction in the viral network or it may suggest that MCMV specific proteins have similar functions to HCMV proteins found in the HCMV YTH and have substituted those HCMV proteins in respect to the M27 network. This is supported by observation that half of the interactions involving the M27 hub are of MCMV specific origins.

The essentiality of the identified hub proteins reveals that MCMV hub proteins can be both essential and non-essential. Two hub proteins are essential, four are non-essential and one is attenuated. Essentiality does not depend on homology to HCMV and the phenotype of the hub protein does not determine the essentiality of the network proteins. Hub proteins in MCMV are both structural and non-structural components.

Of particular interest is the protein encoded by m132.2, exon 2 of what has been termed sgg1. m132.2 interacts with the most partners, twenty-three PPIs. Cytomegalovirus, both MCMV and HCMV, are considered salivary gland viruses [26]. It is in glandular epithelium that large amounts of the virus accumulate and can be excreted via saliva, thus providing an important avenue of transmission. The salivary gland is also the site of persistence where the virus can continue to replicate long after infection in other organs cease. Sgg1, or m132 represents a determinant for salivary gland infection. Deletion of this gene prevents viral

replication in only the salivary gland [27-29]. However, in tissue culture, using fibroblast cells, m132.2 is dispensable for growth. This ORF is a good example of elements of essentiality changing depending on the conditions or environment that the virus is subjected to (Figure 2-6).

While many of the interacting proteins are of unknown function, there are interacting proteins that are components of viral entry and egress. Sgg1 interacts with two glycoproteins, m13 and m74. m74 is potentially involved in entry via fusion with the host cell membrane [30]. CMV facilitates entry via a myriad of glycoproteins and vary in its ability to enter specific cell types from fusion to endocytosis [31]. And it is possible that with respect to the salivary gland, sgg1 could help provide or sequester the necessary components, whether cellular or viral in origin, in order to create viral particles that are successful at infecting a particular cell type. Other interactions of importance are M27, potential immune response inhibitor, components of nuclear egress, M53 and viral replication, m128.3, ie2. The presence of M27 and m128.3 in the sgg1 protein network also adds new layers of interactions as both are hub proteins at the center of large networks. There is no correlation between essentiality and interacting partners as m132.2 interacts with both essential and non-essential components.

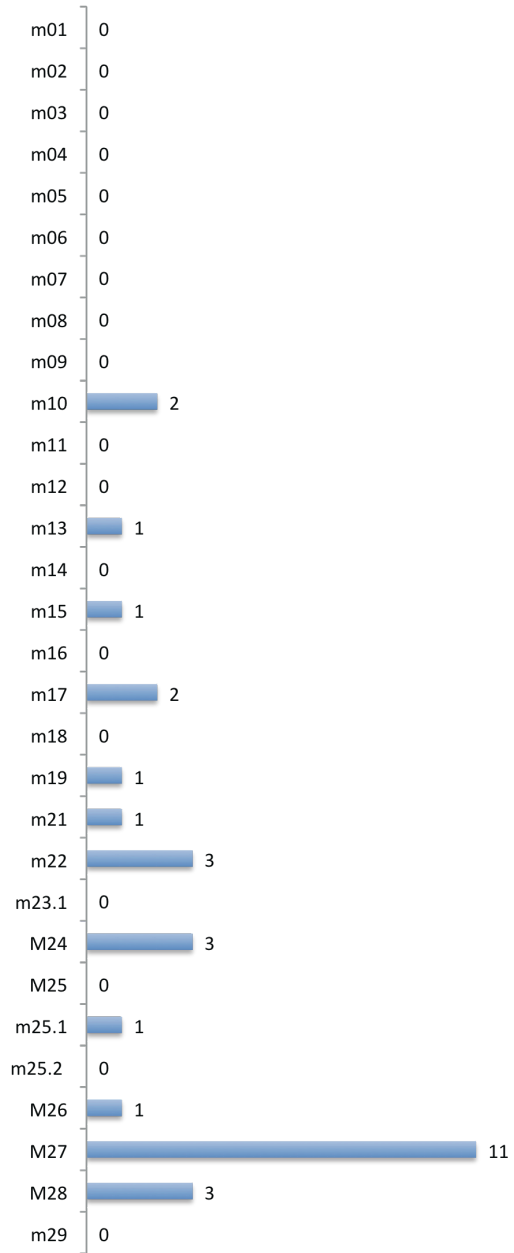
Only one of these hub proteins is one of the core proteins, M72. However, the other interacting hub proteins do interact with core proteins. This contrasts with the five core proteins that have been found to be hubs in HCMV. UL72, the M72 homolog, however, was not identified as one of them. UL72 functions as a dUTPase, while the M72 function has yet to be determined. Interacting partners suggest a wide range of potential functions ranging from immune evasion to viral replication.

## **Conclusion**

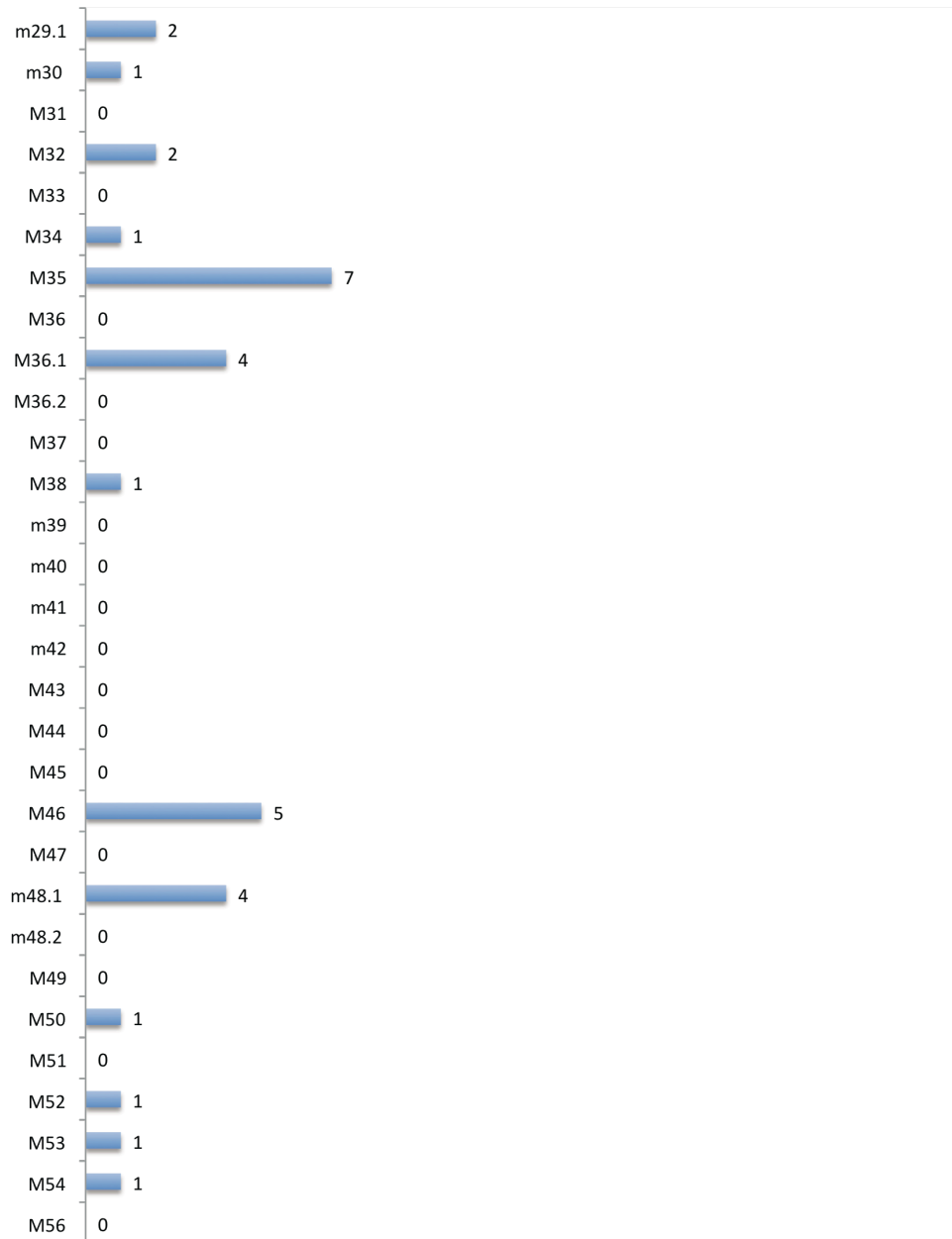
Global screening projects such as yeast two-hybrid can provide many clues to the potential function of a protein; however, they can also cause confusion in these terms as well. Adding other potential data sources such as gene expression kinetics, functional analysis, and growth phenotype can also help provide the clues to help answer potential questions about the function of particular proteins in regards to the whole organism. However, as in the case of growth phenotype, there is a potential for misinterpretation of data if all conditions are not considered. For an organism like CMV that can infect multiple cell types it is important to consider other conditions in which a gene or protein may prove important or essential. Global analysis represents an important stepping-stone for investigating individual genes in depth. It provides a starting point to help direct vertical scientific approaches and the formation of specific detailed hypothesis.



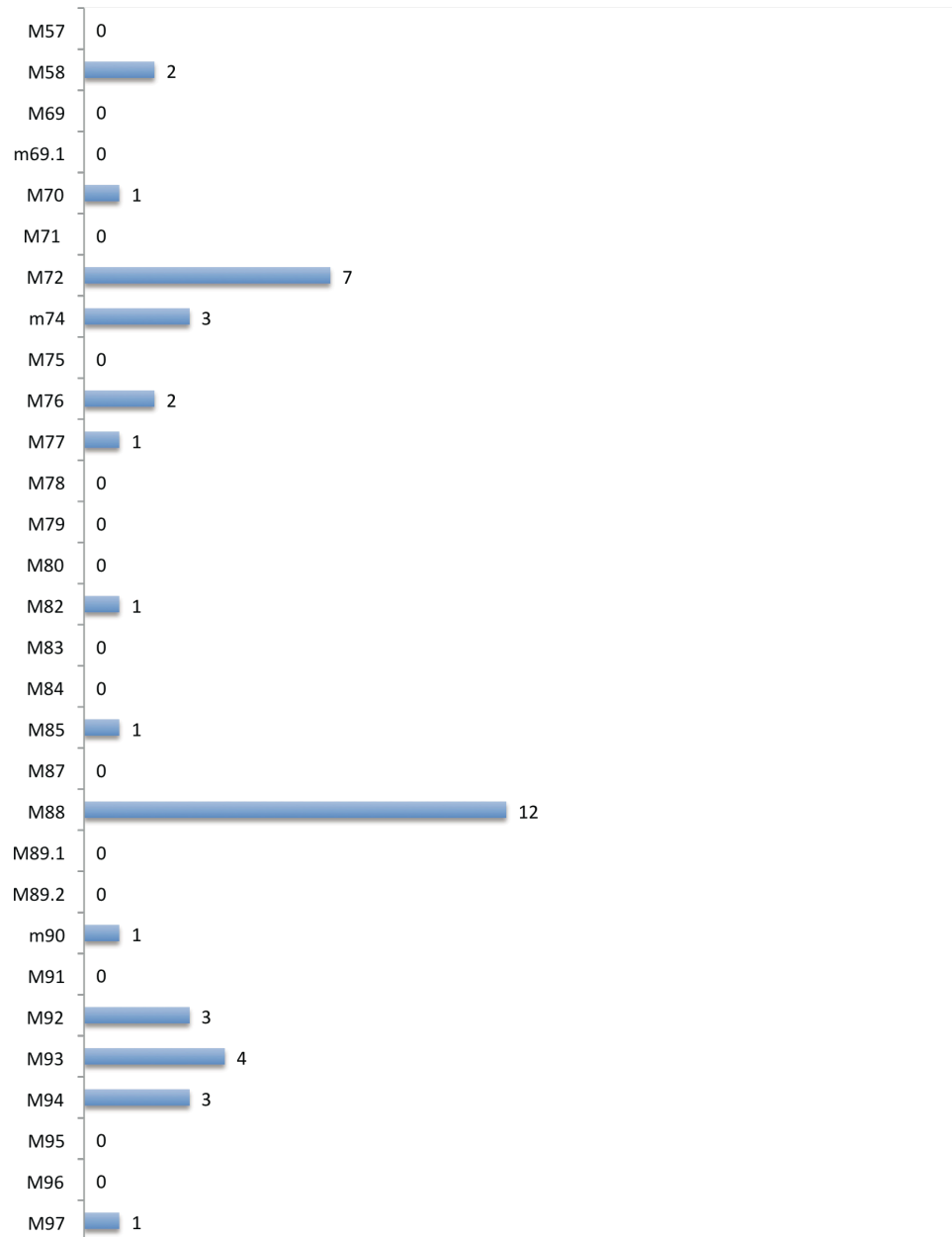
# # of PPIs



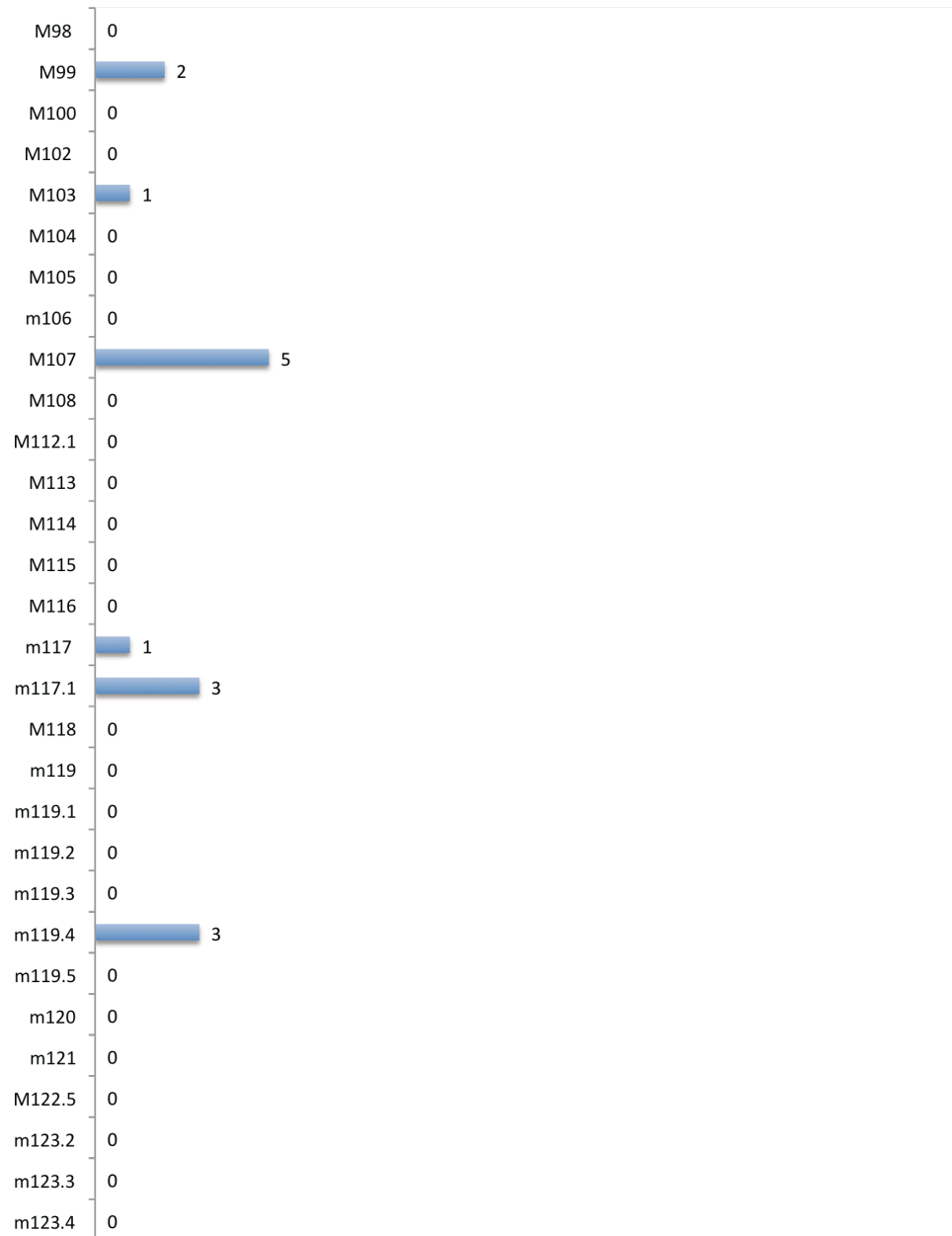
## # of PPIs



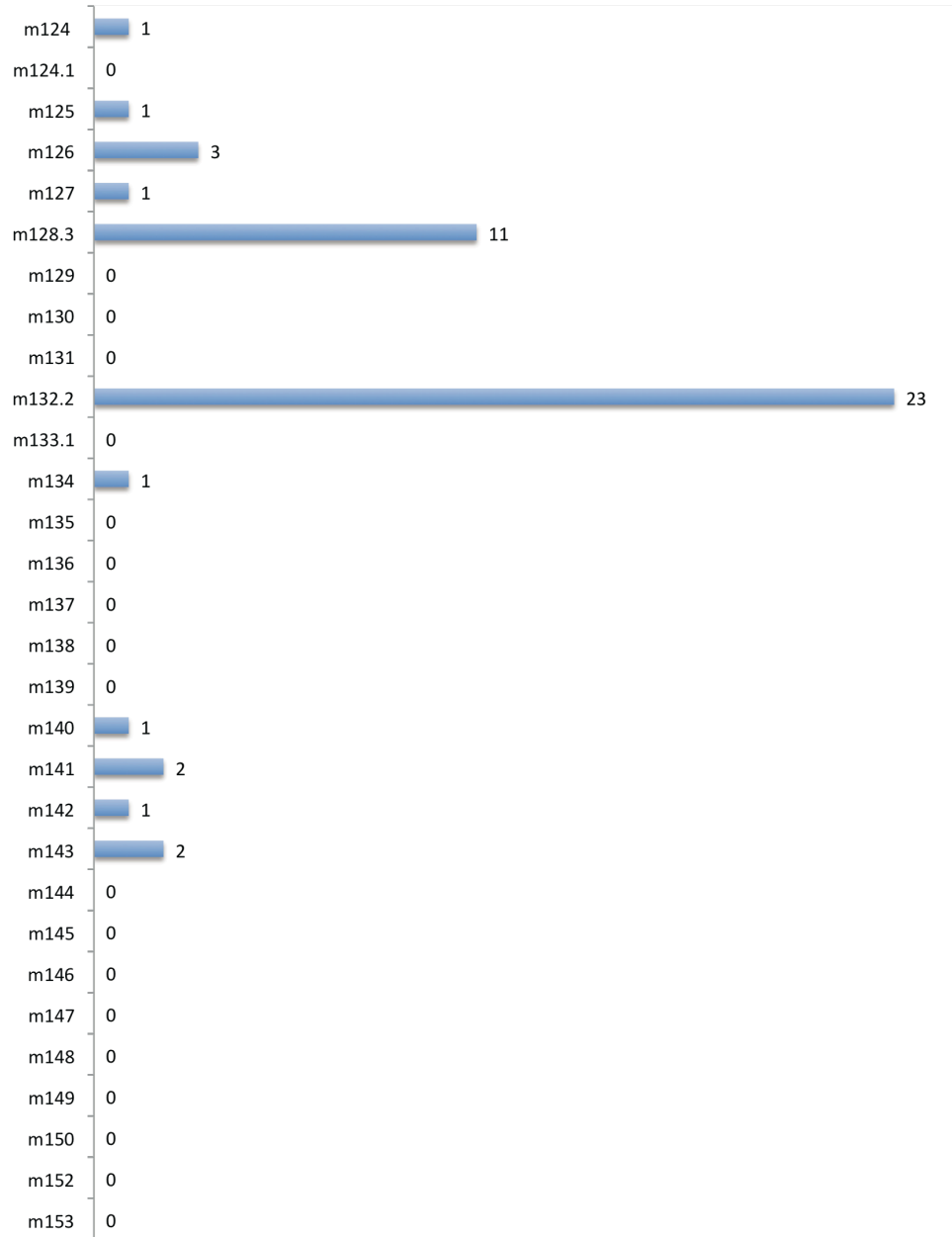
## # of PPIs



## # of PPIs



### # of PPIs



## # of PPIs

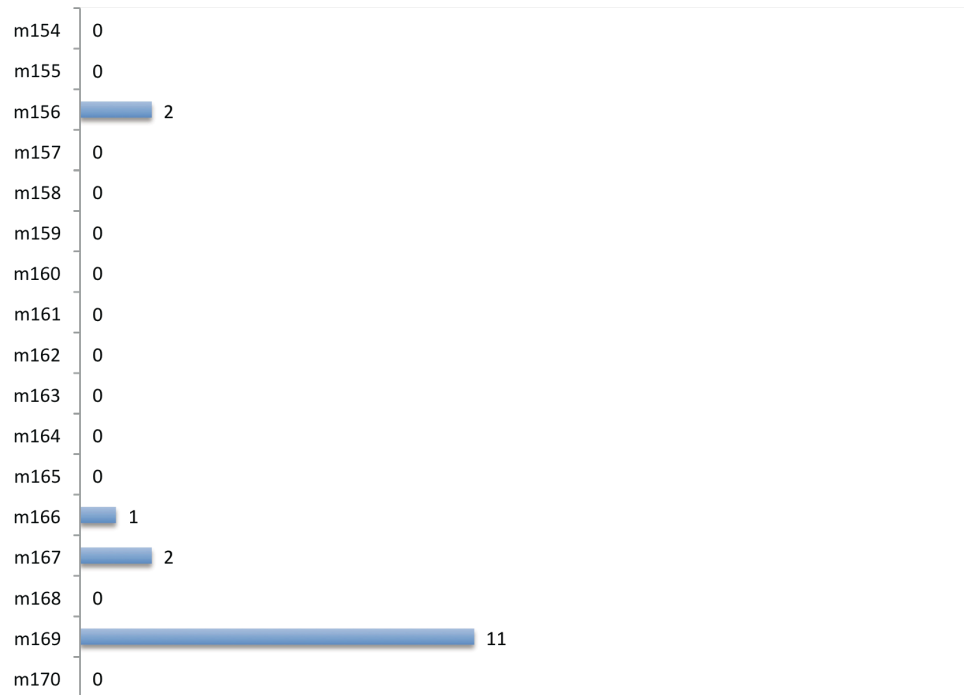


**Figure 1. Distribution of MCMV Protein Interactions.**

The total number of protein-protein interactions for individual MCMV protein found in the yeast two-hybrid assay are listed. The vertical axis represents each MCMV protein and the total number of interactions are shown as bar values.

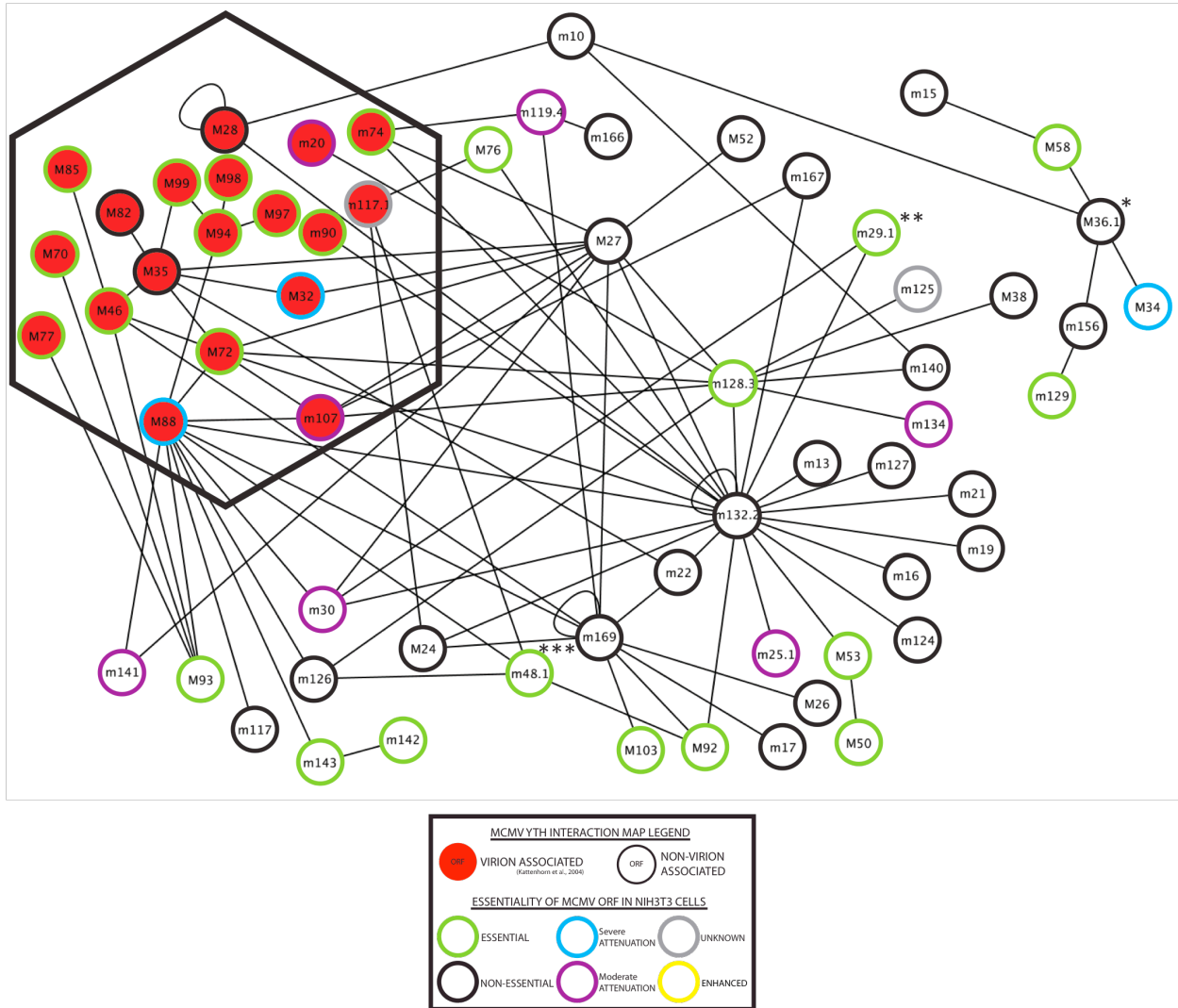


**Figure 2. MCMV interaction Map.**

The interaction map displays the 96 interactions between 63 MCMV proteins as found by yeast two-hybrid analysis. Each node or protein is shown as a circle and each interaction is shown as a single solid line. MCMV proteins which are associated with the virion are represented by a filled red circle. Circle borders are colored to depict the essentiality of each MCMV ORF as determined by viral titration assays using single deletion MCMV BAC mutants (psm3fr) in NIH3T3 murine fibroblast cells. Green: essential gene, black: non-essential gene, blue: severe attenuation, purple: moderate attenuation and grey: unknown phenotype.





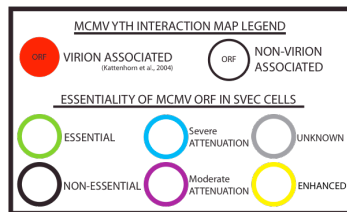
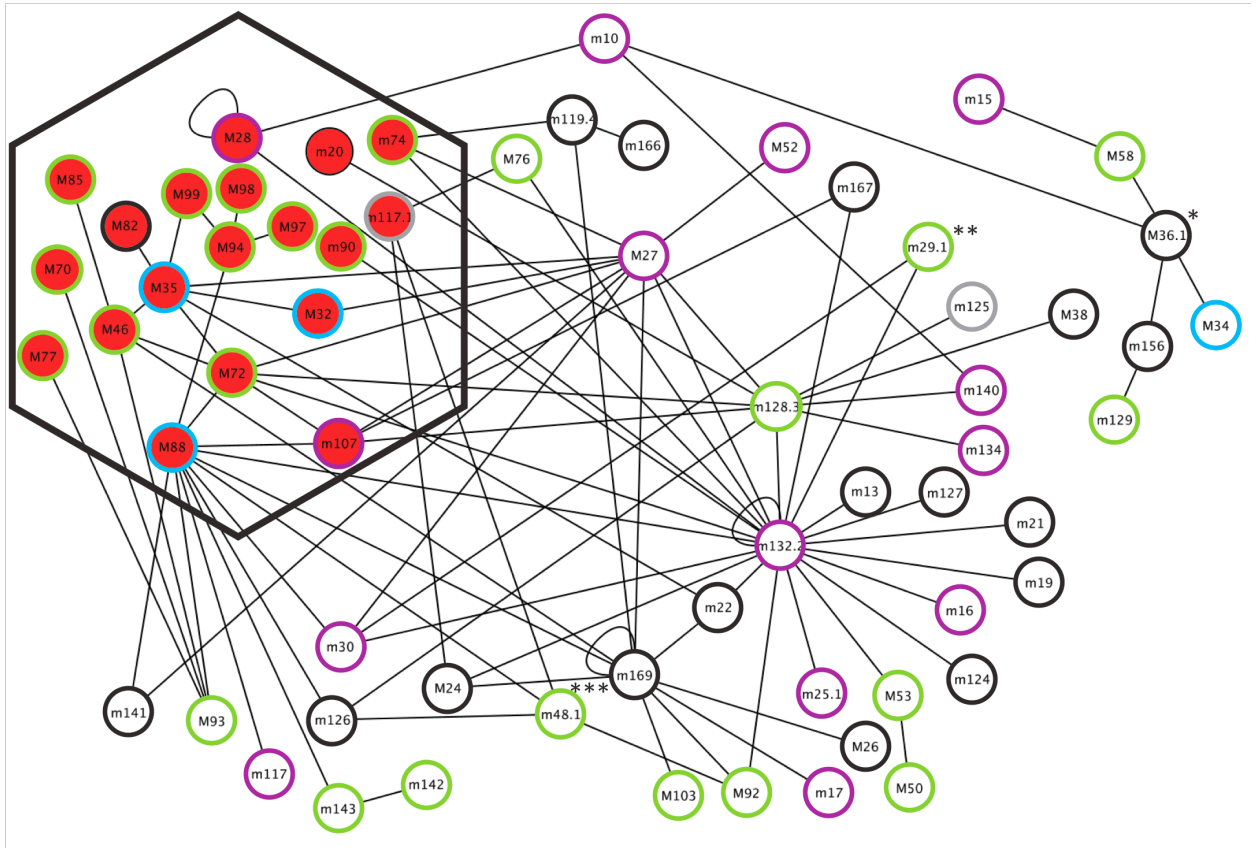


**Figure 4. MCMV interaction Map: SVEC essentiality.**

The interaction map displays the 96 interactions between 63 MCMV proteins as found by yeast two-hybrid analysis. Each node or protein is shown as a circle and each interaction is shown as a single solid line. MCMV proteins which are associated with the virion are represented by a filled red circle. Circle borders are colored to depict the essentiality of each MCMV ORF as determined by viral titration assays using single deletion MCMV BAC mutants (psm3fr) in SVEC cells. Green: essential gene, black: non-essential gene, blue: severe attenuation, purple: moderate attenuation and grey: unknown phenotype.



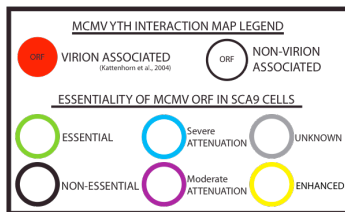
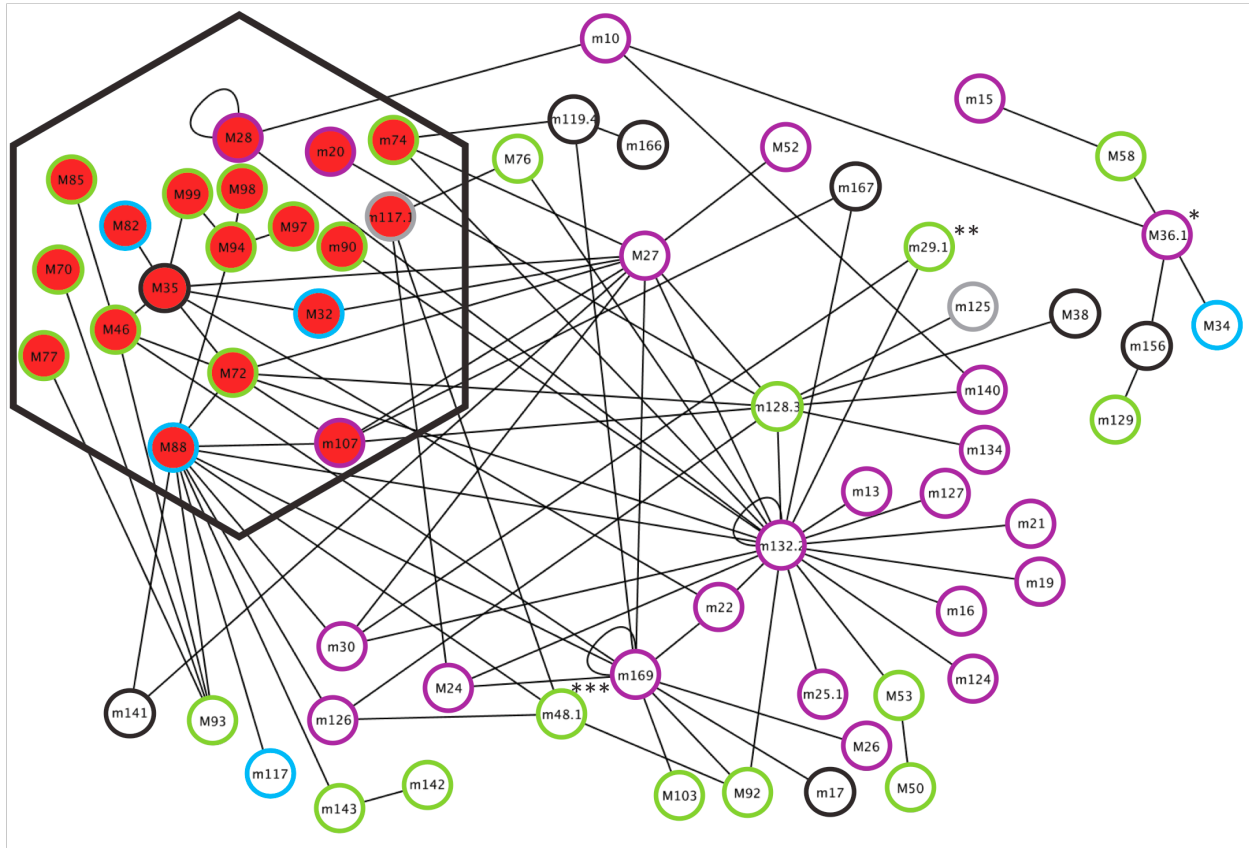


**Figure 6. MCMV interaction Map: SCA-9 essentiality.**

The interaction map displays the 96 interactions between 63 MCMV proteins as found by yeast two-hybrid analysis. Each node or protein is shown as a circle and each interaction is shown as a single solid line. MCMV proteins which are associated with the virion are represented by a filled red circle. Circle borders are colored to depict the essentiality of each MCMV ORF as determined by viral titration assays using single deletion MCMV BAC mutants (psm3fr) in SCA9 cells. Green: essential gene, black: non-essential gene, blue: severe attenuation, purple: moderate attenuation and grey: unknown phenotype.

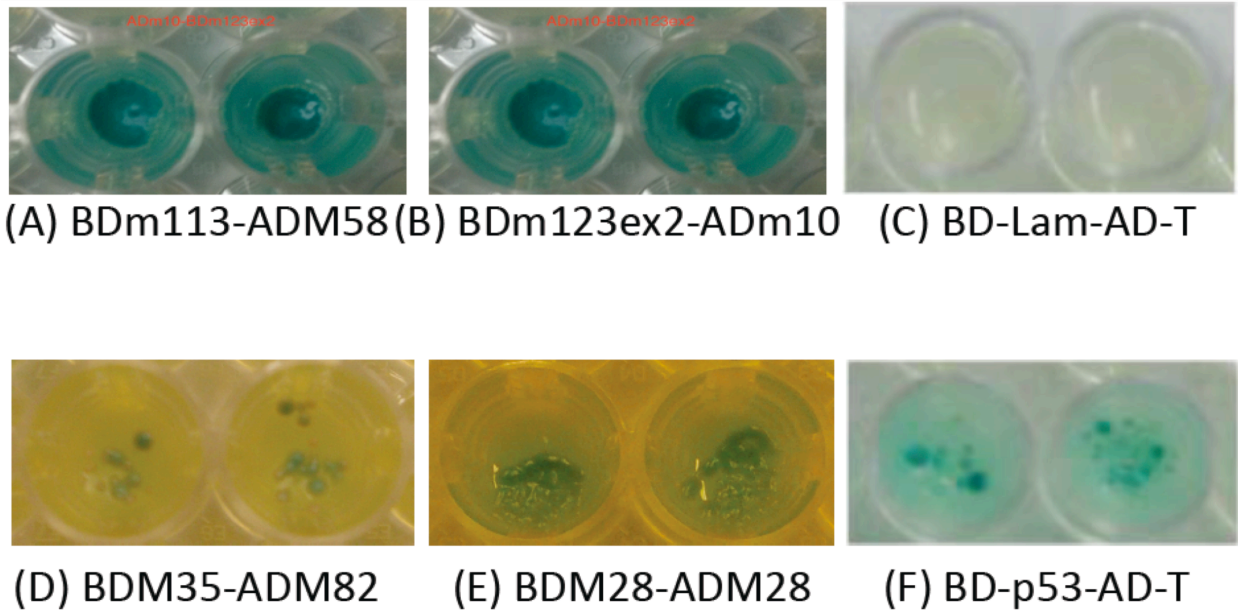


**Figure 7. Yeast Two Hybrid Interactions**

Examples of positive yeast two-hybrid interactions are shown (A, B, D and E). Positive (F) and negative (C) controls were used to test the validity of the assay.

**Table 1. MCMV Protein-Protein Interactions**

							HCMV
AD ORFs	Function	Essentiality	BD ORFs	Function	Essentiality	YTH	
1	m10	glycoprotein family m02	wt	M28	unknown	wt	
2	m10	glycoprotein family m02	wt	M36.1	US22 family homolog	wt	
3	M24	dsRNA binding protein	wt	m117.1	unknown	?	
4	M27	IFN gamma interference	wt	m128.3	ie2	essential	
5	M28	unknown	wt	M28	unknown	wt	
6	M30	unknown	wt	M27	IFN gamma interference	wt	
7	M30	unknown	wt	m29.1	unknown	essential	
8	M30	unknown	wt	M88	tegument	defect	
9	M30	unknown	wt	m128.3	ie2	essential	
10	M32	tegument	defect	M27	IFN gamma interference	wt	
11	M34	transcriptional replication	defect	M36.1	vICA (exon 1)	wt	
12	M35	M25/UL25 gene family	wt	m22	unknown	wt	
13	M35	M25/UL25 gene family	wt	M27	IFN gamma interference	wt	
14	M35	M25/UL25 gene family	wt	M32	tegument	defect	x
15	M35	M25/UL25 gene family	wt	M46	minor capsid protein	essential	
16	M35	M25/UL25 gene family	wt	M99	tegument (pp28 phosphoprotein)	essential	
17	M38	contains part of m38.5 (mitochondrial interaction)	wt	m128.3	ie2	essential	
18	m48.1	unknown	?	M88	tegument	defect	
19	m48.1	unknown	?	M92	unknown	essential	
20	m48.1	unknown	?	m117.1	unknown	?	
21	m48.1	unknown	?	m126	unknown	wt	
22	M52	unknown	wt	M27	IFN gamma interference	wt	
23	M53	nuclear egress	essential	M50	nuclear egress	essential	
24	m58	unknown	essential	m15	glycoprotein family m02	wt	
25	m58	unknown	essential	M36.1	vICA (exon 1)	wt	
26	M70	primase (HCMV)	essential	M93	unknown	essential	
27	M72	dUTPase	essential	M27	IFN gamma interference	wt	
28	M72	dUTPase	essential	M35	M25/UL25 gene family	wt	
29	M72	dUTPase	essential	M46	unknown	essential	
30	M72	dUTPase	essential	M88	tegument	defect	
31	M72	dUTPase	essential	m128.3	ie2	essential	
32	m74	glycoprotein	essential	M27	IFN gamma interference	wt	
33	m74	glycoprotein	essential	m119.4	unknown	defect	
34	M76	unknown	essential	m117.1	unknown	?	
35	M82	upper matrix phosphoprotein	wt	M35	M25/UL25 gene family	wt	x
36	M85	capsid protein	essential	M46	minor capsid protein	essential	x
37	M88	tegument	defect	m143	pkR inhibition	essential	
38	M93	unknown	essential	M46	minor capsid protein	essential	
39	M93	unknown	essential	M77	unknown	essential	
40	M93	unknown	essential	M88	tegument	defect	
41	M94	putative DNA binding protein (HCMV)	essential	M88	tegument	defect	
42	M94	putative DNA binding protein (HCMV)	essential	M97	protein kinase	essential	
43	M99	tegument (pp28 phosphoprotein)	essential	M94	putative DNA binding protein (HCMV)	essential	x
44	m107	unknown	defect	M27	IFN gamma interference	wt	
45	m107	unknown	defect	M72	dUTPase	essential	
46	m107	unknown	defect	M88	tegument	defect	
47	m107	unknown	defect	m128.3	ie2	essential	



				HCMV		
AD ORFs	Function	Essentiality	BD ORFs	Function	Essentiality	YTH
48	m107	unknown	defect	m167	unknown	wt
49	m117	unknown	wt	M88	tegument	defect
50	m125	unknown	?	m128.3	ie2	essential
51	m126	unknown	wt	M88	tegument	defect
52	m126	unknown	wt	m128.3	ie2	essential
53	m132.2	sgg1 (exon2)	wt	m17	unknown	wt
54	m132.2	sgg1 (exon2)	wt	m19	unknown	wt
55	m132.2	sgg1 (exon2)	wt	m21	unknown	wt
56	m132.2	sgg1 (exon2)	wt	m22	unknown	wt
57	m132.2	sgg1 (exon2)	wt	M24	dsRNA binding protein	wt
58	m132.2	sgg1 (exon2)	wt	m25.1	US22 family homolog	defect
59	m132.2	sgg1 (exon2)	wt	M27	IFN gamma interference	wt
60	m132.2	sgg1 (exon2)	wt	M28	unknown	wt
61	m132.2	sgg1 (exon2)	wt	m29.1	unknown	essential
62	m132.2	sgg1 (exon2)	wt	m30	unknown	defect
63	m132.2	sgg1 (exon2)	wt	M53	nuclear egress	essential
64	m132.2	sgg1 (exon2)	wt	M72	unknown	essential
65	m132.2	sgg1 (exon2)	wt	m74	glycoprotein	essential
66	m132.2	sgg1 (exon2)	wt	M76	unknown	essential
67	m132.2	sgg1 (exon2)	wt	M88	tegument	defect
68	m132.2	sgg1 (exon2)	wt	m90	unknown	essential
69	m132.2	sgg1 (exon2)	wt	M92	unknown	essential
70	m132.2	sgg1 (exon2)	wt	m124	unknown	wt
71	m132.2	sgg1 (exon2)	wt	m127	unknown	wt
72	m132.2	sgg1 (exon2)	wt	m128.3	ie2	essential
73	m132.2	sgg1 (exon2)	wt	m132.2	sgg1 (exon 2)	wt
74	m132.2	sgg1 (exon2)	wt	m167	unknown	wt
75	m132.2	sgg1 (exon2)	wt	m13	glycoprotein family m02	wt
76	m134	unknown	defect	m128.3	ie2	essential
77	m140	US22 family homolog	wt	m128.3	ie2	essential
78	m141	US22 family homolog	defect	M27	IFN gamma interference	wt
79	m141	US22 family homolog	defect	M88	tegument	defect
80	m142	US22 family homolog	essential	m143	pkR inhibition	essential
81	m156	unknown	wt	M36.1	vICA (exon 1)	wt
82	m156	unknown	wt	m128.3	ie2	essential
83	m166	unknown	wt	m119.4	unknown	defect
84	m169	unknown	wt	m17	unknown	wt
85	m169	unknown	wt	m22	unknown	wt
86	m169	unknown	wt	M24	dsRNA binding protein	wt
87	m169	unknown	wt	M26	unknown	wt
88	m169	unknown	wt	M27	IFN gamma interference	wt
89	m169	unknown	wt	M46	minor capsid protein	essential
90	m169	unknown	wt	M88	tegument	defect
91	m169	unknown	wt	M92	unknown	essential
92	m169	unknown	wt	M103	unknown	essential
93	m169	unknown	wt	m119.4	unknown	defect
94	m169	unknown	wt	m169	unknown	wt

Table 2. Hub Proteins.

Hub Protein	Essentiality	Function	
<b>M27</b>	wt	Ifn $\gamma$ interference	
Interaction	Essentiality	Function	
1	M30	wt	unknown
2	M32	defect	tegument
3	M35	wt	M25/UL25 family
4	M52	wt	unknown
5	M72	essential	dUTPase
6	m74	essential	glycoprotein
7	m107	defect	unknown
8	m128.3	essential	ie2
9	m132.2	wt	sgg1 (exon 2)
10	m141	defect	US22 family
11	m169	wt	unknown

Hub Protein	Essentiality	Function	
<b>M35</b>	wt	M25/UL25 family	
Interaction	Essentiality	Function	
1	m22	wt	unknown
2	M27	wt	Ifn $\gamma$ interference
3	M32	defect	tegument
4	M46	essential	minor capsid
5	M72	essential	unknown
6	M82	wt	phosphoprotein
7	M99	essential	pp28

Hub Protein	Essentiality	Function	
<b>m128.3</b>	essential	ie2	
Interaction	Essentiality	Function	
1	M27	wt	Ifn $\gamma$ interference
2	M30	wt	unknown
3	M38	wt	mitochondrial (?)
4	M72	essential	dUTPase
5	m107	defect	unknown
6	m125	unknown	unknown
7	m126	wt	unknown
8	m128.3	essential	ie2
9	m132.2	wt	sgg1
10	m134	defect	unknown
11	m140	wt	US22 family
12	m156	wt	unknown

Hub Protein	Essentiality	Function	
<b>M72</b>	essential	unknown	
Interaction	Essentiality	Function	
1	M27	wt	Ifn $\gamma$ interference
2	M35	wt	M25/UL25 family
3	M46	essential	minor capsid
4	M88	defect	tegument
5	m107	defect	unknown
6	m128.3	essential	ie2
7	m132.2	wt	sgg1

Hub Protein	Essentiality	Function	
<b>m132.2</b>	wt	sgg1	
Interaction	Essentiality	Function	
1	m13	wt	m02 family
2	m17	wt	unknown
3	m19	wt	unknown
4	m21	wt	unknown
5	m22	wt	unknown
6	M24	wt	dsRNA binding prt
7	m25.1	defect	US22
8	M27	wt	Ifn $\gamma$ interference
9	M28	wt	unknown
10	m29.1	essential	unknown
11	m30	defect	unknown
12	M53	essential	nuclear egress
13	M72	essential	unknown
14	m74	essential	glycoprotein
15	M76	essential	unknown
16	M88	defect	tegument
17	m90	essential	unknown
18	M92	essential	unknown
19	m124	wt	unknown
20	m127	wt	unknown
21	m128.3	essential	ie2
22	m132.2	wt	sgg1
23	m167	wt	unknown

Hub Protein	Essentiality	Function	
<b>m169</b>	wt	unknown	
Interaction	Essentiality	Function	
1	m17	wt	unknown
2	m22	wt	unknown
3	M24	wt	dsRNA binding prt
4	M26	wt	unknown
5	M27	wt	Ifn $\gamma$ interference
6	M46	essential	minor capsid
7	M88	defect	tegument
8	M92	essential	unknown
9	M103	essential	unknown
10	m119.4	defect	unknown
11	m169	wt	unknown

Hub Protein	Essentiality	Function	
<b>M88</b>	defect	tegument	
Interaction	Essentiality	Function	
1	M30	wt	unknown
2	m48.1	unknown	unknown
3	M72	essential	dUTPase
4	M93	essential	unknown
5	M94	essential	DNA binding prt
6	m107	defect	unknown
7	m117	wt	unknown
8	m126	wt	unknown
9	m132.2	wt	sgg1
10	m141	defect	US22 family
11	m143	essential	pkR inhibition
12	m169	wt	unknown









AD / BD	m01	m02	m03	m04	m05	m06	m07	m08	m09	m10	m11	m12	m13	m14	m15	m16	m17	m18	m19	m20	m21	m22	M23	m23.1	M24	M25	m25.1	m25.2	M26	M27	M28	m29.1	m30	M31	
m142	-	-	-	-	-	-	-	-	-	-	-	-	-	-	-	-	-	AA	-	-	-	-	-	AA	-	-	-	-	-	-	-	-	-	-	
m143	-	-	-	-	-	-	-	-	-	-	-	-	-	-	-	-	-	AA	-	-	-	-	-	AA	-	-	-	-	-	-	-	-	-	-	-
m144	-	-	-	-	-	-	-	-	-	-	-	-	-	-	-	-	-	AA	-	-	-	-	-	AA	-	-	-	-	-	-	-	-	-	-	-
m145	-	-	-	-	-	-	-	-	-	-	-	-	-	-	-	-	-	AA	-	-	-	-	-	AA	-	-	-	-	-	-	-	-	-	-	-
m146	-	-	-	-	-	-	-	-	-	-	-	-	-	-	-	-	-	AA	-	-	-	-	-	AA	-	-	-	-	-	-	-	-	-	-	-
m147	-	-	-	-	-	-	-	-	-	-	-	-	-	-	-	-	-	AA	-	-	-	-	-	AA	-	-	-	-	-	-	-	-	-	-	-
m148	-	-	-	-	-	-	-	-	-	-	-	-	-	-	-	-	-	AA	-	-	-	-	-	AA	-	-	-	-	-	-	-	-	-	-	-
m149	-	-	-	-	-	-	-	-	-	-	-	-	-	-	-	-	-	AA	-	-	-	-	-	AA	-	-	-	-	-	-	-	-	-	-	-
m150	-	-	-	-	-	-	-	-	-	-	-	-	-	-	-	-	-	AA	-	-	-	-	-	AA	-	-	-	-	-	-	-	-	-	-	-
m151	-	-	-	-	-	-	-	-	-	-	-	-	-	-	-	-	-	-	-	-	-	-	-	-	-	-	-	-	-	-	-	-	-	-	-
m152	-	-	-	-	-	-	-	-	-	-	-	-	-	-	-	-	-	AA	-	-	-	-	-	AA	-	-	-	-	-	-	-	-	-	-	-
m153	-	-	-	-	-	-	-	-	-	-	-	-	-	-	-	-	-	AA	-	-	-	-	-	AA	-	-	-	-	-	-	-	-	-	-	-
m154	-	-	-	-	-	-	-	-	-	-	-	-	-	-	-	-	-	AA	-	-	-	-	-	AA	-	-	-	-	-	-	-	-	-	-	-
m155	-	-	-	-	-	-	-	-	-	-	-	-	-	-	-	-	-	AA	-	-	-	-	-	AA	-	-	-	-	-	-	-	-	-	-	-
m156	-	-	-	-	-	-	-	-	-	-	-	-	-	-	-	-	-	AA	-	-	-	-	-	AA	-	-	-	-	-	-	-	-	-	-	-
m157	-	-	-	-	-	-	-	-	-	-	-	-	-	-	-	-	-	AA	-	-	-	-	-	AA	-	-	-	-	-	-	-	-	-	-	-
m158	-	-	-	-	-	-	-	-	-	-	-	-	-	-	-	-	-	AA	-	-	-	-	-	AA	-	-	-	-	-	-	-	-	-	-	-
m159	-	-	-	-	-	-	-	-	-	-	-	-	-	-	-	-	-	AA	-	-	-	-	-	AA	-	-	-	-	-	-	-	-	-	-	-
m160	-	-	-	-	-	-	-	-	-	-	-	-	-	-	-	-	-	AA	-	-	-	-	-	AA	-	-	-	-	-	-	-	-	-	-	-
m161	-	-	-	-	-	-	-	-	-	-	-	-	-	-	-	-	-	AA	-	-	-	-	-	AA	-	-	-	-	-	-	-	-	-	-	-
m162	-	-	-	-	-	-	-	-	-	-	-	-	-	-	-	-	-	AA	-	-	-	-	-	AA	-	-	-	-	-	-	-	-	-	-	-
m163	-	-	-	-	-	-	-	-	-	-	-	-	-	-	-	-	-	AA	-	-	-	-	-	AA	-	-	-	-	-	-	-	-	-	-	-
m164	-	-	-	-	-	-	-	-	-	-	-	-	-	-	-	-	-	AA	-	-	-	-	-	AA	-	-	-	-	-	-	-	-	-	-	-
m165	-	-	-	-	-	-	-	-	-	-	-	-	-	-	-	-	-	AA	-	-	-	-	-	AA	-	-	-	-	-	-	-	-	-	-	-
m166	-	-	-	-	-	-	-	-	-	-	-	-	-	-	-	-	-	AA	-	-	-	-	-	AA	-	-	-	-	-	-	-	-	-	-	-
m167	-	-	-	-	-	-	-	-	-	-	-	-	-	-	-	-	-	AA	-	-	-	-	-	AA	-	-	-	-	-	-	-	-	-	-	-
m168	-	-	-	-	-	-	-	-	-	-	-	-	-	-	-	-	-	AA	-	-	-	-	-	AA	-	-	-	-	-	-	-	-	-	-	-
m169	-	-	-	-	-	-	-	-	-	-	-	-	-	-	-	-	P	AA	-	-	-	P	-	AA	P	-	-	-	P	P	-	-	-	-	-
m170	-	-	-	-	-	-	-	-	-	-	-	-	-	-	-	-	-	AA	-	-	-	-	-	AA	-	-	-	-	-	-	-	-	-	-	-







AD / BD	M32	M33	M34	M35	M36	M36.1	M36.2	M37	M38	m39	m40	m41	m42	M43	M44	M45	m45.1	M46	M47	M48	m48.1	m48.2	M49	M50	M51	M52	M53	M54	M55	M56	M57	M58	m59	M69	m69.1
m142	-	-	AA	-	-	-	-	-	-	-	-	-	-	-	-	-	-	-	-	-	-	-	-	-	-	-	-	-	-	-	-	-	-	-	-
m143	-	-	AA	-	-	-	-	-	-	-	-	-	-	-	-	-	-	-	-	-	-	-	-	-	-	-	-	-	-	-	-	-	-	-	-
m144	-	-	AA	-	-	-	-	-	-	-	-	-	-	-	-	-	-	-	-	-	-	-	-	-	-	-	-	-	-	-	-	-	-	-	-
m145	-	-	AA	-	-	-	-	-	-	-	-	-	-	-	-	-	-	-	-	-	-	-	-	-	-	-	-	-	-	-	-	-	-	-	-
m146	-	-	AA	-	-	-	-	-	-	-	-	-	-	-	-	-	-	-	-	-	-	-	-	-	-	-	-	-	-	-	-	-	-	-	-
m147	-	-	AA	-	-	-	-	-	-	-	-	-	-	-	-	-	-	-	-	-	-	-	-	-	-	-	-	-	-	-	-	-	-	-	-
m148	-	-	AA	-	-	-	-	-	-	-	-	-	-	-	-	-	-	-	-	-	-	-	-	-	-	-	-	-	-	-	-	-	-	-	-
m149	-	-	AA	-	-	-	-	-	-	-	-	-	-	-	-	-	-	-	-	-	-	-	-	-	-	-	-	-	-	-	-	-	-	-	-
m150	-	-	AA	-	-	-	-	-	-	-	-	-	-	-	-	-	-	-	-	-	-	-	-	-	-	-	-	-	-	-	-	-	-	-	-
m151	-	-	-	-	-	-	-	-	-	-	-	-	-	-	-	-	-	-	-	-	-	-	-	-	-	-	-	-	-	-	-	-	-	-	-
m152	-	-	AA	-	-	-	-	-	-	-	-	-	-	-	-	-	-	-	-	-	-	-	-	-	-	-	-	-	-	-	-	-	-	-	-
m153	-	-	AA	-	-	-	-	-	-	-	-	-	-	-	-	-	-	-	-	-	-	-	-	-	-	-	-	-	-	-	-	-	-	-	-
m154	-	-	AA	-	-	-	-	-	-	-	-	-	-	-	-	-	-	-	-	-	-	-	-	-	-	-	-	-	-	-	-	-	-	-	-
m155	-	-	AA	-	-	-	-	-	-	-	-	-	-	-	-	-	-	-	-	-	-	-	-	-	-	-	-	-	-	-	-	-	-	-	-
m156	-	-	AA	-	-	P	-	-	-	-	-	-	-	-	-	-	-	-	-	-	-	-	-	-	-	-	-	-	-	-	-	-	-	-	-
m157	-	-	AA	-	-	-	-	-	-	-	-	-	-	-	-	-	-	-	-	-	-	-	-	-	-	-	-	-	-	-	-	-	-	-	-
m158	-	-	AA	-	-	-	-	-	-	-	-	-	-	-	-	-	-	-	-	-	-	-	-	-	-	-	-	-	-	-	-	-	-	-	-
m159	-	-	AA	-	-	-	-	-	-	-	-	-	-	-	-	-	-	-	-	-	-	-	-	-	-	-	-	-	-	-	-	-	-	-	-
m160	-	-	AA	-	-	-	-	-	-	-	-	-	-	-	-	-	-	-	-	-	-	-	-	-	-	-	-	-	-	-	-	-	-	-	-
m161	-	-	AA	-	-	-	-	-	-	-	-	-	-	-	-	-	-	-	-	-	-	-	-	-	-	-	-	-	-	-	-	-	-	-	-
m162	-	-	AA	-	-	-	-	-	-	-	-	-	-	-	-	-	-	-	-	-	-	-	-	-	-	-	-	-	-	-	-	-	-	-	-
m163	-	-	AA	-	-	-	-	-	-	-	-	-	-	-	-	-	-	-	-	-	-	-	-	-	-	-	-	-	-	-	-	-	-	-	-
m164	-	-	AA	-	-	-	-	-	-	-	-	-	-	-	-	-	-	-	-	-	-	-	-	-	-	-	-	-	-	-	-	-	-	-	-
m165	-	-	AA	-	-	-	-	-	-	-	-	-	-	-	-	-	-	-	-	-	-	-	-	-	-	-	-	-	-	-	-	-	-	-	-
m166	-	-	AA	-	-	-	-	-	-	-	-	-	-	-	-	-	-	-	-	-	-	-	-	-	-	-	-	-	-	-	-	-	-	-	-
m167	-	-	AA	-	-	-	-	-	-	-	-	-	-	-	-	-	-	-	-	-	-	-	-	-	-	-	-	-	-	-	-	-	-	-	-
m168	-	-	AA	-	-	-	-	-	-	-	-	-	-	-	-	-	-	-	-	-	-	-	-	-	-	-	-	-	-	-	-	-	-	-	-
m169	-	-	AA	-	-	-	-	-	-	-	-	-	-	-	-	-	-	P	-	-	-	-	-	-	-	-	-	-	-	-	-	-	-	-	-
m170	-	-	AA	-	-	-	-	-	-	-	-	-	-	-	-	-	-	-	-	-	-	-	-	-	-	-	-	-	-	-	-	-	-	-	-





























## References

1. Davison, A.J., *Herpesvirus Genes*. Reviews in Medical Virology, 1993. 3: p. 237-244.
2. Vidal, M., *A biological atlas of functional maps*. Cell, 2001. 104(3): p. 333-9.
3. Krmpotic, A., et al., *Pathogenesis of murine cytomegalovirus infection*. Microbes Infect, 2003. 5(13): p. 1263-77.
4. Rawlinson, W.D., H.E. Farrell, and B.G. Barrell, *Analysis of the complete DNA sequence of murine cytomegalovirus*. J Virol, 1996. 70(12): p. 8833-49.
5. Scalzo, A.A., et al., *The interplay between host and viral factors in shaping the outcome of cytomegalovirus infection*. Immunol Cell Biol, 2007. 85(1): p. 46-54.
6. Reddehase, M.J., J. Podlech, and N.K. Grzimek, *Mouse models of cytomegalovirus latency: overview*. J Clin Virol, 2002. 25 Suppl 2: p. S23-36.
7. Brocchieri, L., et al., *Predicting coding potential from genome sequence: application to betaherpesviruses infecting rats and mice*. J Virol, 2005. 79(12): p. 7570-96.
8. Fields, S. and O. Song, *A novel genetic system to detect protein-protein interactions*. Nature, 1989. 340(6230): p. 245-6.
9. Giot, L., et al., *A protein interaction map of Drosophila melanogaster*. Science, 2003. 302(5651): p. 1727-36.
10. Ito, T., et al., *A comprehensive two-hybrid analysis to explore the yeast protein interactome*. Proc Natl Acad Sci U S A, 2001. 98(8): p. 4569-74.
11. LaCount, D.J., et al., *A protein interaction network of the malaria parasite Plasmodium falciparum*. Nature, 2005. 438(7064): p. 103-7.
12. Li, S., et al., *A map of the interactome network of the metazoan C. elegans*. Science, 2004. 303(5657): p. 540-3.
13. Rain, J.C., et al., *The protein-protein interaction map of Helicobacter pylori*. Nature, 2001. 409(6817): p. 211-5.
14. McCraith, S., et al., *Genome-wide analysis of vaccinia virus protein-protein interactions*. Proc Natl Acad Sci U S A, 2000. 97(9): p. 4879-84.
15. Calderwood, M.A., et al., *Epstein-Barr virus and virus human protein interaction maps*. Proc Natl Acad Sci U S A, 2007. 104(18): p. 7606-11.
16. Rozen, R., et al., *Virion-wide protein interactions of Kaposi's sarcoma-associated herpesvirus*. J Virol, 2008. 82(10): p. 4742-50.
17. Uetz, P., et al., *Herpesviral protein networks and their interaction with the human proteome*. Science, 2006. 311(5758): p. 239-42.
18. de Chasse, B., et al., *Hepatitis C virus infection protein network*. Mol Syst Biol, 2008. 4: p. 230.
19. Zotenko, E., et al., *Why do hubs in the yeast protein interaction network tend to be essential: reexamining the connection between the network topology and essentiality*. PLoS Comput Biol, 2008. 4(8): p. e1000140.
20. Park, K. and D. Kim, *Localized network centrality and essentiality in the yeast-protein interaction network*. Proteomics, 2009. 9(22): p. 5143-54.
21. Ning, K., et al., *Examination of the relationship between essential genes in PPI network and hub proteins in reverse nearest neighbor topology*. BMC Bioinformatics. 11: p. 505.

22. Cusick, M.E., et al., *Interactome: gateway into systems biology*. Hum Mol Genet, 2005. 14 Spec No. 2: p. R171-81.
23. Lotzerich, M., Z. Ruzsics, and U.H. Koszinowski, *Functional domains of murine cytomegalovirus nuclear egress protein M53/p38*. J Virol, 2006. 80(1): p. 73-84.
24. Kattenhorn, L.M., et al., *Identification of proteins associated with murine cytomegalovirus virions*. J Virol, 2004. 78(20): p. 11187-97.
25. Streblow, D.N., et al., *Rat cytomegalovirus gene expression in cardiac allograft recipients is tissue specific and does not parallel the profiles detected in vitro*. J Virol, 2007. 81(8): p. 3816-26.
26. Shenk, T. and M. Stinski, *Human cytomegalovirus*. 2008, Springer: Berlin. p. xiii, 475 p.
27. Manning, W.C., et al., *Cytomegalovirus determinant of replication in salivary glands*. J Virol, 1992. 66(6): p. 3794-802.
28. Nozawa, N., et al., *Identification of a 1.6 kb genome locus of guinea pig cytomegalovirus required for efficient viral growth in animals but not in cell culture*. Virology, 2008. 379(1): p. 45-54.
29. Lagenaur, L.A., et al., *Structure and function of the murine cytomegalovirus sgg1 gene: a determinant of viral growth in salivary gland acinar cells*. J Virol, 1994. 68(12): p. 7717-27.
30. Scrivano, L., et al., *The m74 gene product of murine cytomegalovirus (MCMV) is a functional homolog of human CMV gO and determines the entry pathway of MCMV*. J Virol. 84(9): p. 4469-80.
31. Fields, B.N., D.M. Knipe, and P.M. Howley, *Fields' virology*. 5th ed ed. 2007, Philadelphia: Wolters Kluwer Health/Lippincott Williams & Wilkins. 2 v. (xix, 3091, 86 p.).

## **Chapter 4**

### **Deletion Mutant Virus Cell Line Screens**

## Introduction

The development of bacterial artificial chromosome (BAC) based mutagenesis has provided researchers with a simple, yet efficient protocol for generating viral mutants that contain single, highly specific, site directed open reading frame (ORF) deletions [1, 2]. The efficiency of this method of mutagenesis has led to global deletion mutagenesis projects involving human cytomegalovirus that has shown some interesting phenotypes in human fibroblast cells and RPMI cells [3, 4]. This technology has been further utilized to create deletion mutant viruses using murine cytomegalovirus (MCMV) BAC constructs. However, until recently these constructs have failed to be viable *in vivo*. An MCMV BAC construct, pSM3fr, has been shown to retain wild-type like growth both *in vitro* and *in vivo* [5]. This allows us to take advantage of the full extent of MCMV research by allowing us to understand how the deletion of MCMV ORFs affects pathogenesis *in vivo*. This BAC construct has been used in our lab to create a library of 170 viral mutants that each contain a single deletion in one of the 170 predicted MCMV ORF [6](Chan et al, unpublished results).

Of these 170 ORF, 60 ORFs have been shown to be essential in murine fibroblast cells, 3 deleted ORFs are severely attenuated and 102 have been shown to be non-essential or of moderate attenuation in fibroblasts (Chan and Umamoto, unpublished results). Many of the essential ORFs represent core components involved in the viral replication process. However, it is the 102 non-essential mutants that may provide an interesting avenue of investigation. As CMV has proven to be a ubiquitous pathogen, able to infect many different types of cells, the question arises to the function of these non-essential ORFs. Due to size and limitations of the CMV genome, the likelihood that the virus has kept 102 non-essential open reading frames seems highly unlikely. We approach this project with the hypothesis that there are other conditions by which these 102 ORFs could potentially be essential or important in viral growth and pathogenesis. While there may be many explanations for the presence of these ORFs, ranging from potential immunologic interactions to other *in vivo* manipulations. Due to the sheer number of non-essential ORFs, we have decided to investigate first the possibility that some of these ORFs may be important in supporting productive infection *in vitro*, in other cell types besides fibroblast cells. The potential for this occurrence is supported in a study using rat cytomegalovirus that shows that there is differential expression of various ORF in different tissues [7].

To investigate this possibility, we have chosen four different cell lines through which infection may be involved in the pathogenesis of MCMV. The cell lines we have chosen are CRL-1972, bone marrow stromal cells, which provide the structural and physiological support for hematopoietic stem cells, a potential site for CMV latency [8]. SCA-9, salivary gland epitheloid cells, where CMV, also known as a salivary gland virus, can persist for many months after infection has been cleared from other major organs. The infection of the salivary gland may also have a role in viral immune evasion and viral persistence [9]. Also screened were J774A.1, macrophage cells, a cell type that may be the transport vehicle for infection of other cellular types and a facilitator in the spread of CMV. It is also relevant in the development of CMV associated atherosclerosis [10]. The final cell type chosen in this screen are SVEC, smooth vascular endothelial cells. CMV infection potentially leads to atherosclerosis and infection of the cells lining the arterial walls may provide the initial insult that leads to the disease [11, 12].



It is our intent to screen the 102 non-essential MCMV mutant viruses in each of these cells to ascertain how each of the represented ORFs may contribute to infection in these various cell types.

## **Materials and Methods**

### **Cells and Viruses**

Mouse NIH 3T3 cells were purchased from ATCC. Cells were maintained in Dulbecco's modified Eagle medium (DMEM) supplemented with 10% NuSerum, essential and nonessential amino acids, penicillin-streptomycin, and sodium bicarbonate (each from a stock solution purchased Invitrogen) and cultured following the guidelines set by ATCC. SCA-9 clone 15 cells (CRL-1734) purchased from ATCC. Cells were maintained using DMEM with 4mM L-glutamine adjusted to contain 1.5 g/L sodium bicarbonate and 4.5 g/L glucose with 10% FBS and penicillin and streptomycin. M2-10B4 (CRL-1972) cells from ATCC were maintained using DMEM supplemented with 10% NuSerum, essential and non-essential amino acids, penicillin-streptomycin, and sodium bicarbonate. SVEC4-10 (CRL2181) cells from ATCC were maintained using DMEM supplemented with 10% NuSerum, essential and nonessential amino acids, penicillin-streptomycin, and sodium bicarbonate. J774A.1 (TIB-67) cells were maintained DMEM with 4mM L-glutamine adjusted to contain 1.5 g/L sodium bicarbonate and 4.5 g/L glucose with 10% FBS and penicillin and streptomycin.

pSM3fr MCMV BAC virus was a gift from the Zhu lab.

pSM3fr MCMV BAC virus and zeocin BAC mutants were propagated in NIH 3T3 cells. To generate stock virus, 2 roller bottles of NIH 3T3 cells at 90% confluence were infected at a low multiplicity of infection (MOI) of 0.1-0.5. When 100% cytopathic effect (CPE) was observed, cells were separated from the flask with a cell scraper. The infected cells and media containing the virus were centrifuged at 400 X g at 4°C for 10 minutes to collect cells. The media was collected as low-titer viral stock for subsequent tissue culture experiments. For the creation of high-titer virus stock, cell pellets from the centrifugation were combined together by resuspension in 1 to 1 ratio with DMEM and 10% non-fat skim milk. The combination was sonicated three times on ice, and 100 ul of the virus stock was aliquoted into cryovials. The media and viral stock were stored at -80°C for long-term storage. Virus titers for the frozen media and viral stock were determined by standard plaque assays. Viral titers ranged from  $2 \times 10^6$  to  $5 \times 10^7$  plaque forming units (PFU) per ml while the media titers ranged from  $5 \times 10^4$  to  $1 \times 10^6$  PFU per ml.

### **Generation of Viral Progeny from BAC DNA Constructs**

NIH 3T3 cells of passage 20 or below were grown to 90-100% confluence. Cells were trypsinized, pelleted and resuspended in DMEM. 3-5 million cells in 260 ul DMEM were mixed with 4.5ug of MCMV BAC DNA in a 4mm electroporation cuvette, and electroporated with a BTX ECM 630 electroporator set at 250 volts, 960  $\mu$ F, and 75 ohms. At these setting the expected pulse time was between 30 to 40 milliseconds. Immediately following electroporation 1ml of DMEM media was added to the cell/DNA mixture in the cuvette. The contents of the transfection were then transferred to a T-25 flask. One day post transfection the media in the T-25 flask was removed and fresh DMEM was added. The cells were then

monitored for CPE. Cells transfected with viral BAC constructs with wild-type like replication kinetics would often exhibit plaque formation 3-5 days post transfection, indicating the presence and spread of infectious viral progeny from the BAC DNA. To remove the BAC vector from the viral genome, the virus was passaged five times in NIH-3T3 cells.

### **Construction of the Viral ORF-Deletion Mutants**

To delete each open reading frame (ORF) two oligonucleotide primers (30 in Zeo 5' and 30 in Zeo 3') were constructed and contained the following components (from 3' to 5'): 64 homologous nucleotides to zeocin LoxP plasmid, a 20-nt unique barcode tag, and a common 19-nt primer. The 30 in Zeo 5' and 30 in Zeo 3' primers were used to amplify the Zeocin LoxP cassette, which contains the zeocin resistance gene flanked by LoxP sites. The product that resulted from the first round of PCR, containing the zeocin resistance cassette with LoxP sites flanked by the barcode tag and the common 19-nt primer, was then subject to a second round of PCR with primers 50 up 5' and 50 dn 3' which contain 20 homologous nucleotides to the 1<sup>st</sup> PCR product and 50 bases of homology to the region upstream and downstream of the targeted ORF, respectively. The resulting product was a Zeocin LoxP cassette flanked by 50-nt homologous sequence targeting the ORF to be deleted in the pSM3fr BAC. This PCR-amplified Zeocin Lox P cassette was then transformed into the DY380 strain of bacteria carrying the pSM3fr BAC. The DY380 strain was engineered from DH10B. DY380 expresses phage-derived recombination genes under the control of a temperature-sensitive repressor [13]. Transformation of the pSM3fr-bearing DY380 strain with the PCR product resulted in the replacement of ORF on selection for zeocin resistance. The unique 20-mer barcode sequences were covalently linked to the sequence that targeted them to the MCMV genome, creating a permanent associate and genetic linkage between a particular deletion strain and the tag sequences.

### **Bacterial Transformation Procedures**

Recombination and electrocompetent cells for transformation were generated by culturing DY380 bacteria at 30°C in low salt Luria Broth (LSLB) media and shaking at 250 rpm for approximately 2-3 hours until the culture reached and OD<sub>600</sub> of 0.4-0.6. Then the bacteria cultures were incubated at 42°C for 15 minutes in shaking water bath rotating at 250 rpm. At 42°C the temperature sensitive repressor suppressing the expression of the recombination protein degrades and expression of the recombination protein is allowed to proceed. This induction process makes the bacteria recombination competent. After the 15 minutes induction period, bacterial cultures are then immediately placed in an ice-water slurry for 10 minutes and gently swirling to ensure uniform cooling of the bacteria. Bacterial cells were then pelleted in a pre-cooled (4°C) centrifuge and washed with 100ml of ice-cold sterile distilled water. Bacterial cells were pelleted again and washed with 10% ice-cold glycerol and pelleted again. Bacterial pellet was resuspend in cold 10% glycerol, aliquoted at a volume of 40ul, and stored at -80°C for long term storage.

Bacterial competent cultures were electroporated with the PCR DNA product that contain the zeocin loxP cassette flanked by the regions targeting the specified ORF for deletion. Approximately 1-5ug of linear PCR product was mixed with 40 ul of the competent bacterial cultures in a 1mm electroporation cuvette. A BTX ECM 630 electroporator was used with

wetting at 1.6kv, 25 uF, and 150 ohms. The transformed bacteria were then incubate for 1-2 hours at 30°C and plated on LSLB agar plates (12.5 ug/ml chloramphenicol/ 50 ug/ml zeocin) at 30°C. BAC DNAs were isolated from the surviving colonies and were screened with PCR assay, restriction profiling, and Southern analysis.

### **Analysis of growth of viruses in vitro in various cell lines**

The growth kinetics of non-essential mutants was initially analyzed on NIH-3T3 cells. NIH-3T3 cells grown to 50 to 60% confluence were infected at with 0.01 PFU per cell. At 0, 1, 2, 4, and 7 days post-infection, the infected cells and medium were harvested, and an equal volume of 10% skim milk were added before being treated to 2 rounds for freeze thaw. Virus titers were determined by plaque assays in duplicate experiments in NIH 3T3 cells. Briefly, cells were first infected with the viruses at 10-fold serial dilutions. After 75 min of incubation with the homogenates diluted in 1 ml of complete medium at 37°C, the cells were overlaid with fresh complete medium containing 2% agarose and culture for 4 to 5 days before the plaques were counted. Viral titers (recorded as PFU per milliliter) for each sample were determined in duplicate. The limit of virus detection was 10 PFU/ml of the freeze thaw mixture. Those samples that were negative at the 10<sup>-1</sup> dilution were assigned a titer value of 10 (10<sup>1</sup>) PFU/ml.

Viral growth determined in screens involving SCA-9, CRL-1972, J774A.1 and SVEC cells were conducted at single time-points and compared against wild-type psm3fr growth. Single time-points were selected for each of the four cell lines based on infection with wild-type MCMV. The criteria for selection was determined by selecting the point at which psm3fr infection reached 50% of its maximum titer and 50% of the cells were infected, determined due to morphological changes in infected cells as visualized by light microscopy. Infected SCA9 cells were harvested as previously described at 4 days post infection at a multiplicity of infection (MOI) of 0.01. For CRL-1972, cells were infected at an MOI of 0.01 and cells were harvested as described in the previous paragraph at 3 days post infection. J774A.1 cells were infected at an MOI of 0.3 and harvested 3 days post infection. And SVEC4-10 cells were infected at an MOI of 0.01 and harvested 3 days post infection (Figure 1).

### **Survival Curves**

Survival curves were conducted as per OLAC and NAF standards of care. 5 SCID mice (NCI) were infected with 1 x 10<sup>4</sup> PFU of either wildtype Smith virus, wildtype pSM3fr BAC virus, or one of four pSM3fr deletion mutants. Mice were observed over a period of 40 days.

### **Southern Analysis of the Deletion Mutant**

Southern analysis of the BAC constructs was performed by digesting 3 ug of BAC DNA with restriction enzyme (AseI), separating on agarose gels (0.8%), and transferred to Zeta-Probe nylon membrane (Bio-Rad). Membrane was hybridized with <sup>32</sup>P-radiolabeled DNA probes that contained the zeocin loxP cassette. Labeled DNA probes were prepared by random primer synthesis (Bio-Rad). Probed membranes were analyzed with a STORM 840 PhosphorImager (Molecular Dynamics).

## **Results**

The determination of the phenotype of infection in the five different cell lines was through the comparison of the log difference in growth between each of the individual mutant viruses and the wild-type pSM3fr construct (Table 1). Positive values reflect the decrease in the growth of the mutants versus the wild-type while negative values represent increased growth of the mutant virus over wild-type infection. Values between 0 and 1 were categorized as WT like growth, as they fell within the error limits of the assay. Values between 1 and 2 were regarded as moderately attenuated and any mutant viruses with values above 2 were determined to be severely attenuated in growth. The same criteria were used in reverse with respect to any viruses that exhibited enhanced growth during infection. However, while there were viruses that were found to be enhanced in growth compared to the wild-type virus, many of them fell within the error of detection and were subsequently classified as wild-type like. There was only one deletion mutant that exhibited a significant increase in infection, at a value of -2.04. This mutant virus contained a deletion in ORF M38 and exhibited this enhanced phenotype in J1774A.1 macrophage cells (Fig. 5, Table 1). In all other cell lines this deletion mutant was wild-type like in growth.

Of the five cell lines screened, MCMV grows readily in fibroblast cells. Most of the studies undertaken have found that in fibroblast cells many of the ORFs are non-essential [14]. In our deletion mutant virus study we found similar results. Of the 102 non-essential deletion mutant viruses screened in NIH-3T3 murine fibroblast cells, eighty-six (84%) of the viruses resulted in a wild-type like growth phenotype, sixteen (15%) showed moderate attenuation and zero (0%) of the viruses showed severe attenuation. NIH-3T3 cells are easily infected by MCMV and of the five cell lines used in the screen they showed the highest percentage of non-essential ORFs.

The cell line with the next highest levels of wild-type like phenotypes was CRL-1972, bone marrow stromal cells (Figure 3, Table 1). These cells are closely related to fibroblast cells and thus have the potential to show similar phenotypes of infection [15]. However, they are not completely similar as only seventy-four (72%) of the ORFs are wild-type like in CRL-1972 cells. Twenty-five (24%) mutant viruses were moderately defective and three (3%) were severely attenuated. These three ORF are M31, M45 and m107, all of which showed signs of moderate attenuation in the NIH-3T3 cells. M45 shares sequence homology to the large subunit of ribonucleotide reductase however studies have shown that it no longer functions in that capacity yet it is still important in pathogenesis in vivo and in various cell lines [6, 16]. The functions for M31 and m107 are unknown. All three of these severely attenuated ORFs are found in the virion [17].

Smooth vascular endothelial cells (SVEC) had the next highest percentage of wild-type like growth but also showed an increase in the number of severely attenuated viruses (Figure 4, Table 1). Fifty-nine (58%) of the deletion viruses screened were non-essential to growth in SVEC cells. Similar to CRL-1972, Twenty-five (24%) mutant viruses showed moderate defects however only nine of these ORFs were similar between the two cell lines. And eight (8%) mutants showed severe attenuation. These eight viruses contained deletion mutations in m20, M27, M31, M35, M41, M45, m139, and m150. The ORFs—M27 and m139 encode proteins important in immune evasion and regulation during infection. M27 is a STAT2 inhibitor, which interferes with gamma interferon signaling pathways [18]. m139 forms a complex with m140

(moderately attenuated in SVEC) and m141 (wild-type like in SVEC) and is important in regulated viral replication in macrophages [19].

The remaining two cell lines were below 50% with respect to non-essential genes. J774A.1, a macrophage cell line, resulted in forty-six (45%) mutant viruses with wild-type like growth phenotype. Forty-nine (28%) of the viruses were moderately attenuated in growth and six (5%) were severely attenuated in growth (Figure 5, Table 1). These six ORFs were m25.2, M31, M41, m119.1, m123ex2 and m165. Only two of these six ORF are of known function. m123ex2 is a component of both the immediate early gene 1 and 3. And m25.2 is a member of the US22 gene family and while previous publications have shown wild-type like phenotypes in fibroblast cells, our data conflicts with previous reports suggesting a non-essential phenotype in macrophage cell lines [20]. However, this may be evidence of similar cell lines resulting in different phenotypes due to location and potential differences in function as the cell line used in previous studies was IC-21, peritoneal macrophages, whereas our study used J774A.1, macrophages isolated from a reticulum sarcoma from a different background of mouse.

Of most interest, is the deletion mutant virus M38 which resulted in a two-log increase in growth in J774A.1 cells while resulting in wild-type like growth in the other four cell lines (Figure 5, Table 1). M38 represents the only ORF that has shown enhanced growth in any of the cell lines screened. The exact function of the M38 protein product is still unknown, however, a region at the beginning of M38 overlaps with the 3' end of the ORF m38.5, an ORF involved in BAX mediated cell death inhibition [21]. The HCMV homolog of M38, UL38 has also been shown to be involved in the inhibition of apoptosis [22].

The final cell line, SCA-9, salivary gland epitheloid cells showed the least number of non-essential ORFs and the highest amounts of attenuated viruses (Figure 2, Table 1). Thirty-six (35%) of the viruses were non-essential, while fifty-six (55%) were moderately attenuated. Of the five cell lines, SCA-9 had the highest number of severely attenuated deletion viruses at ten (10%). Of the ten viruses that were severely attenuated in growth only three of them showed signs of severe attenuation in other cell types, M31, M45, and m150. The remaining seven are m07, M37, m39, M82, M84, m117, and m153.

m07 is a possible glycoprotein. M37 was shown previously in our laboratory to be non-essential in NIH-3T3 cells, an observation that is supported in this study, however severely attenuated in vivo. Interestingly, in a previous study M37 is defective in the salivary glands of BALB/c and SCID mice further supporting the finding of attenuation in salivary gland epitheloid cells [23]. M82 and M84, are matrix phosphoproteins located in the tegument which may be involved in early stages of replication [24]. And m153 is a homolog of the MHC-I complex [25]. The remaining ORFs are of unknown function.

As an investigation into the relationship between in vitro infection and in vivo infection four ORF were chosen for a pilot survival study (Figure 7). m20, m31, m117, and m150 deletion mutant viruses were used to infect four sets of five SCID mice. The survival of mice infected with the mutant virus was compared to five mice infected with wild-type pSM3fr virus. When tested, infection of the pSM3fr wild-type BAC virus showed comparable survival curves to wild-type Smith MCMV, the virus that the BAC was constructed with (Figure 6). The four ORF were chosen due to several different criteria: m20 and m117 was chosen due to its attenuation in only SVEC, m31 due to its severe attenuation in all four of the cell lines screened, and m150 due to its attenuation in SVEC and SCA9 cells, important sites of pathogenesis in mice. Results

of this experiment show that all mice reached 50% survival within 13 days of the curve set by wild-type infection.

## Discussion

Of the 170 ORF predicted in MCMV, 60 ORFs have been shown to be essential in NIH 3T3, murine fibroblast cells, 3 deleted ORFs are severely attenuated and 102 have been shown to be non-essential or of moderate attenuation (Chan and Umamoto, unpublished results). As CMV, has proven to be a ubiquitous pathogen, infecting many different cellular types, the question arises to the function of these non-essential ORFs. Due to size and limitations of the CMV genome, the likelihood that the virus has kept 102 non-essential open reading frames is low. While there are many explanations for the presence of these ORFs, ranging from potential immunologic interactions to other *in vivo* manipulations, due to the sheer number of non-essential ORFs in our screen, we decided to investigate the possibility that some of these ORFs may be important in supporting productive infection in other cell types besides fibroblast cells.

In order to investigate this possibility, we have chosen four different cell lines through which infection may lead to various diseases caused by CMV. The cell lines we have chosen are CRL-1972, bone marrow stromal cells, which provide the structural and physiological support for hematopoietic stem cells, a potential site for CMV latency [8]. SCA-9, salivary gland epitheloid cells, a site where CMV can persist for many months after infection has been cleared from other major organs. J774A.1, macrophage cells, a transport vehicle for MCMV infection of secondary infected organs. And SVEC, smooth vascular endothelial cells, where CMV infection of this type of cell can be the potential trigger that leads to atherosclerosis [11, 12]. It is our intent to screen the 102 non-essential MCMV mutant viruses in each of these cells to ascertain how each of the represented ORFs may contribute to infection in these various cell types.

To determine the essentiality of each ORF in our cell screen, we used the 102 non-essential (fibroblast) deletion mutants to infect SCA-9, CRL-1972, J774A.1 and SVEC cells and titers were analyzed at a single time-point comparing the growth of the mutant virus against wild-type psm3fr growth. Single time-points were selected for each of the four cell lines based on wild-type infection. The criteria for selection was determined by the point at which psm3fr infection reached 50% of its maximum titer and 50% of the cells were infected. Infected SCA9 cells were harvested as previously described at 4 days post infection at a multiplicity of infection (MOI) of 0.01. For CRL-1972, cells were infected at an MOI of 0.01 and cells were harvested as described in the previous paragraph at 3 days post infection. J774A.1 cells were infected at an MOI of 0.3 and harvested 3 days post infection. And SVEC4-10 cells were infected at an MOI of 0.01 and harvested 3 days post infection (Figure 1).

Of the five cell lines screened, MCMV grows readily in fibroblast cells. Many of the studies undertaken have found that in fibroblast cells many of the ORFs are non-essential which was supported by our studies as well [14]. Of the 102 non-essential deletion mutant viruses screened in NIH-3T3 murine fibroblast cells, eighty-six (84%) of the viruses resulted in a wild-type like growth phenotype compared to 72% in CRL1972, 58% in SVEC, 45% in J774A.1 and 35% in SCA9 cells. In 3T3s, sixteen (15%) showed moderate attenuation, 24% in CRL1972, 24% in SVEC, 48% in J774A.1 and 55% in SCA9 cells. None of the ORFs screened in 3T3 showed

severe attenuation. However, in SVEC, eight ORFs were severely attenuated, three in CRL1972, five in J774A.1 and ten in SCA9 cells.

The cell line with the second highest levels of wild-type like phenotypes was CRL-1972, bone marrow stromal cells (Figure 3, Table 1). These cells are closely related to fibroblast cells and thus have the potential to show similar phenotypes of infection [15]. However, they are not completely similar as only seventy-four (72%) of the ORFs are wild-type like in CRL-1972 cells. Twenty-five (24%) mutant viruses were moderately defective and three (3%) were severely attenuated. These three ORF are M31, M45 and m107, all of which showed signs of moderate attenuation in the NIH-3T3 cells. M45 is a homolog of the large subunit of ribonucleotide reductase and while studies have shown that it no longer functions in that capacity it is still important in pathogenesis *in vivo* and in various cell lines [6, 16]. The functions for M31 and m107 are unknown. All three of these severely attenuated ORFs are found in the virion [17].

The eight viruses severely attenuated in SVEC contained deletion mutations in m20, M27, M31, M35, M41, M45, m139, and m150. The ORFs—M27 and m139 encode proteins important in immune evasion and regulation during infection. M27 is a STAT2 inhibitor, which interferes with gamma interferon signaling pathways [18]. m139 complexes with m140 and m141 and is important in controlling replication in macrophages [19].

In J774A.1, a macrophage cell line, the six ORFs that were severely attenuated were m25.2, M31, M41, m119.1, m123ex2 and m165. m25.2 is a member of the US22 gene family and while data has been shown to support the wild-type like phenotype in fibroblast cells the data shown here conflicts with previous reports suggesting no obvious phenotype in macrophage cell lines [20]. However, this may be due to the differences in the macrophage cell lines used. IC-21, peritoneal macrophages, were used in their study whereas our study used J774A.1, macrophages isolated from a reticulum sarcoma which came from a different background of mouse. m123ex2 is a component of both immediate early genes 1 and 3.

In this macrophage cell line, the deletion of the M38 gene resulted in a two-log increase in growth in J774A.1 cells while resulting in wild-type like growth in the other four cell lines (Figure 5, Table 1). This phenomenon has been observed in HCMV deletion mutant viruses, where deletion in several ORF resulted in enhanced viral growth [4]. This enhanced growth was similar to what was observed in our studies where enhanced growth was dependent on the specific cell lines involved and not a universal phenotype. The homolog to M38 however did not exhibit any enhanced phenotype in the cell lines they screened, HFF and RPMI cells.

While the function of the M38 protein product is still unknown, the HCMV homolog, UL38, is involved in the inhibition of apoptosis [22]. The reason behind this phenotype may also be related to a region at the beginning of the coding sequence of M38 that overlaps with the 3' end of the gene, m38.5, an ORF involved in BAX mediated cell death inhibition [21]. M38 may be important in this cell line may explain the significance of macrophages and their monocyte precursors in latency and the dissemination of the virus to secondary infected organs [26, 27]. It is possible that M38 or m38.5 could be involved in a process that not only prevents apoptosis, but also retards the growth of the virus in infected macrophages. Both of which prolong the life of the cell and may result in a greater number of virus released over time, or due to the mobile nature of the macrophage, this attenuation in growth by M38 may be a mechanism to ensure the spread and delivery of the virus to various secondary organs.

The final cell line, SCA-9, salivary gland epithelioid cells showed the least number of non-essential ORFs and the highest amounts of attenuated viruses (Figure 2, Table 1). Of the five cell lines, SCA-9 had the highest number of severely attenuated deletion viruses at ten (10%). Of the ten viruses that were severely attenuated in growth only three of them showed signs of severe attenuation in other cell types, M31, M45, and m150. The remaining seven are m07, M37, m39, M82, M84, m117, and m153.

Of the ORFs with known function, m07 represents a possible glycoprotein. M37 was shown previously in our laboratory to be non-essential in NIH-3T3 cells, an observation that is supported in this study, and attenuated *in vivo*. Interestingly, in the previous study M37 was found to be defective in the salivary glands of BALB/c and SCID mice further supporting the finding of attenuation in salivary gland epithelioid cells [23]. M82 and M84, are matrix phosphoproteins located in the tegument which may be involved in early stages of replication [24]. And m153, is a homolog of the MHC-I complex [25].

As an investigation into the relationship between *in vitro* infection and *in vivo* infection four ORF were chosen for a survival study (Figure 7). m20, m31, m117, and m150 deletion mutant viruses were used to infect four sets of five SCID mice and were compared to five mice infected with wild-type pSM3fr virus. The four ORF were chosen due to several different criteria: m20 and m117 was chosen due to its attenuation in only SVEC, m31 due to its severe attenuation in all four of the cell lines screened, and m150 due to its attenuation in SVEC and SCA9 cells important sites of pathogenesis in mice. Results of this experiment show that all mice reached 50% survival within 13 days of the curve set by wild-type infection. None of the ORFs were essential to viral pathogenesis in terms of the survival of the mice and the length of survival beyond wild-type infection was not dependent on the number of different cell lines that showed attenuation when infected by a specific deletion mutant. While the ORFs studied showed no evident signs of attenuation or defect, it is important to note that this study was focused on determining the overall survival of the mouse with respect to the deleted ORF. It does not investigate the potential differences in infection in specific organ types that have been observed in *in vivo* experiments [23, 28]. It also does not take into account a functional adaptive immune response as these experiments were done in SCID mice.

This study shows that MCMV genes are involved in varying levels of essentiality depending on the cell line in which infection occurs. However, the conditions that we have subjected our deletion viruses to still do not tell the entire story. Testing MCMV virulence *in vivo* is an extremely important next step for this project. How different genes found in the viral genome contribute to infection can only be truly ascertained through analysis of viral pathogenesis in a living host. And as observed with ORFs such as m20 and M31 which show varying degrees of attenuation *in vitro*, *in vivo* this attenuation may not be as pronounced (Figure 6). On the other end of the spectrum, ORF such as M27 and M37, which fail to show signs of attenuation in cell culture, can show signs of defect *in vivo* [23, 29]. As with most global projects, this cell line screen provides a large set of information that represents an important starting point towards further more detailed analysis into the functions of the products encoded by the genes in the virus. This data can be useful in determining the genes or genes that can lead to specific treatments that can be applied to HCMV and herpes infections.



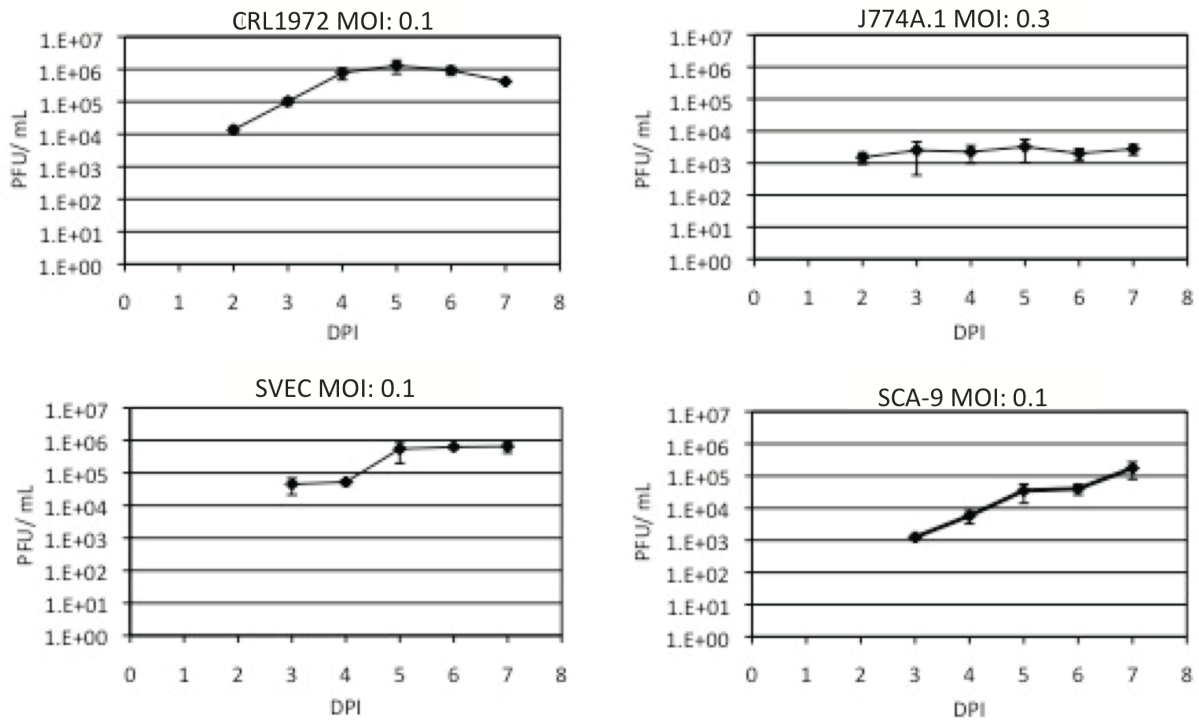


**Figure 1. Cellular screen pilot growth curve study using MCMV BAC pSM3fr.**

Growth curves over the course of seven days were determined in four cell lines that were permissive to MCMV BAC pSM3fr infection. SCA-9, CRL-1972 and SVEC4-10 cells were obtained from ATCC and infected at an M.O.I. of 0.01 and harvested daily from two to seven days post infection (ATCC # CRL-1734, CRL-1972, CRL-2181). J774A.1 cells also obtained from ATCC were infected at an MOI of 0.3 (#TIB-67). Infections were carried on in duplicate.

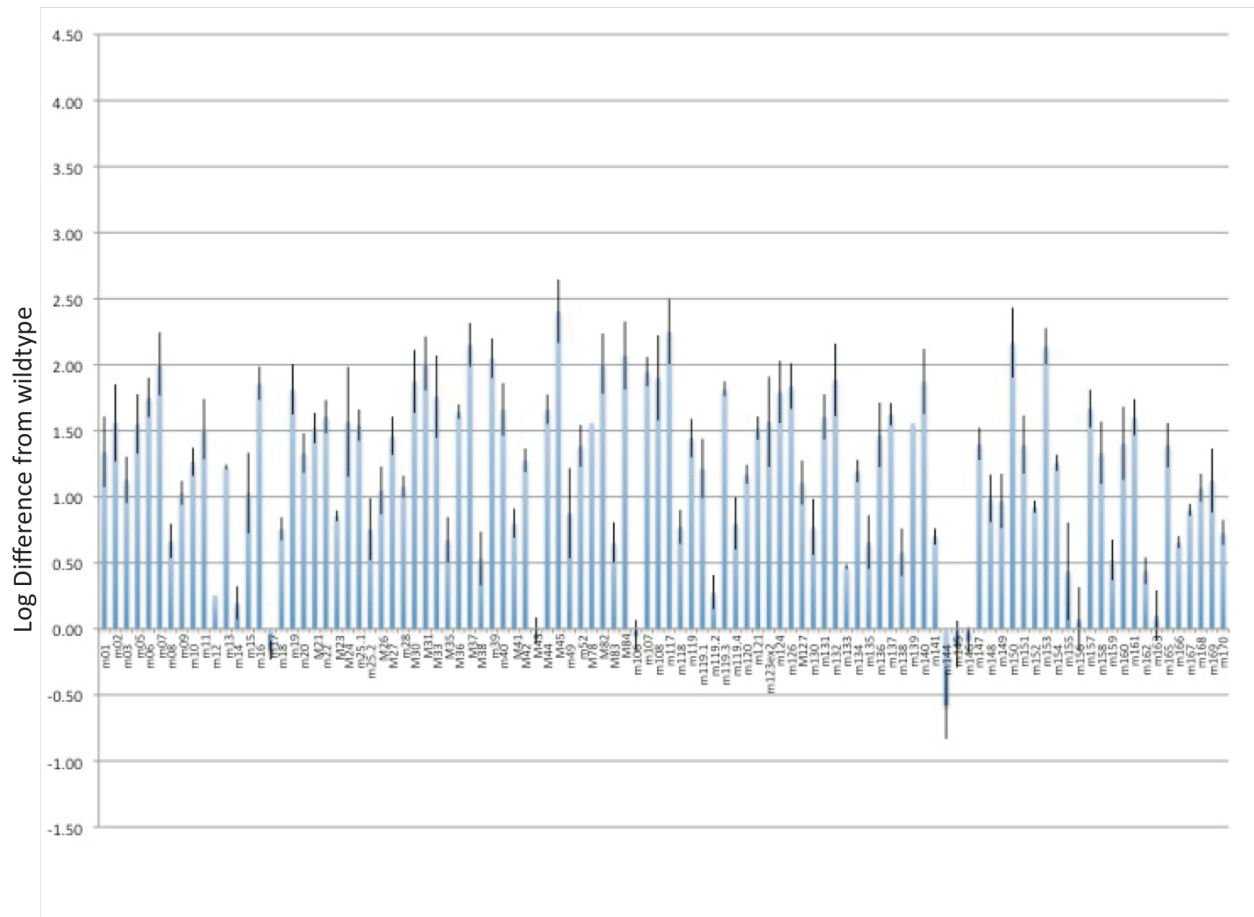


**Figure 2. Single growthpoint screen in SCA-9 cells using single deletion MCMV mutants.**

102 non-essential MCMV BAC mutant viruses constructed from the MCMV BAC construct pSM3fr were screened in duplicate in SCA-9 submandibular salivary gland cells obtained from ATCC (#CRL-1734). Mutant virus was harvested at 4 days post infection and viral growth was compared against wildtype pSM3fr. The chart shows the log difference in titers between each mutant virus and the wildtype control.

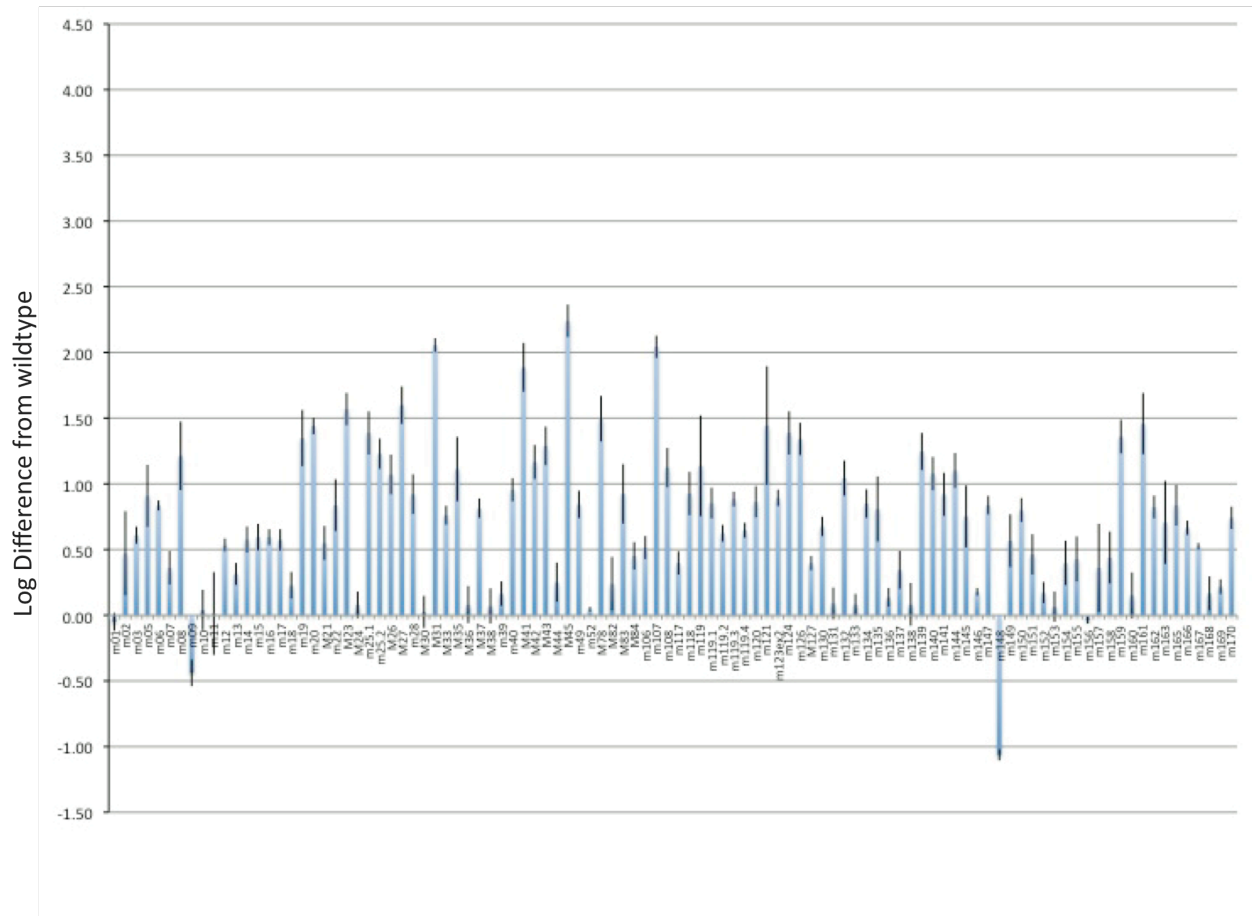


**Figure 3. Single growthpoint screen in CRL-1972 cells using single deletion MCMV mutants.**

102 non-essential MCMV BAC mutant viruses constructed from the MCMV BAC construct pSM3fr were screened in duplicate in CRL-1972 bone marrow stromal cells obtained from ATCC. Mutant virus was harvested at 3 days post infection and viral growth was compared against wildtype pSM3fr. The chart shows the log difference in titers between each mutant virus and the wildtype control.

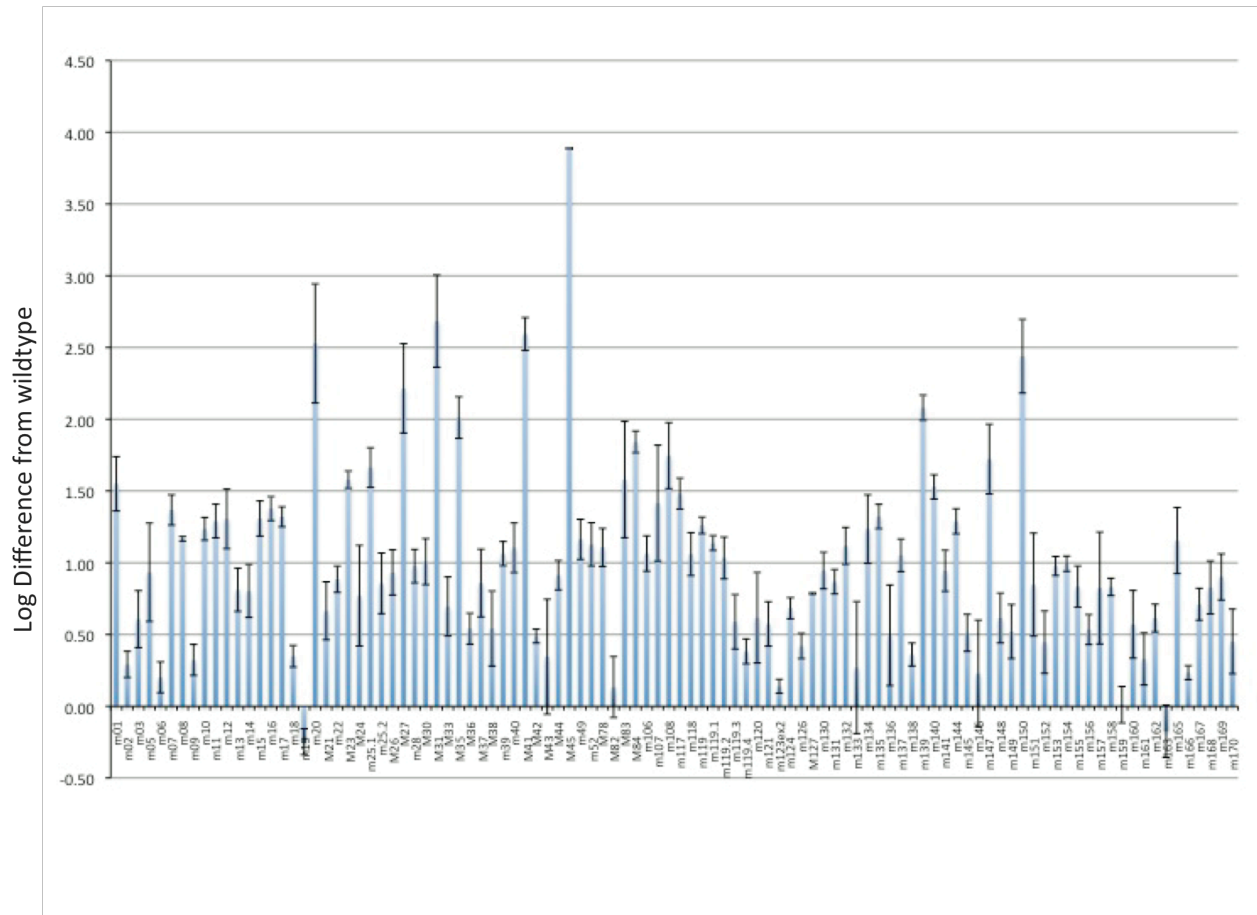


**Figure 4. Single growthpoint screen in SVEC cells using single deletion MCMV mutants.**

102 non-essential MCMV BAC mutant viruses constructed from the MCMV BAC construct pSM3fr were screened in duplicate in SVEC smooth vascular endothelial cells obtained from ATCC (#CRL-2181). Mutant virus was harvested at 3 days post infection and viral growth was compared against wildtype pSM3fr. The chart shows the log difference in titers between each mutant virus and the wildtype control.

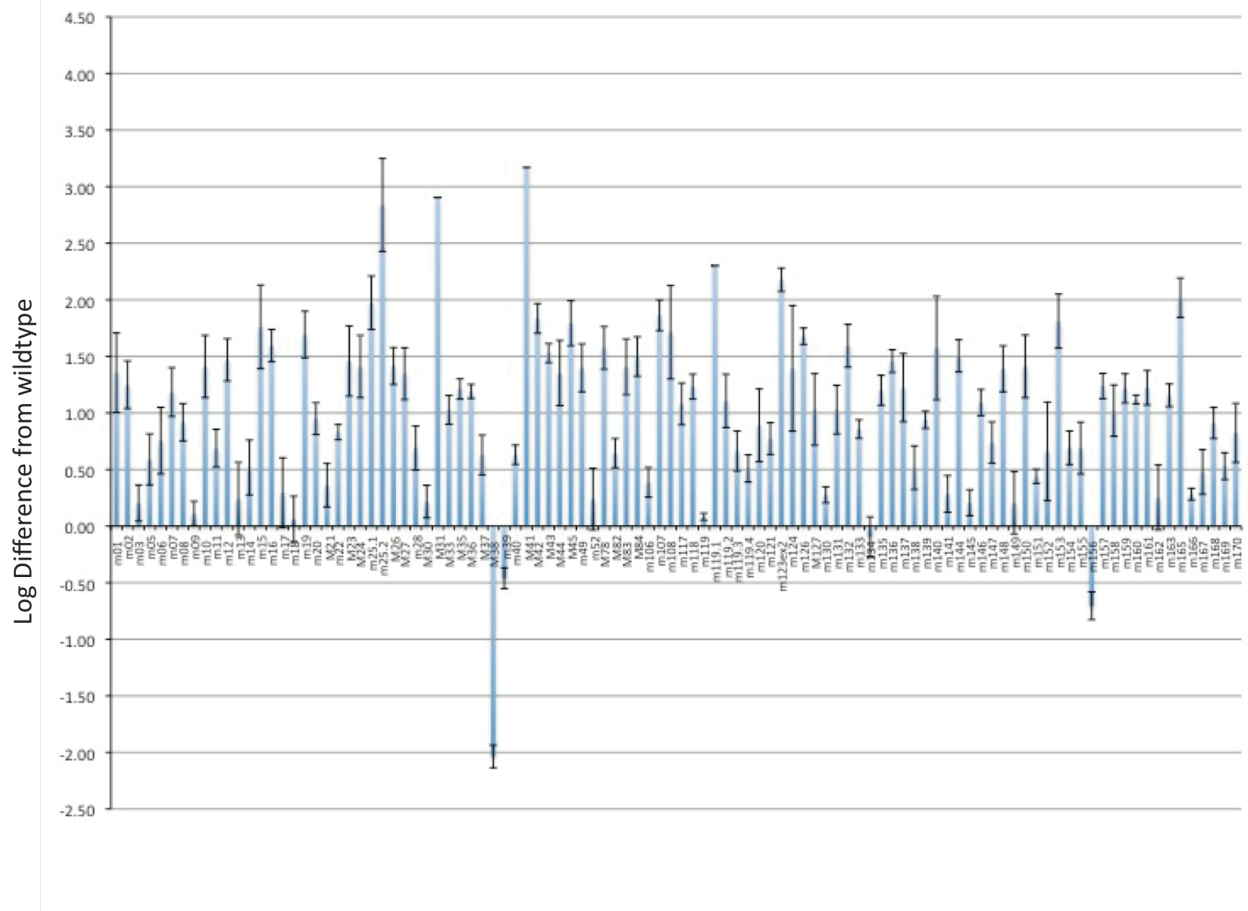


**Figure 5. Single growthpoint screen in J774A.1 cells using single deletion MCMV mutants.**

102 non-essential MCMV BAC mutant viruses constructed from the MCMV BAC construct pSM3fr were screened in duplicate in J774A.1 monocyte/macrophage cells obtained from ATCC (#TIB-67). Mutant virus was harvested at 3 days post infection and viral growth was compared against wild-type pSM3fr. The chart shows the log difference in titers between each mutant virus and the wildtype control.

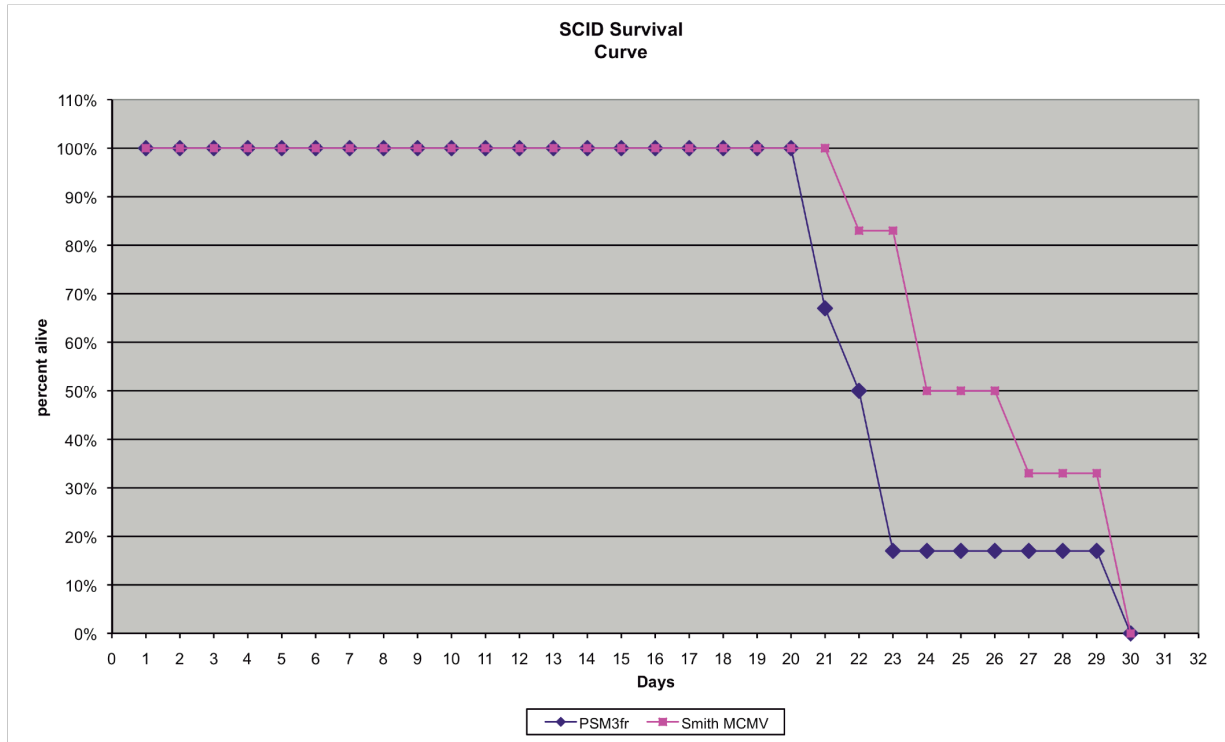


**Figure 6. SCID mice survival curves comparing wildtype Smith MCMV infection to pSM3fr infection**

5 SCID mice were infected with  $1 \times 10^4$  PFU of either wildtype Smith MCMV or the MCMV BAC construct pSM3fr and observed over the period of 30 days. Mice were sacrificed as determined by OLAC and NAF standards.

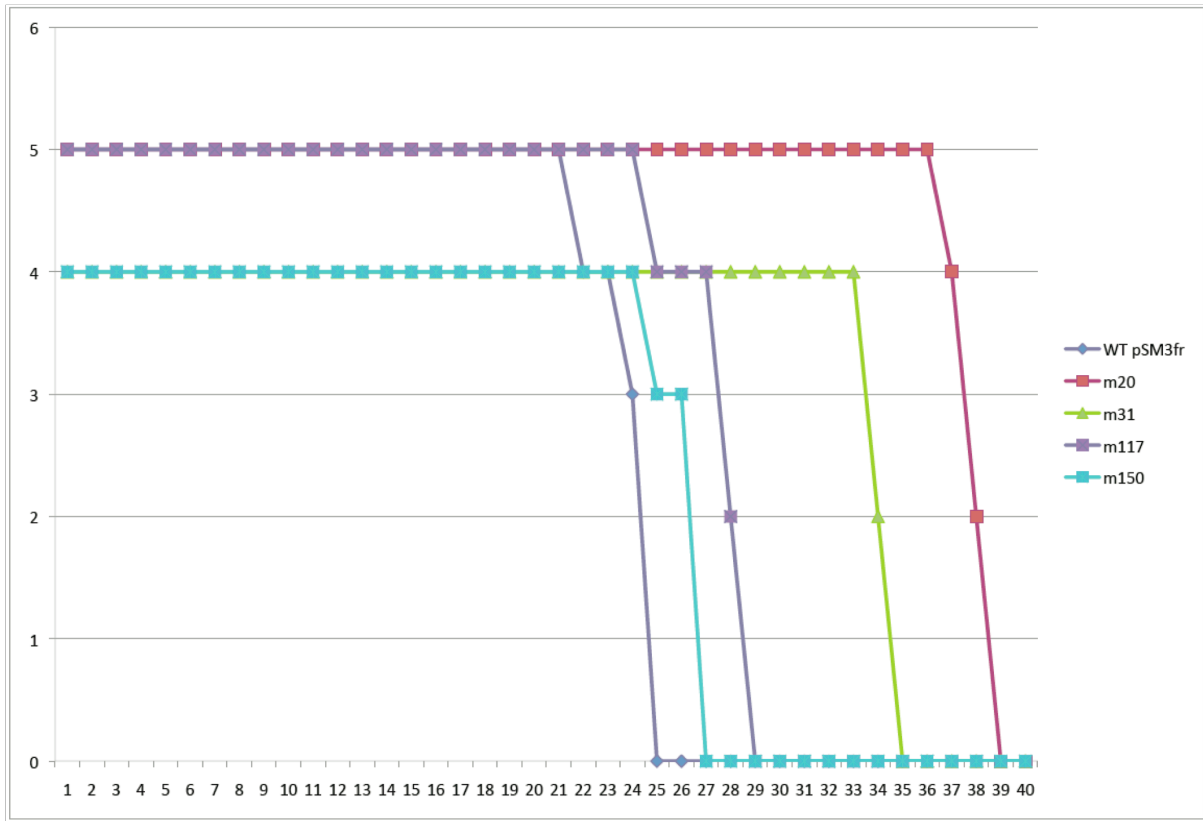


**Figure 7. SCID mice survival curves**

5 SCID mice were infected with  $1 \times 10^4$  PFU of either the wildtype MCMV BAC construct pSM3fr or one of four different MCMV BAC deletion mutant viruses and observed over the period of 40 days. Mice were sacrificed as determined by OLAC and NAF standards.

	3T3	SCA9	CRL1972	SVEC	J774A.1
m01	wt	1.34	-0.05	1.55	1.36
m02	wt	1.56	0.47	0.29	1.25
m03	wt	1.13	0.61	0.61	0.20
m05	wt	1.55	0.91	0.93	0.59
m06	wt	1.75	0.84	0.20	0.76
m07	wt	2.01	0.36	1.37	1.19
m08	moderate	0.67	1.21	1.17	0.92
m09	wt	1.03	-0.44	0.32	0.11
m10	wt	1.26	0.04	1.24	1.41
m11	wt	1.51	0.01	1.29	0.69
m12	wt	0.26	0.53	1.31	1.47
m13	wt	1.23	0.31	0.81	0.24
m14	wt	0.20	0.58	0.80	0.52
m15	wt	1.03	0.59	1.31	1.76
m16	wt	1.86	0.59	1.38	1.60
m17	wt	-0.16	0.57	1.32	0.29
m18	wt	0.76	0.23	0.35	0.06
m19	wt	1.81	1.35	-0.25	1.69
m20	moderate	1.33	1.44	2.53	0.95
m21	wt	1.52	0.55	0.67	0.36
m22	wt	1.61	0.84	0.89	0.83
M23	wt	0.86	1.57	1.58	1.46
M24	wt	1.57	0.08	0.77	1.41
m25.1	wt	1.54	1.39	1.66	1.97
m25.2	wt	0.75	1.23	0.86	2.84
M26	wt	1.05	1.07	0.93	1.42
M27	wt	1.46	1.60	2.22	1.35
M28	wt	1.08	0.92	0.98	0.69
M30	moderate	1.87	0.03	1.01	0.22
M31	moderate	2.01	2.06	2.68	2.90
M33	wt	1.76	0.76	0.70	1.03
M35	wt	0.67	1.11	2.01	1.21
M36	wt	1.64	0.08	0.54	1.19
M37	wt	2.15	0.81	0.86	0.63
M38	wt	0.53	0.07	0.54	-2.04
m39	wt	2.05	0.16	1.06	-0.46
m40	wt	1.66	0.95	1.10	0.63
M41	moderate	0.80	1.89	2.59	3.17
M42	wt	1.28	1.17	0.49	1.84
M43	wt	-0.01	1.29	0.35	1.53
M44	wt	1.66	0.25	0.91	1.35
M45	moderate	2.40	2.24	3.89	1.79
m49	wt	0.88	0.84	1.16	1.40
M52	wt	1.39	0.05	1.13	0.24
M78	moderate	1.56	1.50	1.11	1.58



	3T3	SCA9	CRL1972	SVEC	J774A.1
M82	wt	2.01	0.24	0.13	0.65
M83	wt	0.65	0.92	1.58	1.41
M84	moderate	2.07	0.45	1.84	1.50
m106	wt	-0.05	0.51	1.06	0.39
m107	moderate	1.95	2.04	1.42	1.86
m108	moderate	1.90	1.12	1.75	1.71
m117	wt	2.25	0.40	1.48	1.08
m118	wt	0.77	0.93	1.06	1.23
m119	moderate	1.44	1.14	1.26	0.08
m119.1	wt	1.21	0.85	1.14	2.30
m119.2	wt	0.28	0.62	1.03	1.11
m119.3	wt	1.82	0.88	0.59	0.66
m119.4	moderate	0.80	0.65	0.38	0.51
m120	wt	1.17	0.86	0.62	0.89
m121	wt	1.52	1.44	0.57	0.77
m123ex2	wt	1.57	0.89	0.14	2.18
m124	wt	1.79	1.39	0.68	1.39
m126	wt	1.84	1.34	0.42	1.68
M127	wt	1.11	0.40	0.79	1.03
m130	wt	0.77	0.68	0.95	0.28
m131	moderate	1.60	0.09	0.87	1.03
m132	wt	1.89	1.04	1.12	1.59
m133	wt	0.47	0.08	0.27	0.86
m134	moderate	1.19	0.85	1.23	-0.09
m135	wt	0.66	0.81	1.32	1.20
m136	wt	1.47	0.14	0.49	1.46
m137	wt	1.62	0.34	1.05	1.22
m138	wt	0.58	0.08	0.36	0.52
m139	wt	1.56	1.25	2.08	0.94
m140	wt	1.87	1.08	1.53	1.57
m141	moderate	0.70	0.92	0.94	0.28
m144	wt	-0.58	1.10	1.29	1.50
m145	wt	-0.12	0.75	0.51	0.21
m146	wt	-0.09	0.18	0.23	1.09
m147	wt	1.40	0.84	1.72	0.74
m148	wt	0.99	-1.06	0.61	1.39
m149	wt	0.97	0.57	0.52	0.21
m150	wt	2.17	0.80	2.44	1.41
m151	wt	1.40	0.46	0.85	0.44
m152	wt	0.92	0.17	0.45	0.66
m153	wt	2.14	0.06	0.98	1.81
m154	wt	1.26	0.40	0.99	0.69
m155	wt	0.44	0.43	0.83	0.69
m156	wt	0.07	-0.04	0.53	-0.70
m157	wt	1.67	0.36	0.82	1.24

	3T3	SCA9	CRL1972	SVEC	J774A.1
m158	wt	1.33	0.44	0.83	1.02
m159	moderate	0.52	1.36	0.01	1.22
m160	wt	1.40	0.15	0.57	1.12
m161	wt	1.60	1.46	0.33	1.22
m162	wt	0.44	0.82	0.61	0.25
m163	wt	0.10	0.71	-0.17	1.16
m165	wt	1.39	0.84	1.15	2.02
m166	wt	0.66	0.67	0.23	0.28
m167	wt	0.90	0.52	0.71	0.48
m168	wt	1.07	0.17	0.83	0.91
m169	wt	1.12	0.22	0.90	0.53
m170	wt	0.73	0.74	0.45	0.82

**Table 1. Log differences between mutant MCMV BAC virus in five different cell lines.**

102 single deletion ORF mutant viruses based on the MCMV BAC, pSM3fr, were tested for growth properties on five different cell lines. NIH3T3, SCA9, CRL1972, SVEC and J774A.1 cells were obtained from ATCC. Table shows the log difference between wildtype pSM3fr BAC growth and each mutant virus. Each growth point was tested in duplicate and is color coded based on essentiality. Black: non-essential, purple: moderate attenuation, blue: severe attenuation, yellow: enhanced growth.

## References

1. Zhang, Z., et al., *Genetic analysis of varicella-zoster virus ORF0 to ORF4 by use of a novel luciferase bacterial artificial chromosome system*. J Virol, 2007. 81(17): p. 9024-33.
2. Lee, E.C., et al., *A highly efficient Escherichia coli-based chromosome engineering system adapted for recombinogenic targeting and subcloning of BAC DNA*. Genomics, 2001. 73(1): p. 56-65.
3. Yu, D., M.C. Silva, and T. Shenk, *Functional map of human cytomegalovirus AD169 defined by global mutational analysis*. Proc Natl Acad Sci U S A, 2003. 100(21): p. 12396-401.
4. Dunn, W., et al., *Functional profiling of a human cytomegalovirus genome*. Proc Natl Acad Sci U S A, 2003. 100(24): p. 14223-8.
5. Wagner, M., et al., *Systematic excision of vector sequences from the BAC-cloned herpesvirus genome during virus reconstitution*. J Virol, 1999. 73(8): p. 7056-60.
6. Rawlinson, W.D., H.E. Farrell, and B.G. Barrell, *Analysis of the complete DNA sequence of murine cytomegalovirus*. J Virol, 1996. 70(12): p. 8833-49.
7. Streblow, D.N., et al., *Rat cytomegalovirus gene expression in cardiac allograft recipients is tissue specific and does not parallel the profiles detected in vitro*. J Virol, 2007. 81(8): p. 3816-26.
8. Prosch, S., et al., *Human cytomegalovirus reactivation in bone-marrow-derived granulocyte/monocyte progenitor cells and mature monocytes*. Intervirology, 1999. 42(5-6): p. 308-13.
9. Campbell, A.E., V.J. Cavanaugh, and J.S. Slater, *The salivary glands as a privileged site of cytomegalovirus immune evasion and persistence*. Med Microbiol Immunol, 2008. 197(2): p. 205-13.
10. Milioti, N., et al., *Antigen-induced immunomodulation in the pathogenesis of atherosclerosis*. Clin Dev Immunol, 2008. 2008: p. 723539.
11. Nieto, F.J., et al., *Cohort study of cytomegalovirus infection as a risk factor for carotid intimal-medial thickening, a measure of subclinical atherosclerosis*. Circulation, 1996. 94(5): p. 922-7.
12. Sorlie, P.D., et al., *A prospective study of cytomegalovirus, herpes simplex virus 1, and coronary heart disease: the atherosclerosis risk in communities (ARIC) study*. Arch Intern Med, 2000. 160(13): p. 2027-32.
13. Varnum, S.M., et al., *Identification of proteins in human cytomegalovirus (HCMV) particles: the HCMV proteome*. J Virol, 2004. 78(20): p. 10960-6.
14. Fields, B.N., D.M. Knipe, and P.M. Howley, *Fields' virology*. 5th ed ed. 2007, Philadelphia: Wolters Kluwer Health/Lippincott Williams & Wilkins. 2 v. (xix, 3091, 86 p.).
15. Haniffa, M.A., et al., *Mesenchymal stem cells: the fibroblasts' new clothes?* Haematologica, 2009. 94(2): p. 258-63.
16. Lembo, D., et al., *The ribonucleotide reductase R1 homolog of murine cytomegalovirus is not a functional enzyme subunit but is required for pathogenesis*. J Virol, 2004. 78(8): p. 4278-88.
17. Kattenhorn, L.M., et al., *Identification of proteins associated with murine cytomegalovirus virions*. J Virol, 2004. 78(20): p. 11187-97.

18. Khan, S., et al., *A cytomegalovirus inhibitor of gamma interferon signaling controls immunoproteasome induction*. J Virol, 2004. 78(4): p. 1831-42.
19. Karabekian, Z., et al., *Complex formation among murine cytomegalovirus US22 proteins encoded by genes M139, M140, and M141*. J Virol, 2005. 79(6): p. 3525-35.
20. Menard, C., et al., *Role of murine cytomegalovirus US22 gene family members in replication in macrophages*. J Virol, 2003. 77(10): p. 5557-70.
21. Jurak, I., et al., *Murine cytomegalovirus m38.5 protein inhibits Bax-mediated cell death*. J Virol, 2008. 82(10): p. 4812-22.
22. Terhune, S., et al., *Human cytomegalovirus UL38 protein blocks apoptosis*. J Virol, 2007. 81(7): p. 3109-23.
23. Lee, M., et al., *Murine cytomegalovirus containing a mutation at open reading frame M37 is severely attenuated in growth and virulence in vivo*. J Virol, 2000. 74(23): p. 11099-107.
24. Cranmer, L.D., et al., *Identification, analysis, and evolutionary relationships of the putative murine cytomegalovirus homologs of the human cytomegalovirus UL82 (pp71) and UL83 (pp65) matrix phosphoproteins*. J Virol, 1996. 70(11): p. 7929-39.
25. Mans, J., et al., *Cellular expression and crystal structure of the murine cytomegalovirus major histocompatibility complex class I-like glycoprotein, mI53*. J Biol Chem, 2007. 282(48): p. 35247-58.
26. Smith, M.S., et al., *Roles of phosphatidylinositol 3-kinase and NF-kappaB in human cytomegalovirus-mediated monocyte diapedesis and adhesion: strategy for viral persistence*. J Virol, 2007. 81(14): p. 7683-94.
27. Smith, M.S., et al., *HCMV activates PI(3)K in monocytes and promotes monocyte motility and transendothelial migration in a PI(3)K-dependent manner*. J Leukoc Biol, 2004. 76(1): p. 65-76.
28. Xiao, J., et al., *In vitro and in vivo characterization of a murine cytomegalovirus with a transposon insertional mutation at open reading frame M43*. J Virol, 2000. 74(20): p. 9488-97.
29. Abenes, G., et al., *Murine cytomegalovirus open reading frame M27 plays an important role in growth and virulence in mice*. J Virol, 2001. 75(4): p. 1697-707.

## Chapter 5

M43

## Introduction

HCMV represents one of the most common opportunistic infections associated with AIDS patients. In HIV infected individuals, HCMV infection can lead to severe diseases such as CMV-associated pneumonia, gastrointestinal diseases, and CNS complications. Furthermore, HCMV is among the most common causes of oral diseases associated with AIDS patients [1-3]. During primary infection, HCMV infection will progress to the salivary glands after infection of the primary organs [1, 4]. Subsequently, the virus engages in a high level of replication in the serous acinar cells of the salivary glands and can be shed via saliva, making the salivary glands a major source of persistent virus [1, 4]. Extremely high levels of viral production in the salivary glands are a hallmark of CMV primary infections and reactivation from latent infections [1, 4]. Protection of immunodeficient patients from developing CMV-associated oral infections and possibly systematic infections requires eliminating HCMV infection from the salivary glands and blocking viral replication in these organs. Understanding the mechanism of CMV infections, such as identifying viral determinants for CMV pathogenesis in these organs, will provide insight into the development of new drugs and novel strategies for blocking CMV infection and transmission.

Understanding the mechanism of CMV infection of the salivary glands will provide insight into the treatment and prevention of CMV-associated oral diseases as well as systematic infections in AIDS patients. However, little is known about the nature of the viral determinants required for CMV replication in the salivary glands. In a previous study, an MCMV mutant with a deletion in ORF m133, also called salivary gland gene 1 (sgg1), exhibited a titer approximately 5,000 folds lower than that of wild-type Smith virus in the salivary glands when the animals were infected intraperitoneally [5]. Moreover, the titer of the MCMV sgg1 mutant in the salivary glands was about 30-100 fold lower than that of the wild type Smith strain when the animals were directly inoculated in the salivary glands. These observations suggest that sgg1 is important for MCMV replication in the salivary glands [5]. However, HCMV does not contain an ORF whose sequence is homologous to m133 of MCMV thereby diminishing the importance of sgg1 with respect to human infection [6, 7]. Meanwhile, the mechanism of how the sgg1 mutant is defective in replicating in the salivary glands and how sgg1 functions to support viral growth in this organ is currently not known. More recently, viral mutants, including those with mutations at M83, have exhibited attenuated growth in the salivary glands as well as in other organs, suggesting that the genes are important for viral growth in multiple organs and are not specifically required for viral replication in the salivary glands [8-11].

Using a genetic approach, previous studies in our laboratory have provided the first direct evidence that MCMV open reading frame M43 is important for viral infection in salivary gland. A viral mutant, RvM43, which contained a transposon inserted in the ORF M43 [12], was constructed. Our results showed that M43 is not essential for viral replication *in vitro* in NIH-3T3 cells. Moreover, RvM43 exhibited a titer similar to that of the wild-type virus in the lungs, livers, spleens, and kidneys of both Balb/c and SCID mice, and was as virulent as the wild-type virus in killing the SCID mice when these animals were intraperitoneally infected. In contrast, the titers of the mutant virus in the salivary glands of the intraperitoneally-infected animals were significantly (100-1000 fold) lower than those of the wild type virus [12]. When inoculated directly into the salivary glands, RvM43 remained defective in growth when

compared to the wild-type and rescued virus. Similar results were also observed using another viral mutant, DM43, which contains a deletion of the entire M43 ORF (Zhu, J., Chan, K., Li, H., Umamoto, S., and Liu, F., unpublished results). These results suggest that M43 encodes a determinant for MCMV infection in the salivary glands.

M43 is the second ORF known (other than *sgg1*) that is specifically required for MCMV replication in the salivary glands and in which a mutation diminishes the ability of the virus to replicate in the salivary glands, but does not affect its infection in other organs (e.g. spleens) *in vivo*. The gene coding for M43 is highly conserved among MCMV, HCMV and other animal CMVs. It also has been found to be a component of the infectious particle [13]. However, the function of UL43, the HCMV counterpart of M43, as well as its homologues in other animal CMVs, is currently unknown.

The development of bacterial artificial chromosome (BAC) based mutagenesis has provided researchers with a simple, yet efficient protocol for generating viral mutants that contain single, highly specific, site directed open reading frame (ORF) deletions [14, 15]. The efficiency of this method of mutagenesis has led to global deletion mutagenesis projects involving human cytomegalovirus that has shown some interesting phenotypes in human fibroblast cells and RPMI cells [16, 17]. This technology has been further utilized to create deletion mutant viruses using murine cytomegalovirus (MCMV) BAC constructs. However, until recently these constructs have failed to be viable *in vivo*. An MCMV BAC construct, pSM3fr, has been shown to retain wildtype like growth both *in vitro* and *in vivo* [18]. This allows us to take advantage of the full extent of MCMV research by allowing us to understand how the deletion of MCMV ORFs affects pathogenesis *in vivo*. An M43 deletion mutant virus created using this technology and a yeast two-hybrid system that allows us to screen interaction between the M43 protein product and cDNA from mouse cells will help us investigate the potential mechanism by which M43 deletion results in defects in the salivary gland.

## **Materials and Methods**

### **Cells and Viruses**

Mouse NIH 3T3 cells were purchased from ATCC. Cells were maintained in Dulbecco's modified Eagle medium (DMEM) supplemented with 10% NuSerum, essential and nonessential amino acids, penicillin-streptomycin, and sodium bicarbonate (each from a stock solution purchased Invitrogen) and cultured following the guidelines set by ATCC. SCA-9 clone 15 cells (CRL-1734) purchased from ATCC. Cells were maintained using DMEM with 4mM L-glutamine adjusted to contain 1.5 g/L sodium bicarbonate and 4.5 g/L glucose with 10% FBS and penicillin and streptomycin. M2-10B4 (CRL-1972) cells from ATCC were maintained using DMEM supplemented with 10% NuSerum, essential and non-essential amino acids, penicillin-streptomycin, and sodium bicarbonate. SVEC4-10 (CRL2181) cells from ATCC were maintained using DMEM supplemented with 10% NuSerum, essential and nonessential amino acids, penicillin-streptomycin, and sodium bicarbonate. J774A.1 (TIB-67) cells were maintained using DMEM with 4mM L-glutamine adjusted to contain 1.5 g/L sodium bicarbonate and 4.5 g/L glucose with 10% FBS and penicillin and streptomycin. IC-21 (TIB-186) cells were maintained using RPMI 1640 with 2mM L-glutamine adjusted to contain 1.5g/L Sodium bicarbonate, 4.5 g/L glucose, 10mM HEPES, 1mM sodium pyruvate and 10% FBS.

pSM3fr MCMV BAC virus was a gift from the Zhu lab.

pSM3fr MCMV BAC virus and zeocin BAC mutants were propagated in NIH 3T3 cells. To generate stock virus, 2 roller bottles of NIH 3T3 cells at 90% confluence were infected at a low multiplicity of infection (MOI) of 0.1-0.5. When 100% cytopathic effect (CPE) was observed, cells were separated from the flask with a cell scraper. The infected cells and media containing virus were centrifuged at 400 X g at 4°C for 10 minutes to collect cells. The media was collected as low titer viral stock for subsequent tissue culture experiments. For the virus stock, cell pellets from the centrifugation were combined together by resuspension in 1 to 1 ratio with DMEM and 10% non-fat skim milk. The stock was sonicated three times on ice, and 100ul of the virus stock was aliquoted into cryovials. The media and viral stock were stored at -80°C for long-term storage. Virus titers for the frozen media and viral stock were determined by standard plaque assays. Viral titers ranged from  $2 \times 10^6$  to  $5 \times 10^7$  plaque forming units (PFU) per ml while the media titers ranged from  $5 \times 10^4$  to  $1 \times 10^6$  PFU per ml.

### **Generation of Viral Progeny from BAC DNA Constructs**

NIH 3T3 cells of passage 20 or below were grown to 90-100% confluence. Cells were trypsinized, pelleted and resuspended in DMEM. 3-5 million cells in 260 ul DEME were mixed with 4.5ug of MCMV BAC DNA in a 4mm electroporation cuvette, and electroporated with a BTX ECM 630 electroporator set at 250 volts, 960  $\mu$ F, and 75 ohms. At these setting the expected pulse time was between 30 to 40 milliseconds. Immediately following electroporation 1ml of DMEM media was added to the cell/DNA mixture in the cuvette. The contents of the transfection were then transferred to a T-25 flask. One day post transfection the media in the T-25 flask was removed and fresh DMEM was added. The cells were then monitored for CPE. Cells transfected with viral BAC constructs with wild-type like replication kinetics would often exhibit plaque formation 3-5 days post transfection, indicating the presence and spread of infectious viral progeny from the BAC DNA. To remove the BAC vector from the viral genome, the virus was passaged five times in NIH3T3 cells.

### **Construction of the Viral ORF-Deletion Mutants**

To delete each open reading frame (ORF) two oligonucleotide primers (30 in Zeo 5' and 30 in Zeo 3') were constructed and contained the following components (from 3' to 5'): 64 homologous nucleotides to zeocin LoxP plasmid, a 20-nt unique barcode tag, and a common 19-nt primer (Figure 1). The 30 in Zeo 5' and 30 in Zeo 3' primers were used to amplify the Zeocin LoxP cassette, which contains the zeocin resistance gene flanked by LoxP sites. The product that resulted from the first round of PCR, containing the zeocin resistance cassette with LoxP sites flanked by the barcode tag and the common 19-nt primer, was then subject to a second round of PCR with primers 50 up 5' and 50 dn 3' which contain 20 homologous nucleotides to the 1<sup>st</sup> PCR product and 50 bases of homology to the region upstream and downstream of the targeted ORF, respectively. The resulting product was a Zeocin LoxP cassette flanked by 50-nt homologous sequence targeting the ORF to be deleted in the pSM3fr BAC. This PCR-amplified Zeocin Lox P cassette was then transformed into the DY380 strain of bacteria carrying the pSM3fr BAC. The DY380 was engineered from DH10B. DY380 strain expresses phage-derived recombination genes under the control of a temperature-sensitive repressor [19]. Transformation of the pSM3fr-bearing DY380 strain with the PCR product resulted in the



replacement of ORF on selection for zeocin resistance. The unique 20-mer barcode sequence were covalently linked to the sequence that targeted them to the MCMV genome, creating a permanent associate and genetic linkage between a particular deletion strain and the tag sequences.

### **Bacterial Transformation Procedures**

Recombination and electrocompetent cells for transformation were generated by culturing DY380 bacteria at 30°C in low salt Luria Broth (LSLB) media and shaking at 250 rpm for approximately 2-3 hours until the culture reached an OD<sub>600</sub> of 0.4-0.6. Then the bacteria cultures were incubated at 42°C for 15 minutes in shaking water bath rotating at 250 rpm. At 42°C the temperature sensitive repressor suppressing the expression of the recombination protein degrades and expression of the recombination protein is allowed to proceed. This induction process makes the bacteria recombination competent. After the 15 minutes induction period, bacterial cultures are then immediately placed in an ice-water slurry for 10 minutes and gently swirling to ensure uniform cooling of the bacteria. Bacterial cells were then pelleted in a pre-cooled (4°C) centrifuge and washed with 100ml of ice cold sterile distilled water. Bacterial cells were pelleted again and washed with 10% ice cold glycerol and pelleted again. Bacterial pellet was resuspended in cold 10% glycerol, aliquoted at a volume of 40ul, and stored at -80°C for long term storage.

Bacterial competent cultures were electroporated with the PCR DNA product that contain the zeocin loxP cassette flanked by the regions targeting the specified ORF for deletion. Approximately 1-5ug of linear PCR product was mixed with 40 ul of the competent bacterial cultures in a 1mm electroporation cuvette. A BTX ECM 630 electroporator was used with wetting at 1.6kv, 25 uF, and 150 ohms. The transformed bacteria were then incubated for 1-2 hours at 30°C and plated on LSB agar plates (12.5 ug/ml chloramphenicol/ 50 ug/ml zeocin) at 30°C. BAC DNAs were isolated from the surviving colonies and were screened with PCR assay, restriction profiling, and Southern analysis.

### **Analysis of growth of viruses in vitro in various cell lines**

Growth kinetics of non-essential mutants analyzed on NIH3T3 cells. NIH 3T3 cells grown to 50 to 60% confluence were infected at with 0.01 PFU per cell. At 0, 1, 2, 4, and 7 days post-infection, the infected cells and medium were harvested, and an equal volume of 10% skim milk were added before being treated to 2 rounds for freeze thaw. Virus titers were determined by plaque assays in duplicate experiments in NIH 3T3 cells. Briefly, cells were first infected with the viruses at 10-fold serial dilutions. After 75 min of incubation with the homogenates diluted in 1 ml of complete medium at 37°C, the cells were overlaid with fresh complete medium containing 2% agarose and culture for 4 to 5 days before the plaques were counted. Viral titers (recorded as PFU per milliliter) for each sample were determined in duplicate. The limit of virus detection was 10 PFU/ml of the freeze thaw mixture. Those samples that were negative a 10<sup>-1</sup> dilution were assigned a titer value of 10 (10<sup>1</sup>) PFU/ml.

Growth kinetics of non-essential mutants analyzed on SCA9 cells. SCA-9 cells grown to 50 to 60% confluence were infected at with 0.01 PFU per cell. At 0, 1, 3, and 5 days post-infection, the infected cells and medium were harvested, and an equal volume of 10% skim milk

were added before being treated to 2 rounds for freeze thaw. Virus titers were determined by plaque assays in duplicate experiments in NIH-3T3 cells.

Growth kinetics of non-essential mutants analyzed on IC-21 cells. IC-21 cells grown to 50 to 60% confluence were infected at with 0.1 PFU per cell and 1 PFU per cell. At 0, 1, 2, 4, and 7 days post-infection, the infected cells and medium were harvested, and an equal volume of 10% skim milk were added before being treated to 2 rounds for freeze thaw. Virus titers were determined by plaque assays in duplicate experiments in NIH 3T3 cells.

Viral growth determined in screens involving SCA-9, CRL-1972, J774A.1 and SVEC cells were conducted at single time-point comparisons against wild-type psm3fr growth. Single time-points were selected for each of the four cell lines based on wild-type infection. Criteria for selection was determined by the point at which psm3fr infection reached 50% of maximum titers and 50% of the cells were infected, determined due to morphological changes in infected cells as visualized by light microscopy. Infected SCA9 cells were harvested as previously described at 4 days post infection at a multiplicity of infection (MOI) of 0.01. For CRL-1972, cells were infected at an MOI of 0.01 and cells were harvested as described in the previous paragraph at 3 days post infection. J774A.1 cells were infected at an MOI of 0.3 and harvested 3 days post infection. And SVEC4-10 cells were infected at an MOI of 0.01 and harvested 3 days post infection.

### **Southern Analysis of the Deletion Mutant**

Southern analysis of the BAC constructs was performed by digesting 3 ug of BAC DNA with restriction enzyme (AseI), separating on agarose gels (0.8%), and transferred to Zeta-Probe nylon membrane (Bio-Rad). Membrane was hybridized with <sup>32</sup>P-radiolabeled DNA probes that contained the zeocin loxP cassette. Labeled DNA probes were prepared by random primer synthesis (Bio-Rad). Probed membranes were analyzed with a STORM 840 PhosphorImager (Molecular Dynamics).

### **Construction of plasmids**

MCMV Smith and pSM3fr, a MCMV Smith<sub>BAC</sub> construct, were used for all PCR amplification of full-length virion ORFs. Primers to virion ORFs (Table 1) were designed for cloning into the pGBK-T7 bait and pGAD-T7 prey plasmids for yeast expression and further subcloning in pCMV-myc and pCMV-HA mammalian expression plasmids (Clontech). Each primer sequence contains an outer and inner restriction enzyme site for cloning in the multiple cloning site (MCS) of the yeast and mammalian expression plasmids, respectively (Table 1). PCR amplification was through the use of iProof High-fidelity DNA polymerase (Bio-Rad). The resulting constructs were confirmed by restriction digest profile and sequencing. A total of fifty-seven MCMV-encoded virion ORFs were cloned into each of the pGBK-T7 and pGAD-T7 vectors.

### **Yeast two-hybrid library screen**

The M43 ORF cloned into pGBK-T7 was transformed into AH109 (*MATa*) and a universal normalized mouse library cloned into pGAD-T7-RecAB plasmid was transformed into Y187 (*MATα*) yeast strains, respectively (Matchmaker 3 System, Clontech). AH109 strains harboring pGBK-T7 plasmids were maintained in minimal SD media with tryptophan dropout supplement

(SD/-Trp) while Y187 strains harboring pGAD-T7 plasmids were maintained in minimal SD media with leucine dropout supplement (SD/ -Leu).

Prior to performing the matings, the M43 pGBK-T7-fusion protein in the AH109 strain was tested for autoactivation. The AH109 strain was plated on SD/ -Ade/ -His/ -Trp agar with 40 µg/mL X-α-Gal. AH109 strains containing pGBK-T7 ORFs were determined to be autoactivators if growth was detected in the absence of any pGAD-T7 cloned ORFs, and subsequently eliminated from further matings.

Yeast mating was carried out by inoculating 1 mL of the library strain with 5 mL of the M43 bait strain in a 2L flask with 45 mL of 2xYPDA and 50 µg/mL of kanamycin. The 2L flask was incubated at 30 degrees C for 24 hours at 50 rpm. Cells were pelleted at 1000 g for 10 min and resuspended using 10 ml of 0.5xYPDA/Kan. 100 µl of a 1/1000 and 1/10,000 dilution of the matings were spread onto SD/-Trp, SD/-Leu and SD/-Leu/-Trp in order to calculate the number of screened clones. The rest of the inoculum was plated on SD/-Ade/-His/-Leu/-Trp/X-alpha-Gal (QDO) agar plates and incubated for 3-8 days.

Yeast colonies were harvested and plasmids were extracted using yeast DNA extraction kits (Pierce). Extracted plasmid DNAs were then transformed into Top 10 cells and plated on LB/ Amp agar plates and allowed to grow overnight. Bacterial colonies were picked and grown overnight to amplify plasmid DNA. Plasmid DNA was harvested using Qiagen miniprep kits. Extracted DNA was sent for sequencing to determine the sequence of the insert in pGAD-T7-RecAB vectors. Gene identity of the insert was determined using nucleotide BLAST.

Mating controls used was via the comparison of combinations of transformed AH109 and Y187 strains together and individually in 0.5 mL of YPDA, that were shaken overnight at 200 rpm. These mating cultures were plated onto SD/ -Leu/ -Trp plates. Only diploid yeasts from the mating of AH109 and Y187 yeast were able to grow on the SD/ -Leu/ -Trp plates while individual AH109 and Y187 yeast were unable to grow.

QDO/ X-α-Gal plates were used as a high stringency screen for eliminating possible false positives. AH109 strains contained three reporters—ADE2, HIS3, and MEL1 (encodes a-galactosidase)—under the control of unique GAL4 upstream activating sequences (UAS) and TATA boxes. The positive control used was AH109 yeast transformed with BD-p53 fusion protein mated with Y187 yeast transformed with AD-T (SV40 T-antigen), while the negative control was transformation of AH109 with BD-Lamin C with and Y187 with AD-T.

## Results

The M43 deletion mutant virus was created using the MCMV BAC virus pSM3fr [18]. pSM3fr is a BAC mutant virus that contains several features beyond the simplicity of using a bacterial artificial chromosome backbone to facilitate homologous recombination and mutagenesis in a bacterial system. In the bacterial system there are no size constraints to the MCMV genome however due to packaging limitations of the viral capsid there is a constraints in vitro and in vivo. These packaging constraints can lead to unforeseen mutations or recombination events that lead to a non-infectious MCMV virus particle in vivo (Lee, unpublished results). The pSM3fr BAC virus was designed with this limitation in mind. Using the MCMV Smith virus strain, this strain is infectious in vivo and retains characteristic of MCMV pathogenesis that make it similar to infection and pathogenesis of HCMV. In order to

accomplish this it was designed to contain a 527 nt repeated fragment from the MCMV genome that flanked the BAC backbone. This repeated sequence is required to excise the BAC in cell culture after mutagenesis. This leaves a full-length infectious genome that is able to replicate in mice.

Our lab has taken advantage of this construct to create a mutant virus library of which the M43 deletion mutant virus was created (Chan and Umamoto, unpublished results). In order to create the M43 deletion mutant two sets of primers were designed to create the fragment used to delete the ORF. The first set of 5' and 3' primers contained fifty nucleotides upstream or downstream, respectively, of the M43 predicted ORF (Figure 1A). The fifty nucleotides were combined with a portion of either an upstream or downstream unique sequence tag (signature tag). The second set of primers contained the full length upstream or down signature tag sequence, LoxP sites and either an upstream or downstream sequence of zeocin. Using these two sets of primers a recombination cassette was created featuring fifty nt sequences upstream and downstream of the M43 ORF, two unique signature tags, two LoxP sites and the gene that encodes for zeocin. Using homologous recombination the M43 genome was replaced with this cassette allowing for selection of the deletion mutant via zeocin. After confirmation of successful deletion via southern, the mutant virus was passaged five times in NIH-3T3 fibroblasts to remove the BAC backbone.

The resulting M43 deletion mutant virus was used to infect a variety of different cell types. As part of a larger screen involving all the MCMV mutant viruses created, the M43 deletion virus was used to infect NIH-3T3 cells at a multiplicity of infection (MOI) of 0.01 (Figure 3A). At one viral particle for every 100 cells, infected cells were harvested at zero, one, three, five and seven days post infection (dpi) and reached a titer of  $1 \times 10^6$  plaque forming units per mL (PFU/mL). Comparison of the M43 deletion mutant to wild-type infection showed that in NIH-3T3 cells deletion of M43 was non-essential.

As M43 had been shown previously to be defective in vivo in the salivary gland, SCA9 salivary gland epitheloid cells were infected at zero, one, three and five dpi at an MOI of 0.01 (Figure 3A). When compared to wild-type infection both viruses reached a titer of  $1 \times 10^5$  PFU/mL. Again showing that M43 was not essential in SCA9 cells.

Three other cell lines were tested at one timepoint (Figure 3B). CRL1972—bone marrow stromal cells, SVEC—smooth vascular endothelial cells and J774A.1—macrophage cells. In SVEC cells, deletion of M43 was wild-type like and in CRL1972 and J774A.1 the deletion mutant showed moderate signs of attenuation.

Growth curve analysis in IC-21—peritoneal macrophages showed an interesting phenotype. Infected cells were harvested at one, three, five and seven dpi and compared to wild-type pSM3fr infection. When infecting at high MOI, MOI of 1.0, M43 showed moderate signs of attenuation that fell within the one log margin of error that represented the limitation of our technique. However, at low MOI, MOI of 0.1, M43 showed a two-log defect at three and five dpi. At seven dpi, the M43 deletion mutant virus seemed to recover and regain wildtype-like growth characteristics.

Using the Matchmaker yeast two-hybrid system from Clontech, the M43 ORF was cloned into the bait vector, pGBK-T7 plasmid, containing the binding domain of Gal4 (BDM43). A library of normalized mouse cDNA was cloned into the pGAD-T7-RecAB vector fusing the Gal4 activation domain to each cDNA fragment (AD-fusion). Both BDM43 and the cDNA AD-fusion

plasmids were transformed into AH109 and Y187 yeast cells and mated (Figure 2). Matings were plated on QDO selection plates and colonies were screened for their inserted cDNA sequences. The library screened a total of 11,900,000 clones, well above the minimum of the one million required for complete coverage of the cDNA library. Calculation of mating efficiency resulted in 5% efficiency based on the limiting partner bait plasmid. This falls well above the limit of 2% required to screen one million clones. Yeast two-hybrid library screen mating resulted in the growth of twelve colonies that yielded two genes that have potential interaction with the M43 ORF (Figure 5). The M43 fusion protein interacted with proteins created from nine hundred nucleotide fragments of cDNA. Of the interacting proteins, Fibulin 5 was found in two of the yeast colonies that grew on the QDO plates and represented a 402 bp fragment that spanned position 946 to 1347 of the 1347 bp Fibulin 5 mRNA. The other protein, Kelch-like 1 represented a fragment from 1825 to 2256 of the 2256 bp mRNA.

## Discussion

HCMV is among the most common causes of oral diseases associated with AIDS patients [1-3]. In the salivary glands the virus engages in a high level of replication in the serous acinar cells of the salivary glands making the salivary glands a major source of persistent virus [1, 4]. Understanding how CMV leads to productive and latent infection in the salivary glands represents a key step in potentially developing treatments and therapies that can prevent transmission or reduce the level of infection in affected individuals.

Previous studies in our laboratory have provided evidence that the MCMV open reading frame M43 is important for viral infection in salivary gland. M43 represents an important avenue of investigation as it contains homology to the HCMV ORF UL43. By using a murine model of infection we can investigate the effects of pathogenesis of the virus to a greater extent than we could using HCMV. In these earlier studies, a viral mutant, RvM43, was constructed which contained a transposon inserted in the ORF M43 [12]. Our results showed that M43 is not essential for viral replication *in vitro* in NIH-3T3 cells. Moreover, RvM43 exhibited similar titers to that of the wild-type virus in the lungs, livers, spleens, and kidneys of both Balb/c and SCID mice, and was as virulent as the wild-type virus in killing SCID mice when these animals were intraperitoneally infected. In contrast, the titers of the mutant virus in the salivary glands of the intraperitoneally-infected animals were significantly (100-1000 fold) lower than those of the wild-type virus [12]. When inoculated directly into the salivary glands, RvM43 remained defective in growth when compared to the wild-type and rescued virus. Similar results were also observed using another viral mutant, DM43, which contained a deletion of the entire M43 ORF (Zhu, J., Chan, K., Li, H., Umamoto, S., and Liu, F., unpublished results). These results suggest that M43 encodes a determinant for MCMV infection in the salivary glands.

Recently, a new M43 deletion mutant virus was created using the MCMV BAC virus pSM3fr [18]. pSM3fr is a BAC mutant virus that contains several features that facilitate investigation of deleted ORF *in vivo*. This system takes advantage of the ease and simplicity of a bacterial system of mutagenesis but accounts for packaging limitations of the viral capsid when grown *in vitro* and *in vivo*. These packaging constraints can lead to unforeseen mutations or recombination events that lead to a non-infectious MCMV viral particle *in vivo* (Lee, unpublished results). The pSM3fr BAC virus was designed using the MCMV Smith virus strain,

this strain is infectious *in vivo* and retains characteristic of MCMV pathogenesis that make it similar to infection and pathogenesis of HCMV. In order to allow our deletion mutant to grow with a roughly full-length genome the virus was designed to contain a 527 nt repeated fragment from the MCMV genome that flanked the BAC backbone. This repeated sequence is important in excising the BAC in cell culture after mutagenesis. Five passages in cell culture results in a hundred percent removal of the BAC from all mutant viruses.

Our lab has taken advantage of this construct to create a mutant virus library of which the M43 deletion mutant virus was created (Chan and Umamoto, unpublished results). In order to create the M43 deletion mutant, two sets of primers were designed to create the fragment used to delete the ORF. The first set of 5' and 3' primers contained fifty nucleotides upstream or downstream, respectively, of the M43 predicted ORF (Figure 1A). The fifty nucleotides were combined with a portion of either an upstream or downstream unique sequence tag (signature tag). The second set of primers contained the full length upstream or down signature tag sequence, *LoxP* sites and either an upstream or downstream sequence of Zeocin. Using these two sets of primers a recombination cassette was created featuring fifty nt sequences upstream and downstream of the M43 ORF, two unique signature tags, two *LoxP* sites and the gene that encodes for zeocin. Using homologous recombination the M43 genome was replaced with this cassette allowing for selection of the deletion mutant via zeocin. After confirmation of successful deletion via southern, the mutant virus was passaged five times in NIH-3T3 fibroblast cells to remove the BAC backbone. In addition to the removal of the backbone, the virus was created with the ability to remove the zeocin cassette through *LoxP* recombination to limit any toxic effects *in vivo*. The mutant virus also contains two unique signature sequences designed to be used with real-time PCR as an additional method for quantitation. The M43 mutant virus and all other viruses found in the mutant virus library created contain these tags and can be used in a high-throughput method to determine levels of infection of these various viruses in various organs using less mice [20].

The resulting M43 deletion mutant virus was used to infect a variety of different cell types. As part of a larger screen involving all the MCMV mutant viruses created, the M43 deletion virus was used to infect NIH-3T3 cells at a multiplicity of infection (MOI) of 0.01 (Figure 3A). At one viral particle for every 100 cells, infected cells were harvested at zero, one, three, five and seven days post infection (dpi) and reached a titer of  $1 \times 10^6$  plaque forming units per mL (PFU/mL). Comparison of the M43 deletion mutant to wildtype infection showed that in NIH-3T3 cells deletion of M43 was non-essential.

As M43 had been shown previously to be defective *in vivo* in the salivary gland, SCA9 salivary gland epitheloid cells were infected at zero, one, three and five dpi at an MOI of 0.01 (Figure 3A). When compared to wildtype infection both viruses reached a titer of  $1 \times 10^5$  PFU/mL. Again showing that M43 was not essential in SCA9 cells. This may be due to the nature of SCA-9 cells as epitheloid. While derived from salivary gland cells, transformation of the cell line has resulted in epithelial cell characteristics which may influence the ability of the virus to productively infect these cells.

Three other cell lines were tested at one timepoint (Figure 3B). CRL1972—bone marrow stromal cells, SVEC—smooth vascular endothelial cells and J774A.1—macrophage cells. In SVEC cells, deletion of M43 was wildtype like and in CRL1972 and J774A.1 the deletion mutant showed moderate signs of attenuation.

Growth curve analysis in IC-21—peritoneal macrophages showed an interesting phenotype. Infected cells were harvested at one, three, five and seven dpi and compared to wildtype pSM3fr infection. When infecting at high MOI, MOI of 1.0, M43 showed moderate signs of attenuation that fell within the one log margin of error that represented the limitation of our technique. However, at low MOI, MOI of 0.1, M43 showed a two-log defect at three and five dpi. At seven dpi, the M43 deletion mutant virus seemed to recover and regain wildtype-like growth characteristics. The ability of M43 to grow like wild-type at high MOI where the majority of the cells are infected seems to suggest that M43 has no involvement in the processes that involve replication. The MOI we used represented an infection ratio of one virus per cell and may account for the moderate attenuation in the growth phenotype from wild-type infection. Using Poisson distribution full coverage of all cells with at least viral particle involves an MOI of 5. Suggesting that there were still cells available for both the wild-type and deletion virus to infect. This is of importance when analyzing growth of the viruses at low MOI where a 2-log difference in growth is seen at days three and five post infection. There could be many reasons for a defect at low MOI however, due to the ability of the virus to infect like wild-type at high MOI, there is a potential for the defect caused by the M43 ORF deletion to occur in cell to cell spread. And comparison of the deletion mutant and wild-type viral titers at one day post infection in both high and low MOI, we can infer that the defect is not in viral adsorption as the mutant virus shows similar levels of infection to wild-type infection. The data from both high and low MOI experiments suggests a potential defect in the ability of the virus to spread from cell to cell and may involve elements of viral egress. In support of this theory is the recovery of the M43 deletion mutant virus at high MOI seen at seven days post infection. At this late timepoint the majority of the cells are already infected and the amount of virus does not depend on the spread of the viral particle but rather the replication of the virus as in low MOI experiments. The macrophage represents an important cell line for persistence and latency for CMV [21]. But more importantly, the macrophage may function as an important transporter for infectious virus both active and latent virus. The ability to infect this cell type may provide implications for the spread and level of CMV infection in the host. The salivary gland generally shows signs of viral titers at later times than other organs leading to its characterization as a secondary infected tissue. Due to the nature of infection of the salivary glands, the virus may require cells like the macrophage to spread and infiltrate this organ. The rate at which CMV can spread among macrophages may result in the phenotype seen in our previous studies. In both Balb/c and SCID mice, virus levels of the M43 transposon mutant do increase over time even though they do not obtain wildtype levels suggesting that there is not the absence of growth when deleting M43 but a potential retardation [12].

In our yeast two-hybrid interaction screen, when screened against all of the ORF, we did not find any viral protein interaction involving M43. While a negative result using yeast two-hybrid is usually ignored and does not infer a result due to the many reasons explained in the previous chapters that could lead to false negatives. It raised the idea that the M43 protein could potentially interact with cellular components to cause the phenotypes that we observed when using the deletion virus. Several of the viral yeast two-hybrid studies published investigated interactions between the virus and host cells. Using hepatitis C virus (HCV) yeast two-hybrid analysis, investigators found that viral proteins interacted with multiple host cell proteins potentially elucidating disease manifestations. For example, networks of HCV proteins

interacted with components in insulin-Jak/stat pathways showing a connection between the increased risk of insulin resistance seen during infection and viral products [22]. And construction of the Epstein Barr interactome involved the screening of a spleen cDNA library that resulted in 173 EBV-human protein interactions [23].

Our laboratory utilized the Matchmaker yeast two-hybrid system from Clontech to clone the M43 ORF into the bait vector, pGBK-T7, containing the binding domain of Gal4 (BDM43). A library of normalized mouse cDNA was cloned into the pGAD-T7-RecAB vector fusing the Gal4 activation domain to each cDNA fragment (AD-fusion). Both BDM43 and the cDNA AD-fusion plasmids were transformed into AH109 and Y187 yeast cells and mated (Figure 2). Matings were plated on QDO selection plates and colonies were screened for their inserted cDNA sequences. In the assay, 11,900,000 clones were screened. The amount of clones screened was well above the minimum of one million required for coverage of the cDNA library. The mating efficiency was 5% also above the minimum limit of 2% required to screen one million clones. Mating resulted in the growth of twelve colonies that yielded two genes that potentially interacted with the M43 ORF (Figure 5). Of the interacting proteins, Fibulin 5 was found in two of the yeast colonies that grew on the QDO plates and represented a 402 bp fragment that spanned position 946 to 1347 of the 1347 bp Fibulin 5 mRNA. The other protein, Kelch-like 1 represented a fragment from 1825 to 2256 of the 2256 bp mRNA.

Fibulin 5, also known as DANCE or EVEC, is an extracellular matrix (ECM) protein that has a variety of functions that involve cell growth, motility, adhesion and wound healing in endothelial, epithelial and fibroblast cells [24]. It is an antagonist of angiogenesis and can function to prevent the migration and degradation of ECM components in endothelial cells [25]. The Fibulin 5 protein contains six calcium-binding EGF motifs and an RGD motif that can interact with cell surface integrins. Knock-out mice show that Fibulin 5 serves an important function in elastic fiber elasticity, as these mice show severe signs of elastinopathy in skin, lungs, aorta and genitals [26]. The inserted sequence that has been shown to potentially interact with M43 may involve binding or disruption of a region containing one of the six calcium-binding EGF motifs however the fragment does not contain the RGD motif found at the N terminus of Fibulin 5. The fragment in the yeast two-hybrid library screen that interacts with M43 falls within the last motif of the six calcium-binding EGF motifs found at amino acids (a.a.) 288 to 333. The fragment contains amino acids at position 315 to the end. These protein motifs are thought to provide stability to the protein and may facilitate interaction with other interacting proteins. The potential involvement with ECM proteins involved with cellular adhesion seem to suggest that the role of M43 may fall somewhere in allowing infected cells to migrate and thus spread to other areas of the body. M43 binding of fibulin 5 internally may sequester the protein and prevent it from functioning as an anti-adhesion molecule. While many of the studies link fibulin 5 to endothelial and epithelial cells. The function of adhesion molecules in cells such as macrophages cannot be ignored and may prove a link to M43 involvement in infection of IC-21 peritoneal macrophages. In general, the potential for M43 to facilitate transport of the virus through manipulation of adhesion and ECM proteins support the decrease in infection levels of the salivary gland when M43 is deleted thus interfering with processes that have an affect on spread to secondary organs.

The other protein identified in the yeast two-hybrid library screen also supports M43's role in promoting cellular motility. Kelch-like protein 1 (KLHL 1) is a protein involved in actin



binding and may have similar functions to the Kelch protein found in *Drosophila* that facilitates the formation of canals required for transport [27]. KLHL 1 is highly expressed in brain tissues and may have a role in organizing the cytoskeleton of cells in the cerebellum. The structure of KLHL 1 contains six Kelch-like repeats from a.a. position 462 to a.a. 752 involved in actin binding. The fragment recovered in the yeast two-hybrid library screen represents a.a. 609 to 752 suggesting a potential role in the disruption of the last three actin binding sites. Studies have also shown that KLHL 1 is a cytoplasmic protein. The role KLHL 1 has in potentially modifying the cytoskeletal structure shows the potential involvement of M43 in processes that may serve to facilitate transport and motility of cells infected by MCMV. There is also another possibility that can be inferred from the data obtained from IC-21 infections, the cytoplasmic localization of KLHL 1 and its interaction with the cell cytoskeleton combined with the presence of M43 in the structure of the virus particle may suggest a role for M43 in viral assembly or egress. KLHL 1 could be potentially used as a vehicle to move the virus through the cellular network using M43 as a linker protein.

While KLHL1 is primarily expressed in neuronal tissues suggesting a function of M43 other than in relation to macrophage or salivary gland tissues. The involvement of KLHL 1 in actin and cytoskeleton arrangement highlights a similar role in motility and adhesion for M43 to its interaction with fibulin 5. The possibility also exists that binding of M43 to KLHL 1 may not be specifically to KLHL 1 but to its Kelch-like repeats, which facilitate the protein's ability to bind actin. These repeats are found in multiple different proteins including proteins of orthopoxviruses which are proposed to help transport the virus to various cell compartments [28]. The limitations of the yeast two-hybrid system may have prevented interaction with proteins expressing these repeats. Although the possibility exists that the viral protein may have multiple roles that vary depending on the cell type infected and interaction with KLHL 1 may have no connection to infection of macrophages or the salivary gland.

The M43 ORF represents an interesting avenue of investigation into the potential pathogenesis of the MCMV virus that may provide insight into HCMV infection and persistence. Its involvement in processes and cell types that require motility may suggest a unique and intriguing interplay between components that allow the virus to traffic in the cell and through the human host. And it may be through the understanding of such components that treatments can be developed to limit the potential spread and severity of CMV associated disease.



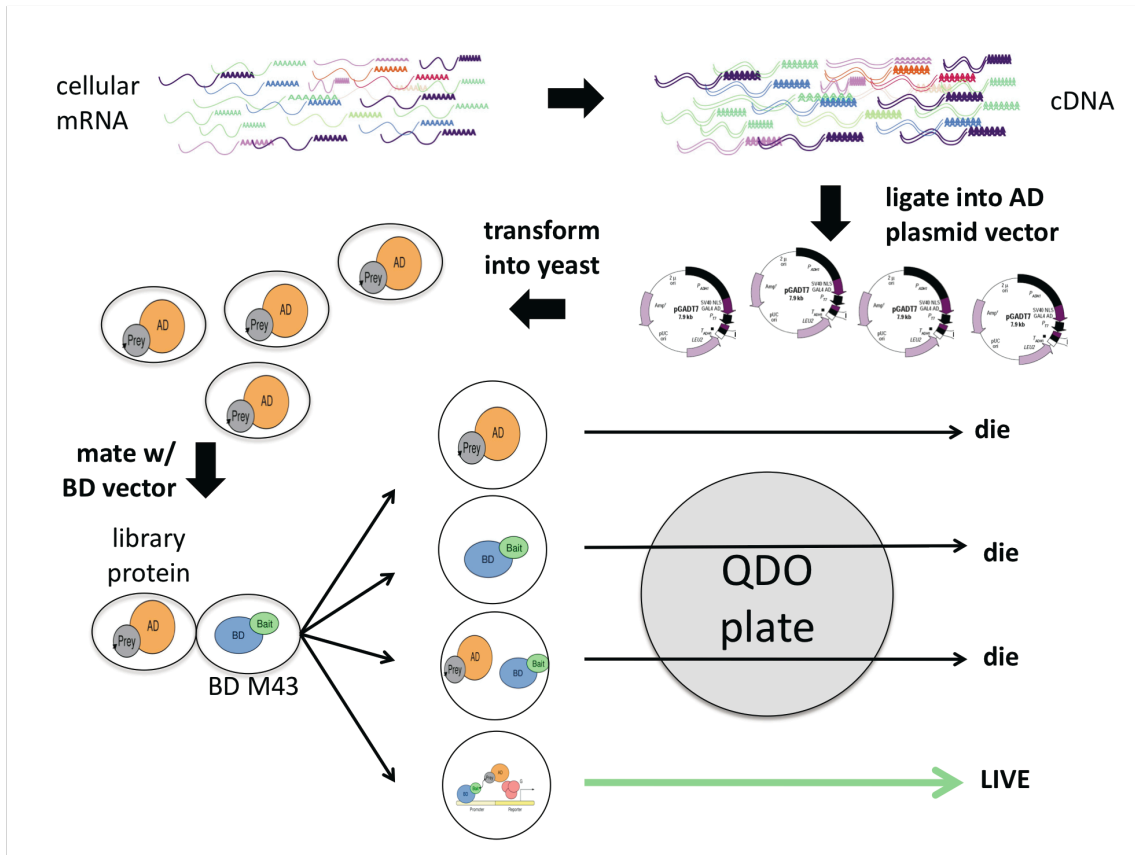
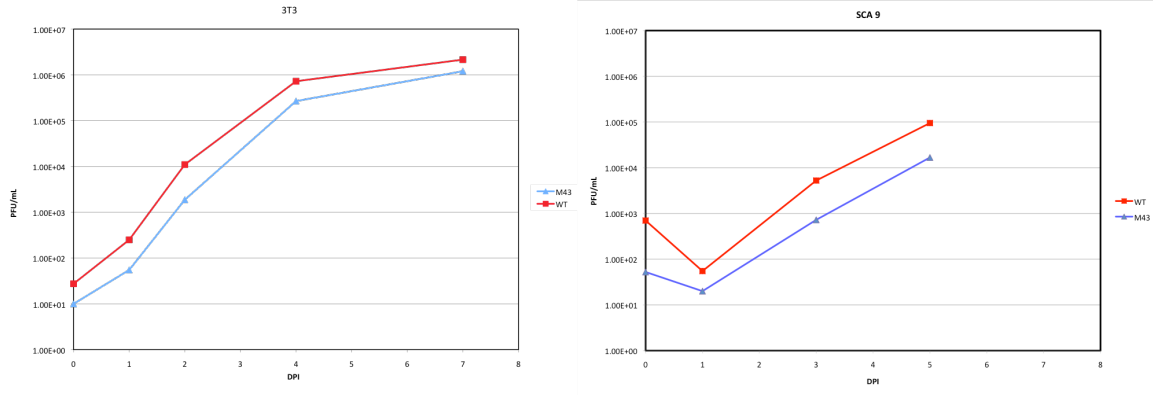


**Figure 2. Yeast Two-Hybrid Library Screen.**

The MCMV ORF M43 was cloned into the pGBK-T7 (BD) yeast two-hybrid bait vector. BD-M43 was transformed into AH109 yeast cells and mated with yeast containing a normalized cDNA mouse library cloned into pGAD-T7-RecAB (AD) vector. Mated yeasts were plated on QDO plates and yeast growth represented mated yeast that contained successful AD vector interaction with BD-M43.

A



B

	3T3	SCA9	CRL1972	SVEC	J774A.1
M43	wt	-0.01	1.29	0.35	1.53

**Figure 3. Growth Curve Analysis Using M43 Deletion BAC virus**

(A) Viral growth of the M43 deletion mutant was conducted in NIH-3T3 and SCA-9 cells (ATCC). M43 and wild-type pSM3fr virus was used to infect both cell lines at a multiplicity of infection of 0.01. In both cell lines, the M43 deletion virus grew similar to wildtype. (B) The growth of the M43 deletion mutant was compared to wildtype at a single timepoint in four different cell lines. SCA9 - 4 dpi, MOI: 0.01. CRL1072 - 3 dpi, MOI: 0.01. SVEC - 3 dpi, MOI: 0.01. J774A.1 - 3 dpi, MOI: 0.3. Growth of the M43 deletion mutant was wildtype like in SCA9 and SVEC cells and showed signs of moderate attenuation in CRL1972 and J774A.1 cells as compared to wildtype growth in each of the mentioned cell lines.

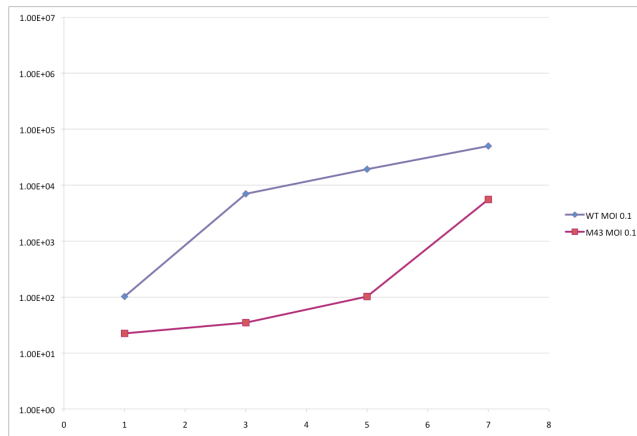
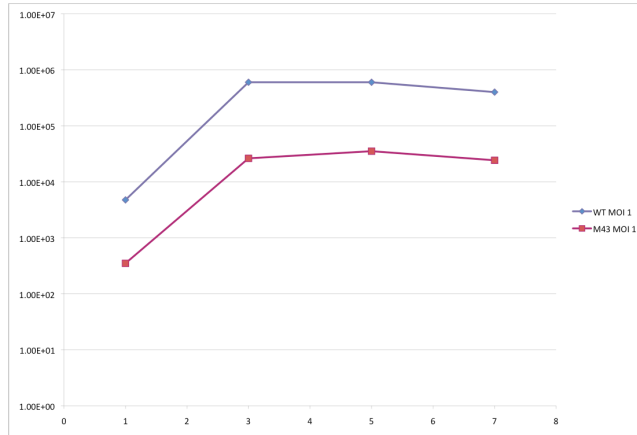


**Figure 4. Growth Curve Analysis of M43 Deletion Mutant in IC-21 Peritoneal Macrophages**

IC-21, peritoneal macrophages were infected at a MOI of 0.1 and 1.0 using the M43 deletion mutant virus. Growth analysis of the M43 deletion mutant at both low MOI and high MOI was compared to wildtype pSM3fr growth. Deletion of the M43 ORF results in wildtype like growth at high MOI and a 2-log defect at low MOI.

Yeast two-hybrid cDNA library screen

HITS	12
GENE MATCHES	2

<b>GENES IDENTIFIED</b>	<b>HITS</b>	<b>FUNCTION</b>
FIBULIN 5	2	EXTRACELLULAR MATRIX PROTEIN
KELCH-LIKE PROTEIN 1	1	ACTIN ORGANIZATION

**Figure 5. Yeast Two-Hybrid Library Screen**

The M43 ORF was cloned into the pGBK-T7 yeast bait vector and mated to pGAD-T7-RecAB vectors containing a normalized mouse cDNA library (clontech). 11,900,000 clones were screened resulting in a 5% mating efficiency. 12 colonies were identified and harvested for sequence analysis. 3 of these colonies resulted in genes matching Fibulin 5 and Kelch-like protein 1.

## References

1. Pass, R.F., *Cytomegalovirus*, in *Fields Virology*, D.M. Knipe and P.M. Howley, Editors. 2001, Lippincott-William & Wilkins: Philadelphia, Pa. p. 2675-2706.
2. Itin, P.H. and S. Lautenschlager, *Viral lesions of the mouth in HIV-infected patients*. *Dermatology*, 1997. 194(1): p. 1-7.
3. Greenberg, M.S., *HIV-associated lesions*. *Dermatol Clin*, 1996. 14(2): p. 319-26.
4. Mocarski, E.S. and C.T. Courcelle, *Cytomegalovirus and their replication*, in *Fields Virology*, D.M. Knipe and P.M. Howley, Editors. 2001, Lippincott-William & Wilkins: Philadelphia, Pa. p. 2629-2673.
5. Manning, W.C., et al., *Cytomegalovirus determinant of replication in salivary glands*. *J Virol*, 1992. 66(6): p. 3794-802.
6. Chee, M.S., et al., *Analysis of the protein-coding content of the sequence of human cytomegalovirus strain AD169*. *Curr Top Microbiol Immunol*, 1990. 154: p. 125-69.
7. Rawlinson, W.D., H.E. Farrell, and B.G. Barrell, *Analysis of the complete DNA sequence of murine cytomegalovirus*. *J Virol*, 1996. 70(12): p. 8833-49.
8. Cavanaugh, V.J., et al., *Murine cytomegalovirus with a deletion of genes spanning HindIII-J and -I displays altered cell and tissue tropism*. *J Virol*, 1996. 70(3): p. 1365-74.
9. Davis-Poynter, N.J., et al., *Identification and characterization of a G protein-coupled receptor homolog encoded by murine cytomegalovirus*. *J Virol*, 1997. 71(2): p. 1521-9.
10. Morello, C.S., Cramner, L.D., and Spector, D.H., *In vivo replication, latency, and immunogenicity of murine cytomegalovirus mutants with deletions in the M83 and M84 genes, the putative homologs of human cytomegalovirus pp65 (UL83)*. *Journal of Virology*, 1999. 73: p. 7678-7693.
11. Zhan, X., et al., *Construction and characterization of murine cytomegaloviruses that contain transposon insertions at open reading frames m09 and M83*. *J Virol*, 2000. 74(16): p. 7411-21.
12. Xiao, J., et al., *In vitro and in vivo characterization of a murine cytomegalovirus with a transposon insertional mutation at open reading frame M43*. *J Virol*, 2000. 74(20): p. 9488-97.
13. Kattenhorn, L.M., et al., *Identification of proteins associated with murine cytomegalovirus virions*. *J Virol*, 2004. 78(20): p. 11187-97.
14. Zhang, Z., et al., *Genetic analysis of varicella-zoster virus ORF0 to ORF4 by use of a novel luciferase bacterial artificial chromosome system*. *J Virol*, 2007. 81(17): p. 9024-33.
15. Lee, E.C., et al., *A highly efficient Escherichia coli-based chromosome engineering system adapted for recombinogenic targeting and subcloning of BAC DNA*. *Genomics*, 2001. 73(1): p. 56-65.
16. Yu, D., M.C. Silva, and T. Shenk, *Functional map of human cytomegalovirus AD169 defined by global mutational analysis*. *Proc Natl Acad Sci U S A*, 2003. 100(21): p. 12396-401.
17. Dunn, W., et al., *Functional profiling of a human cytomegalovirus genome*. *Proc Natl Acad Sci U S A*, 2003. 100(24): p. 14223-8.
18. Wagner, M., et al., *Systematic excision of vector sequences from the BAC-cloned herpesvirus genome during virus reconstitution*. *J Virol*, 1999. 73(8): p. 7056-60.

19. Varnum, S.M., et al., *Identification of proteins in human cytomegalovirus (HCMV) particles: the HCMV proteome*. J Virol, 2004. 78(20): p. 10960-6.
20. Song, M.J., et al., *Identification of viral genes essential for replication of murine gamma-herpesvirus 68 using signature-tagged mutagenesis*. Proc Natl Acad Sci U S A, 2005. 102(10): p. 3805-10.
21. Fields, B.N., D.M. Knipe, and P.M. Howley, *Fields' virology*. 5th ed ed. 2007, Philadelphia: Wolters Kluwer Health/Lippincott Williams & Wilkins. 2 v. (xix, 3091, 86 p.).
22. de Chasse, B., et al., *Hepatitis C virus infection protein network*. Mol Syst Biol, 2008. 4: p. 230.
23. Calderwood, M.A., et al., *Epstein-Barr virus and virus human protein interaction maps*. Proc Natl Acad Sci U S A, 2007. 104(18): p. 7606-11.
24. Lee, M.J., et al., *Fibulin-5 promotes wound healing in vivo*. J Am Coll Surg, 2004. 199(3): p. 403-10.
25. Albig, A.R. and W.P. Schiemann, *Fibulin-5 antagonizes vascular endothelial growth factor (VEGF) signaling and angiogenic sprouting by endothelial cells*. DNA Cell Biol, 2004. 23(6): p. 367-79.
26. Yanagisawa, H., M.K. Schluterman, and R.A. Brekken, *Fibulin-5, an integrin-binding matricellular protein: its function in development and disease*. J Cell Commun Signal, 2009. 3(3-4): p. 337-47.
27. Nemes, J.P., et al., *The SCA8 transcript is an antisense RNA to a brain-specific transcript encoding a novel actin-binding protein (KLHL1)*. Hum Mol Genet, 2000. 9(10): p. 1543-51.
28. Shchelkunov, S.N., *Interaction of orthopoxviruses with the cellular ubiquitin-ligase system*. Virus Genes. 41(3): p. 309-18.



## **Chapter 6**

## **Conclusion**

Cytomegalovirus, a beta-herpesvirus, represents an important pathogen that causes morbidity and mortality in a wide range of immunocompromised and immunocompetent individuals. It is also an important source of knowledge as its large genome holds many genes responsible for both infection, modulation of the host and replication of the virus. However, the function of many of the 170 predicted genes in CMV remain unknown. These functions can be elucidated through a variety of different methods from traditional vertical approaches that investigate the function and mechanism of individual genes in great detail to newer global approaches that can cover the functions of large amounts of the genome through the use of high-throughput techniques [1].

An approach that has proven invaluable in our global investigations is the discovery and utilization of bacterial artificial chromosome (BAC) technology. BAC based mutagenesis has given researchers an elegant and efficient tool for generating large amounts of viral mutants that can contain single, highly specific, site directed open reading frame (ORF) deletions [2, 3]. This technology has allowed us to determine the deletion phenotypes of CMV viral genes in both cell culture and in animal models.

Understanding the essentiality of individual genes can give us important clues as to the importance of a particular gene or gene product in the course of infection but may not provide any information as to a gene's function or role with respect to the virus or infection of the host. This role can potentially be elucidated by determining the interactions between proteins found in both the virus and the host, in order to construct a network of interacting proteins called an interactome. The yeast two-hybrid system allows for a simple and efficient method for building these interactomes and has been used in determining interactions in a variety of different organisms from humans to bacteria [4-8]. Through these networks we can potentially determine the function of unknown proteins by looking at its interacting partners.

While powerful techniques by themselves, both BAC mutagenesis and the yeast two-hybrid system can benefit through the merging of data discovered in each system. It is through the integration of multiple global screens that a larger more detailed picture can be drawn. And through the combination of both horizontal and vertical techniques we can determine avenues of investigation to determine the functions of unknown proteins in CMV.

The investigation of large genomes of organisms, including those of viruses like CMV, can prove to be a daunting task. The sheer amount of proteins, by itself, can prove to be a nightmare when determining their individual functions. And can become impossible to determine when considering the multiple cellular conditions and environments that CMV can infect. However, with information from both, global analyses and individual highly detailed investigations, we can come closer to understand the role or roles by which each individual gene participates in the infection of the host. And it is through the understanding of the functions and importance of genes in various conditions that we can develop new methods and therapies to treat CMV infection and CMV associated diseases.

## References

1. Vidal, M., *A biological atlas of functional maps*. Cell, 2001. **104**(3): p. 333-9.
2. Zhang, Z., et al., *Genetic analysis of varicella-zoster virus ORF0 to ORF4 by use of a novel luciferase bacterial artificial chromosome system*. J Virol, 2007. **81**(17): p. 9024-33.
3. Lee, E.C., et al., *A highly efficient Escherichia coli-based chromosome engineering system adapted for recombinogenic targeting and subcloning of BAC DNA*. Genomics, 2001. **73**(1): p. 56-65.
4. Giot, L., et al., *A protein interaction map of Drosophila melanogaster*. Science, 2003. **302**(5651): p. 1727-36.
5. Ito, T., et al., *A comprehensive two-hybrid analysis to explore the yeast protein interactome*. Proc Natl Acad Sci U S A, 2001. **98**(8): p. 4569-74.
6. LaCount, D.J., et al., *A protein interaction network of the malaria parasite Plasmodium falciparum*. Nature, 2005. **438**(7064): p. 103-7.
7. Li, S., et al., *A map of the interactome network of the metazoan C. elegans*. Science, 2004. **303**(5657): p. 540-3.
8. Rain, J.C., et al., *The protein-protein interaction map of Helicobacter pylori*. Nature, 2001. **409**(6817): p. 211-5.